

METHODS IN PHARMACOLOGY AND TOXICOLOGY

# Apoptosis Methods in Pharmacology and Toxicology

Approaches to  
Measurement  
and Quantitation

---

Edited by

Myrtle A. Davis

 HUMANA PRESS

# **Apoptosis Methods in Pharmacology and Toxicology**

**METHODS IN PHARMACOLOGY AND TOXICOLOGY**

---

*Mannfred A. Hollinger, PhD* SERIES EDITOR

*Apoptosis Methods in Pharmacology and Toxicology: Approaches to  
Measurement and Quantification*

edited by **Myrtle A. Davis**, 2002

*Ion Channel Localization: Methods and Protocols*

edited by **Anatoli N. Lopatin** and **Colin G. Nichols**, 2001

**Methods in Pharmacology and Toxicology**

# **Apoptosis Methods in Pharmacology and Toxicology**

**Approaches to Measurement  
and Quantification**

Edited by

**Myrtle A. Davis**

*University of Maryland School of Medicine,  
Baltimore, MD*

**Humana Press**



**Totowa, New Jersey**

© 2002 Humana Press Inc.  
999 Riverview Drive, Suite 208  
Totowa, New Jersey 07512

**www.humanapress.com**

All rights reserved. No part of this book may be reproduced, stored in a retrieval system, or transmitted in any form or by any means, electronic, mechanical, photocopying, microfilming, recording, or otherwise without written permission from the Publisher.


The content and opinions expressed in this book are the sole work of the authors and editors, who have warranted due diligence in the creation and issuance of their work. The publisher, editors, and authors are not responsible for errors or omissions or for any consequences arising from the information or opinions presented in this book and make no warranty, express or implied, with respect to its contents.

Cover Illustration:

Cover design by Patricia F. Cleary.

Production Editor: Jessica Jannicelli.

For additional copies, pricing for bulk purchases, and/or information about other Humana titles, contact Humana at the above address or at any of the following numbers: Tel.: 973-256-1699; Fax: 973-256-8341; E-mail: [humana@humanapr.com](mailto:humana@humanapr.com) or visit our website: <http://humanapress.com>

This publication is printed on acid-free paper.  ANSI Z39.48-1984 (American National Standards Institute) Permanence of Paper for Printed Library Materials.

**Photocopy Authorization Policy:**

Authorization to photocopy items for internal or personal use, or the internal or personal use of specific clients, is granted by Humana Press Inc., provided that the base fee of US \$10.00 per copy, plus US \$00.25 per page, is paid directly to the Copyright Clearance Center at 222 Rosewood Drive, Danvers, MA 01923. For those organizations that have been granted a photocopy license from the CCC, a separate system of payment has been arranged and is acceptable to Humana Press Inc. The fee code for users of the Transactional Reporting Service is: [0-89603-890-4/02 \$10.00 + \$00.25].

Printed in the United States of America. 10 9 8 7 6 5 4 3 2 1

Library of Congress Cataloging-in-Publication Data

## Series Foreword

---

Dr. Davis is to be congratulated for assembling an outstanding list of contributors for *Apoptosis Methods in Pharmacology and Toxicology: Approaches to Measurement and Quantification*. Of all the books published yearly in the fields of pharmacology and toxicology, methods books are by far the most difficult to compile. But, when successful, the rewards are correspondingly high. This, I believe, is the case with Dr. Davis and her contributors' efforts in the present volume.

The importance of apoptosis as a biological, cellular process can be illustrated by the following examples. Programmed cell death occurs during: metamorphosis of tadpole tail, removal of interdigital material between the fingers and toes of the developing fetus (a necessary occurrence during gestation), the sloughing off of the endometrium at the start of the monthly menstruation event in younger women, and the elimination of surplus cells in the brain (necessary in order to form proper synaptic connections). With such diverse examples as these, the potential impact of pharmacological and toxicological factors that can perturb the apoptotic process is obvious. Central to studies relating to apoptosis in these, and other areas, is the availability of appropriate methodological protocols.

The contributors in Dr. Davis' book have provided state-of-the-art descriptions of numerous relevant protocols that should contribute to increasing our understanding of this exciting field.

*Mannfred A. Hollinger*

## Preface

---

The topic of apoptotic cell death has received a lion's share of attention, especially within the last 15 years. This heightened interest likely results from recent recognition of the relevance of apoptosis to a variety of scientific disciplines; pharmacology and toxicology are no exceptions. The major goals for toxicologists who study apoptosis, however, often differ from the investigative goals of other disciplines. In many cases, a toxicologist or pharmacologist is faced with the task of quantifying an apoptotic response or assessing, in a quantitative way, the mechanism by which a chemical or drug interacts with apoptotic signaling factors. Frequently, the final outcome of this task is to apply results to safety evaluation or assess relevance to environmental exposures. Although there are several publications that review and instruct the reader about detection of apoptosis, many of these texts do not pair the methods used for evaluating apoptosis with the need to evaluate safety or risk assessment. The primary aim of this book is to review methods that can be used by toxicologists, pathologists, or pharmacologists in the analysis of chemical-induced apoptosis. *Apoptosis Methods in Pharmacology and Toxicology: Approaches to Measurement and Quantification* provides a concise source of information on the detection, mechanisms, and quantification of apoptosis that is useful for the design of toxicology and pharmacology studies.

The range of methods covered may seem surprisingly narrow at first glance, but there are few methods that have proven to have broad application to numerous tissue and cell types or that can be applied to unknown induction mechanisms. The number of methods for detection may also seem small compared with the exciting and abundant activity in apoptosis research over the past 10 years. For example, PubMed lists 19,167 publications with apoptosis in the title between 1991 and 2001. Since research in the area of apoptosis has yielded reports of an overwhelming number of inducing agents, regulatory factors, and mechanisms, one might ask why the number of biological assays for measurement of apoptosis is comparatively low. One reason may be that despite the plethora of molecular factors and events that have been found to participate in the apoptotic process, only a few of these appears to have the sensitivity, specificity, and universal application

required to merit acceptance as reliable biological assays for measurement of apoptosis. The search for molecular and biochemical events in apoptosis common to most cell types and induction pathways has resulted in assays that are largely based on the biochemical mechanisms that regulate the morphologic features of apoptosis. Even after years of use, several of the current methods used to identify or quantify apoptosis are still developing because of limited testing in different cell types, in experimental models, or in tissue sections.

In *Apoptosis Methods in Pharmacology and Toxicology*, meaningful and cutting edge chapters were contributed by authors with substantial knowledge of the technical challenges and caveats of methods used for analysis of apoptosis. Each chapter emphasizes how the method can be used in evaluation of apoptosis, the limitations of the method, and how the technique may be applied for large-scale screening applications. In the introductory chapter, there is a brief overview of study design and approaches to mechanistic studies of toxicant-induced apoptosis. The remaining chapters provide a concise source of information on detection and quantification of apoptosis that can be incorporated into the design of toxicological evaluations. In Chapter 2, Martin Poot, Robert H. Pierce, and Terrance J. Kavanagh review the flow cytometric and fluorometric methods of quantifying and characterizing apoptosis. Measurement of several biochemical features of apoptosis are discussed and protocols are provided for the measurement of cell-cycle stage-specific apoptosis and the simultaneous measurement of mitochondrial membrane potential, and reduced thiol and NAD(P)H levels. Chapter 3, contributed by Zbigniew Darzynkiewicz, Elzbieta Bedner, and Piotr Smolewski, is *the only comprehensive review* to date on the application of laser scanning cytometry in analysis of apoptosis. This relatively new and powerful method is discussed and detailed protocols are provided.

Chapter 4, contributed by Matthew A. Wallig, Curtis M. Chan, and Nancy A. Gillett, emphasizes challenges to tissue-based methods and reemphasizes the need to keep morphologic assessment of apoptosis as a “gold standard.” Immunocytochemical approaches to the measurement of several biochemical and molecular endpoints in tissue sections are discussed. Quantification and qualitative analysis of morphology is also emphasized, along with quantification. This section will be highly useful for those carrying out studies in whole animal models, in contrast to cell culture systems.

DNA microarray technology is reviewed in Chapters 5 and 6. Chapter 5 by Helmut Zarbl reviews microarray analysis as a general technique, and Chapter 6 by Richard W. E. Clarkson, Catherine A. Boucher, and Christine



J. Watson focuses on the application of microarray technology in the measurement of apoptosis. Finally, relatively new ELISA techniques are described in detail in Chapter 7 by Calvin F. Roff and colleagues. This chapter is unique in that it describes approaches that can be applied as high throughput screens for functional quantification of protein or chemical inhibitors that target active caspases and the Bcl-2 family of proteins.

*Apoptosis Methods in Pharmacology and Toxicology* is expected to serve as a useful reference for all scientists who face the challenge of identifying apoptosis, or elucidating mechanisms of drug-induced injury, as well as those scientists bewildered by the abundant flow of new information on apoptosis whose practical application is difficult to discern. This volume should equally serve as a reference for any laboratory that has a general interest in studying apoptosis. In such an evolving field, new developments are continually being reported. It is recommended that everyone with a serious interest in apoptosis and cell death make use of one of the web-based discussion groups or attend conferences or workshops on the topic to stay informed about research that may have application to research questions in their labs.

*Myrtle A. Davis*

# Contents

---

Foreword .....	v
Preface .....	vii
List of Contributors .....	xiii
1 Introduction	
<i>Myrtle A. Davis</i> .....	1
2 Flow Cytometric and Fluorometric Methods of Quantifying and Characterizing Apoptotic Cell Death	
<i>Martin Poot, Robert H. Pierce, and Terrance J. Kavanagh</i> .....	11
3 Analysis of Apoptosis by Laser-Scanning Cytometry	
<i>Zbigniew Darzynkiewicz, Elzbieta Bedner,     and Piotr Smolewski</i> .....	37
4 Specific Methods for Detection and Quantification of Apoptosis in Tissue Sections	
<i>Matthew A. Wallig, Curtis M. Chan, and Nancy A. Gillett</i> .....	59
5 DNA Microarrays: <i>An Overview of Technologies     and Applications</i>	
<i>Helmut Zarbl</i> .....	77
6 Microarray Analysis of Apoptosis	
<i>Richard W. E. Clarkson, Catherine A. Boucher,     and Christine J. Watson</i> .....	97
7 ELISAs for Quantification of Bcl-2 Family Activities and Active Caspases	
<i>Calvin F. Roff, Amy M. Walz, Lisa B. Niehoff,     David J. Sdano, Antoinette M. Bennaars, Jeffrey A. Cooper,     Becky L. Senft, Anatoli A. Sorkin, Steven P. Stoesz,     and Paul A. Saunders</i> .....	119
Index .....	149

## Contributors

---

- ELZBIETA BEDNER • *Department of Pathology, Pomeranian School of Medicine, Szczecin, Poland*
- ANTOINETTE M. BENNAARS • *R & D Systems Inc. Minneapolis, MN*
- CATHERINE A. BOUCHER • *Biorobotics Ltd., Cambridge, UK*
- CURTIS M. CHAN • *Sierra Biomedical, A Division of Charles River Laboratories, Inc., Sparks, NV*
- RICHARD W. E. CLARKSON • *Department of Pathology, University of Cambridge, Cambridge, UK*
- JEFFREY A. COOPER • *R & D Systems Inc., Minneapolis, MN*
- ZBIGNIEW DARZYNKIEWICZ • *Brander Cancer Research Institute, New York Medical College, Valhalla, NY*
- MYRTLE A. DAVIS • *Department of Pathology, University of Maryland School of Medicine, Baltimore, MD*
- NANCY A. GILLET • *Sierra Biomedical, A Division of Charles River Laboratories, Inc., Sparks, NV*
- MANNFRED A. HOLLINGER • *Emeritus Professor of Pharmacology, School of Medicine, University of California, Davis, CA*
- TERRANCE J. KAVANAGH • *Department of Environmental Health, University of Washington, Seattle, WA*
- LISA B. NIEHOFF • *R & D Systems Inc., Minneapolis, MN*
- ROBERT H. PIERCE • *Department of Pathology, University of Rochester, Rochester, NY*
- MARTIN POOT • *Department of Pathology, University of Washington, Seattle, WA*
- CALVIN F. ROFF • *R & D Systems Inc., Minneapolis, MN*
- PAUL A. SAUNDERS • *R & D Systems Inc., Minneapolis, MN*
- DAVID J. SDANO • *R & D Systems Inc., Minneapolis, MN*
- BECKY L. SENFT • *R & D Systems Inc., Minneapolis, MN*
- PIOTR SMOLEWSKI • *Department of Hematology, School of Medicine, Lodz, Poland*
- ANATOLI A. SORKIN • *R & D Systems Inc., Minneapolis, MN*
- STEVEN P. STOESZ • *R & D Systems Inc., Minneapolis, MN*

MATTHEW A. WALLIG • *Department of Veterinary Pathobiology, University of Illinois at Urbana-Champaign, Urbana, IL*

AMY M. WALZ • *R & D Systems Inc., Minneapolis, MN*

CHRISTINE J. WATSON • *Department of Pathology, University of Cambridge, Cambridge, UK*

HELMUT ZARBL • *Cancer Biology Program, Fred Hutchinson Cancer Research Center, Seattle, WA*

## Introduction

---

Myrtle A. Davis

### 1. TERMINOLOGY AND FEATURES OF CELL DEATH

The term “apoptosis” (introduced by Kerr, Wyllie, and Currie in a seminal paper in 1972; [1]) is now widely accepted as a fundamental mechanism of cell death that contributes to the pathogenesis of disease or removal of cells in the adult organism. Although there are still instances in which the term apoptosis is used interchangeably with programmed cell death, it is well-accepted that the two terms have very distinct interpretations. Programmed cell death is a term that depicts the physiological cell death that was first described as it occurred in ovarian follicles by Walther Flemming in 1885 (2). The impact of the process during development was subsequently appreciated by many others including Glücksman in 1951 (3) and Lockshin and Williams in 1965 (4). In general, programmed cell death should be used to describe a temporally and spatially restricted cell death that follows a distinct biological program in the developing organism and is usually limited to the field of developmental biology. In contrast, the term “apoptosis” was originally chosen to replace the term “shrinkage necrosis” previously used to describe the morphologic features of dying cells observed in hepatic lobes of adult liver after ligation of the portal vein, excised basal cell carcinoma, and in the adrenal cortex following removal of adrenocorticotrophic hormone (ACTH) (5–7). The morphologic features of apoptosis are summarized and contrasted with other pathways of cell death in Table 1.

### 2. MEASUREMENT OF APOPTOSIS

Although the morphologic features of apoptosis are the gold standard for definitive identification of apoptotic cells, there are often limitations to the

**Table 1**  
**Morphologic Features of Cell Death**

Apoptosis	Oncosis	Alternate forms of cell death
<ul style="list-style-type: none"> <li>• Cell shrinkage</li> <li>• Cellular budding</li> <li>• Chromatin margination</li> <li>• Chromatin fragmentation</li> <li>• DNA fragmentation</li> <li>• Nuclear fragmentation</li> <li>• Cellular fragmentation</li> <li>• Phagocytosis by neighboring cells</li> <li>• Organelles appear morphologically normal (including membranes)</li> <li>• Most changes occur while cell retains an intact cell membrane</li> </ul>	<ul style="list-style-type: none"> <li>• Cell swelling</li> <li>• Organelle swelling</li> <li>• Cellular blebbing (fluid-filled structures)</li> <li>• Increased cytoplasmic membrane permeability</li> <li>• Karyolysis</li> <li>• Nonspecific DNA fragmentation</li> <li>• Incites inflammation and recruitment of professional inflammatory cells cell</li> </ul>	<ul style="list-style-type: none"> <li>• Also called cytoplasmic death, type 3B death, paraptosis (8–10)</li> <li>• Cytoplasmic vacuolation</li> <li>• Mitochondrial swelling</li> <li>• No chromatin or DNA damage</li> <li>• Requires protein synthesis (in some cases)</li> </ul>

use of morphological criteria for quantification and identification of apoptotic cells. For example, early morphologic changes are usually identifiable in cell culture, but in the whole organ rapid elimination (via sloughing into lumens or engulfment by other cells) may limit observation of late morphologic changes in tissue sections. Late changes may include nuclear and DNA fragmentation. In addition, limited numbers of tissue sections may limit the three-dimensional profile needed to adequately quantify the numbers of apoptotic cells in a whole organ.

Biochemical endpoints have been used to establish markers or indicators of apoptosis that can accompany, but not replace, morphologic criteria and provide readily quantifiable endpoints. The biochemical or molecular events that have been reported to accompany apoptosis are numerous, but only a few of these events can be regarded as universal indicators of apoptosis, and even fewer of these are accepted as regulatory events (Table 2). The stringency required to characterize a universal indicator of apoptosis and subsequently develop an assay based on this indicator is a challenge to researchers and commercial entities. One obvious criterion for an apoptosis-specific indicator is that it does not occur or show similar changes during other types of cell death, namely an oncotic or swelling form of death. This is frequently the most critical distinction that needs to be made by a biochemical or molecular marker used for tissue-based assays because both events may occur simultaneously in the same tissue. An oncotic event may also be a continuum of an apoptotic pathway in tissue-culture systems. For example, cell death may continue from apoptosis to secondary oncotic necrosis if the apoptotic cell is not engulfed. In this scenario, positive identification of a biochemical marker of apoptosis may be made in a cell with morphologic features consistent with oncotic-necrotic death. These possibilities make it even more critical that the biochemical marker for apoptosis be stringently tested for specificity. In other cases, a biochemical event may occur in both pathways of death, but differ by extent of the alteration. For example, a measurable decrease in mitochondrial transmembrane potential (MMP) or permeability transition (PT) may occur during oncotic-death and apoptosis, but the magnitude of the decrease may influence the ATP-generating capacity of the cell. ATP dissipation may then determine whether the cell undergoes apoptosis or oncotic death (11,12). When combined with morphologic assessment however, extent of MMP decrease or PT opening can be a useful way to measure apoptosis in cell culture systems.

A question that commonly arises is: "why is it necessary to distinguish the pathway of death?" The answer depends on the primary goal of the study. If the goal is to understand the primary molecular or biochemical events that

**Table 2**  
**The Basis for Commonly Used Apoptosis Assays**

Basis for the assay	Assay(s)	Drawbacks <sup>a</sup>
Fragmentation of DNA into internucleosomal fragments; chromatin condensation; chromatin fragmentation	<ul style="list-style-type: none"> <li>• Terminal deoxynucleotidyl dUTP nick end labeling (TUNEL)</li> <li>• <i>In situ</i> end labeling (ISEL)</li> <li>• DNA agarose gel electrophoresis</li> <li>• JAM assay</li> <li>• Nuclear stains (i.e., Hoechst, DAPI)</li> <li>• Transverse or pulse field electrophoresis</li> <li>• Assessment of Soluble DNA</li> <li>• Flow cytometric analysis of DNA content</li> </ul>	DNA fragmentation occurs very late in some cell types; not always quantitative for numbers of apoptotic cells; some assays can be expensive and time-consuming (i.e., TUNEL)
Apoptotic cells expose phosphotidyl serine (PS) on the outer surface of the cell membrane	All Annexin V assays	Not all cells expose PS—this needs to be confirmed for each cell type; need live cell culture or unfixed specimens; doesn't work as well for adherent cells; does not work at all for fixed cells or tissues; necrotic cells will also stain positive and will require morphologic assessment or combination assay ( <i>see</i> below)
Caspases are cleaved and activated during apoptosis	<ul style="list-style-type: none"> <li>• Active caspase immunoblotting</li> <li>• Measurement of caspases activity using substrate peptides</li> <li>• Assay of cleavage of known intracellular caspases substrates (i.e., Poly ADP Ribose Polymerase)</li> </ul>	Several caspase activities may need to be surveyed some models may be caspase-independent (i.e., calpain-mediated)



**Table 2 (Continued)**

Basis for the assay	Assay(s)	Drawbacks <sup>a</sup>
Increase in mitochondrial membrane permeability; permeability transition pore opening (PT); decrease in mitochondrial membrane potential (MMP)	<ul style="list-style-type: none"> <li>• JC-1 and JC-9 carboxyanine dyes</li> <li>• Mito Tracker and MitoFluor dyes</li> <li>• TMRME and Rhodamine 123</li> <li>• Fluorescent probe, calcein redistribution</li> <li>• Radiolabeled deoxyglucose</li> </ul>	Large changes may not be specific for apoptosis; subtle changes, more characteristic of apoptosis may not be measurable; alterations may be reversible
Differential loss in cell membrane integrity between apoptotic and oncotic cells	Combination assays <ul style="list-style-type: none"> <li>• Propidium iodide—YO-PRO-1</li> <li>• Acridine Orange-Ethidium Bromide</li> <li>• Annexin V-Propidium iodide</li> </ul>	Useful for live, unfixed cells or unfixed organs only
Proteins from the intermembrane space of the mitochondria are released from mitochondria of apoptotic cells	Quantitation of cytoplasmic amounts of: <ul style="list-style-type: none"> <li>• Cytochrome C</li> <li>• Apoptosis inducing factor (AIF)</li> <li>• Adenylate kinase</li> <li>• Sulfite oxidase</li> <li>• Procaspase 9</li> </ul>	All need confirmation of release in conjunction with apoptotic death; may also require confirmation of regulatory role for the factor on the apoptosis
Proteins migrate to the mitochondria during apoptosis	Quantitation of mitochondrial amounts of: <ul style="list-style-type: none"> <li>• Caspase 9</li> <li>• Cytosolic adapter protein, Apaf-1</li> <li>• Bid, Bax, Bak</li> </ul>	Same as above

<sup>a</sup>All assays require a morphologic study that confirms and differentiates apoptosis from oncotic or other forms of cell death to confirm specificity of the assay.

led to the cellular response observed, knowing the primary cellular response is key to a mechanistic investigation. If, on the other hand, the goal of the study is to determine evidence of organ toxicity, then documentation and quantification of the toxic cellular response will suffice. It could be argued, however, that even in the latter case, knowing the primary cellular response may be critical to identification of a toxic event that may have primarily affected cellular engulfment or recognition processes. An example of this is acetaminophen toxicosis, in which a cytotoxic effect on Kupffer cells may influence engulfment of apoptotic hepatocytes, contributing to an eventual picture of widespread necrosis in the liver (13).

### **3. APPROACHES TO MECHANISTIC INVESTIGATIONS OF APOPTOSIS**

The question of how apoptosis is regulated and controlled is one of the most intriguing questions for an investigator. Indeed, regulation of the apoptotic response is the focus of the vast majority of research on apoptosis. There is no road map for those interested in pursuing answers to these mechanistic questions when apoptosis is initiated by a chemical or toxicant, but knowledge of the pathways that have contributed to elucidating several mechanisms of apoptosis can provide a general scheme for mechanistic study design. At the onset, it is probably best to keep an open mind and consider that the biochemical and molecular events that regulate cellular responses to a toxicant are unique. From that basic principal, clues can be drawn from chemical and structural features of the toxicant or compound. Chemical and structural features may allow identification of a list of potential intracellular targets for the compound. We can take for example, compound X. Compound X was found to interact with and activate a cellular receptor. Knowledge about the expected cell-signaling pathways utilized by the receptor can provide a basis for a logical series of experiments to elucidate the primary events that regulate the cellular response to compound X. Several examples of this type of mechanistic approach can be found including the approaches used to elucidate effects of therapeutic concentrations of doxorubicin and cisplatin. Both of these anticancer compounds were reported to lead to the induction of cell death receptor, CD95 and CD95 ligand in neuroblastoma cells and subsequent activation of the now well-recognized pro-apoptotic series of events characteristic of death-inducing ligand/receptor systems (reviewed in ref. 14). To elucidate mechanisms for new compounds, experimental evidence documenting a sequence of apoptotic events is the first step. Altered regulation of the cellular response when these events are inhibited or directly activated will be critical to determining the apoptotic signaling pathway used by the compound.

Another possible approach is to demonstrate that the chemical interacts with or alters the activity of a known regulator of apoptosis. This type of approach is usually considered when there is structural evidence that the toxicant may interact with an apoptotic regulatory protein. A chemical may inhibit pathways or factors that promote cellular survival or augment cell death-inducing pathways. Protein interactions may be identified by yeast-two hybrid, immunoprecipitation studies, expression studies, and mutation analysis accompanied by activity assays of events that lie downstream of the factor studied. An intriguing example of a toxin that appears to fit this mechanism is verotoxin II (15). Interestingly, verotoxin II was reported to bind Bcl-2 and it is hypothesized that in complex with Bcl-2, verotoxin II gains access to the mitochondria and induces cell death. Unfortunately, most toxicants induce multiple intracellular effects often making it difficult to discern epiphenomenon from events that regulate the cellular response. The challenges for those who study chemical-induced mechanisms of apoptosis can be daunting, but knowledge about chemical structure, protein–toxicant interaction, and dose-response will aid in proposing reasonable and testable hypotheses. Initial use of protein structure databases (Protein Data Bank, Brookhaven, NY, containing over 6500 proteins) and genetic responses can also provide useful information about molecular events.

#### 4. APPLICATION OF MICROARRAY DATA

The use of microarray data, to assess whether expression of pro- and anti-apoptotic genes are induced or downregulated by potential apoptotic stimuli, is gaining popularity among toxicologists, however, the relationship between transcriptional regulation of a protein and other events that occur during apoptosis will need to be considered. Apart from a few notable exceptions, it is clear from an abundance of experimental evidence that in most cell types, apoptosis does not require *de novo* synthesis of protein and gene transcription is seldom responsible for the death of the cell. There is also lack of evidence for transcriptional control of several known pro- and anti-apoptotic proteins by pro-apoptotic stimuli, but rather several proteins have been shown to be regulated via post-translational mechanisms that include: protein phosphorylation, organelle sequestration, translocation, and protein interactions. Microarray analyses do not measure post-translational events. Thus microarray analyses that assess *bim* mRNA, the product of which is a pro-apoptotic BH3-only protein that uses protein translocation to activate the apoptotic program, may have limited value to primary regulation of apoptosis. In contrast, including *nox* and *puma* on a microarray platform is highly useful because they are p53-inducible genes normally subject to tran-

scriptional regulation. Similarly, caspases appear to be regulated post-translationally during apoptosis and thus the interpretation of cellular mRNA expression of caspases after treatment with an apoptotic stimulus may be of limited mechanistic value because activation of caspase protein has committed the cell to death. In contrast, gene-expression analysis of known apoptosis regulatory proteins can have important mechanistic relevance to sublethal concentrations of toxicants or evaluation of cellular responses to multiple exposures or exposure to chemical mixtures. For example, pre-exposure to a nonlethal dose of a toxicant or chemical may alter the expression of pro- or anti-apoptotic factors. If the observed change in mRNA expression causes a change in protein expression, the cellular response to a subsequent toxicant exposure may be altered. Another common application of microarray techniques is to obtain an expression footprint of mRNA alterations. These data can be used to identify common transcriptional regulation among these mRNAs and subsequently traced back to signal-transduction pathways activated by the chemical. These types of mechanistic studies and applications of microarray data are anticipated with great enthusiasm.

## 5. CONCLUSION

Measurement of apoptosis has become an essential component of the evaluation of cytotoxicity of chemicals. In some cases, the primary goal of investigators will be to elucidate the mechanism by which a compound induces an apoptotic response. In other instances, the primary goal will be to identify and measure apoptosis. The discovery and development of new drugs directed to specific cellular targets will depend on screening methods that include measurement of functional cellular responses, including apoptosis. In any case, the ability to accurately measure and quantify apoptosis is critical. The following chapters review methods that can be used to detect and quantify apoptosis in a wide variety of experimental situations.

## REFERENCES

1. Kerr, J. F., Wyllie, A. H., and Currie, A. R. (1972) Apoptosis: a basic biological phenomenon with wide-ranging implications in tissue kinetics. *Br. J. Cancer* **26**, 239–257.
2. Flemming, W. (1885) über die Bildung Von Richtungsfiguren in Sägethiereiern beim Utergang Graaf'scher Follikel. *Arch Anat. EntwGesch*, 221–244.
3. Glücksmann, A. (1951) Cell deaths in normal vertebrae ontogeny. *Biol. Rev. Camb. Philos. Soc.* **26**, 59–86.
4. Lockshin, R. A. and Williams, C. M. (1964) Programmed cell death. II. Endocrine potentiation of the breakdown of the intersegmental muscles of silkmooths. *J. Insect Physiol.* **10**, 643–649.

5. Kerr, J. F. (1965) Histochemical study of hypertrophy. *J. Pathol. Bacteriol.* **190**, 419–435.
6. Kerr, J. F. (1971) Shrinkage necrosis: a distinct mode of cellular death. *J. Pathol.* **105**, 13–20.
7. Kerr, J. F. (1972) Shrinkage necrosis of adrenal cortical cells. *J. Pathol.* **107**, 217–219.
8. Sperandio, S., de Belle, I., Bredesen, D. E. (2000) An alternative, nonapoptotic form of programmed cell death. *Proc. Natl. Acad. Sci. USA* **97**, 14,376–14,381.
9. Clarke, P. G. (1990) Developmental cell death: morphological diversity and multiple mechanisms. *Anat. Embryol.* **181**, 195–213.
10. Pilar, G. and Landmesser, L. (1976) Ultrastructural differences during embryonic cell death in normal and peripherally deprived ciliary ganglia. *J. Cell Biol.* **68**, 339–356.
11. Crompton, M. (1999) The mitochondrial permeability transition pore and its role in cell death. *Biochem. J.* **341**, 233–249.
12. Crompton, M. (2000) Mitochondrial intermembrane junctional complexes and their role in cell death. *J. Physiol.* **529(Pt 1)** 11–21.
13. Goldin, R. D., Ratnayaka, I. D., Breach, C. S., Brown, I. N., and Wickramasinghe, S. N. (1996) Role of macrophages in acetaminophen (paracetamol)-induced hepatotoxicity. *J. Pathol.* **179**, 432–435.
14. Walczak, H. and Krammer, P. H. (2000) The CD95 (APO-1/Fas) and the TRAIL (APO-2L) apoptosis systems. *Exp. Cell Res.* **256**, 58–66.
15. Suzuki, A., Doi, H., Matsuzawa, F., Aikawa, S., Takiguchi, K., Kawano, H., et al. (2000) Bcl-2 antiapoptotic protein mediates verotoxin II-induced cell death: possible association between bcl-2 and tissue failure by E. coli O157:H7. *Genes Dev.* **14**, 1734–1740.

# Flow Cytometric and Fluorometric Methods of Quantifying and Characterizing Apoptotic Cell Death

---

Martin Poot, Robert H. Pierce, and Terrance J. Kavanagh

## 1. INTRODUCTION

Cell death is a major endpoint in toxicologic assessment both in vivo and in vitro and numerous methods have become available for the characterization and quantitation of cell death. Recent developments in cell biology have made great strides in articulating two generally distinct modes of cell death. Although the Cell Death Nomenclature Committee of the Society of Toxicologic Pathologists has recommended replacing the terms “apoptosis” and “necrosis” with “apoptotic necrosis” and “oncotic necrosis,” emphasizing that necrosis simply refers to the fact that the cells are dead (1), in this chapter we will utilize the more generally used terms apoptosis and necrosis. This chapter will focus on the relative advantages and inherent disadvantages of a number of flow and image cytometry assays with an eye to helping investigators to choose among the many available techniques to measure apoptosis.

Although in some experimental systems a “hybrid” death phenotype has been identified (2–4) in general, apoptosis and necrosis involve different biochemical features and, possibly, kinetics (5). Necrosis appears to be a rapid response (often to exogenous agents) involving cellular injury, cell swelling, loss of cytoplasmic ATP, release of sequestered calcium, and uncontrolled activation of calcium-dependent enzymes (proteases, lipases, DNAases) leading to early loss of cytoplasmic membrane integrity (6). DNA

**Table 1**  
**Fluorescent Dyes Used in Assays of Apoptosis**

Parameter	Fluor	Excitation maximum (nm)	Emission maximum (nm)
NAD(P)H level	NAD(P)H	350	450
Mito membrane potential	Rhodamine 123	505	530
	DiOC <sub>6</sub> (3)	480	500
	JC-1	515	530/610
	CMXRosamine	590	610
Mitochondrial mass	MitoTracker Green FM	490	520
Cardiolipin	Nonyl Acridine Orange	490	520
Reduced thiols (GSH)	Monochlorobimane (MCB)	360	450
Cytosolic oxidants	CDCFDA	490	530

single-strand breaks are formed, but the morphology of the cell nucleus usually remains intact. Apoptosis, in contrast, is a more controlled process involving a decrease in cell size, the loss of mitochondrial membrane potential, alterations in mitochondrial structure and function, altered cellular redox status (7,8), as well as activation of caspases, exposure of cell-surface phosphatidylserine residues, and ordered double-strand DNA fragmentation. Although loss of cytoplasmic membrane integrity may eventually occur in the very late stages of apoptosis, maintenance of plasma membrane function in the early phase is a characteristic feature of apoptotic cell death. The exact apoptotic phenotype manifested appears to depend both on the cell type and the nature of the apoptotic trigger.

In view of the diversity of manifestations of the apoptotic process, no single method can encompass all stages and forms of apoptosis. Consequently, numerous techniques to analyze apoptosis have been developed, each with its advantages and limitations. In this review, the cardinal features of apoptosis and the fluorometric assessment of these features will be discussed, including specific examples of assays useful in the assessment of apoptosis based on nuclear appearance of DNA double-strand breaks, nuclear fragmentation, changes in mitochondrial function, and cellular redox status (*see* Table 1). The advantages and limitations of analyses using a confocal microscope, a flow cytometer, or a fluorescence plate reader will be discussed and are summarized in Table 2.

### **1.1. Nuclear Morphology and Apoptosis**

A major morphologic hallmark of apoptosis is nuclear fragmentation. This can be detected by viewing cell and tissue samples after staining with a DNA-

**Table 2**  
**Advantages and Limitations of Assays for Apoptosis**

Parameter of apoptosis	Assay method	Advantages	Limitations
Nuclear fragmentation	Microscopy	Morphological proof of apoptosis	Time-consuming; depends on judgement
DNA degradation	Gel electrophoresis	End stage of apoptosis	Limited sensitivity; prone to artifacts
DNA breaks	Flow cytometry (Sub-G1) TUNEL	End stage of apoptosis Highly specific	Debris and noise may look like false-positives Laborious; loss of apoptotic bodies
Mitochondrial parameters	Flow cytometry and confocal microscopy	Fast; large cell numbers Early stages of apoptosis Multiparameter option	Indirect; early stage changes may not be definitive proof
Phosphatidyl-serine exposure	Flow cytometry and confocal microscopy	Fast; large cell numbers Early stages of apoptosis Multiparameter option	False-positives due to over-trypsinization



specific dye. When samples are stained with fluorescent DNA dyes (e.g., Hoechst 33342 and 33258 dyes; 4',6-diamidino-2-phenylindole [DAPI]; SYTOX Green, ethidium bromide, propidium iodide, 7-aminoactinomycin D) a confocal microscope can be used to view such fragmentation (*see* below). An advantage of using fluorescent dyes is that their emission covers only part of the visible spectrum. Thus, additional parameters can be determined simultaneously in the same sample by staining with other fluorescent dyes. This multiparameter approach will be discussed below.

It has been reasoned that nuclear fragmentation during apoptosis is the result of DNA degradation. This hypothesis is supported by morphologic evaluation and by the observation that there is an increased level of DNA containing debris in cell samples undergoing apoptosis. Thus, counting the number of DNA-containing subcellular particles (for instance by flow cytometry) relative to the number of intact cells could be taken as a measure of apoptosis. However, this approach is fraught with difficulties. First, it is not likely that each apoptotic nucleus will give rise to the same number of debris particles. In other words, the number of apoptotic nuclei cannot be calculated as a fixed fraction of the number of debris particles. Second, debris particles are much smaller than intact nuclei. Thus, it may be difficult to distinguish debris particles from the electronic noise produced at the lower limits of resolution of flow cytometers.

To overcome these problems, various protocols based on cell fixation with ethanol have been developed (9,10). Cell fixation keeps nuclear fragments within a cell together. Thus, a cell with a fragmented nucleus will still be counted as one unit. Since apoptosis involves the formation double-strand breaks in the DNA, loose DNA fragments will arise. Some of these DNA fragments can be extracted from fixed cells with low-phosphate containing buffers (11). After this wash, apoptotic cells will be detected as cells with a less than G1 phase DNA content. Enumerating the number of sub-G1 cells relative to cells with G1, S, and G2 phase DNA content then allows quantitation of the number of cells that have undergone apoptosis. Thus, cell fixation before quantitation of apoptosis overcomes the problem that multiple cell fragments may be counted as multiple apoptotic events. Still it remains necessary to standardize the assay, such that electronic noise will be avoided. These methodological issues have been discussed in depth (12).

In the assay outlined earlier, apoptotic cells are detected because of lowered signal intensity resulting from DNA degradation. The finding that apoptosis involves a specific form of DNA degradation allows one to detect these unique events with a specific labeling procedure. With the aid of terminal deoxynucleotide transferase, fluorescently labeled dUTP residues are

added to the 3' sides of these double-strand DNA breaks (13). Since the amount of fluorescence thus generated is higher in apoptotic cells than in cells without this specific form of DNA damage, the apoptotic cells can be distinguished. For each new cell type, this assay needs to be optimized (14).

### ***1.2. Mitochondrial Alterations in Apoptosis***

Mitochondria have recently been shown to play an important role in apoptosis, acting as either in the upstream initiation (15) or downstream execution phase (7), depending on the specific experimental model. Although no unified picture of mitochondrial alterations in apoptosis has yet emerged, several features have been shown to be important in a variety of disparate apoptosis models (8), including: loss of cytochrome c, opening of the mitochondrial permeability transition pore, loss of mitochondrial membrane potential, catabolism of cardiolipin, mitochondrial proliferation (16), redistribution of cytoplasmic BAX to the mitochondria (17), and pH alterations (18).

Mitochondrial respiration (reviewed in ref. 19) involves a complex series of redox reactions beginning with reduced NAD and FAD species and ending with molecular oxygen as the ultimate electron acceptor. Several important characteristics of the process of electron transport include the generation of free-radical intermediates through single electron transfers and the production of an electro-chemical gradient as the transfer of electrons down the electron-transport chain is coupled to proton pumping from the mitochondrial matrix into the intermembrane space. Thus, the matrix and the cytoplasm are alkaline (proton-depleted) relative to the proton-rich (low pH) intermembrane space. The inner mitochondrial membrane is uniquely suited to act as a proton-diffusion barrier and the F0/F1-ATPase couples diffusion of protons down this gradient ( $\Delta\Psi_{\mu}$ ) to the generation of ATP. Alterations in  $\Delta\Psi_{\mu}$ , (usually decreased  $\Delta\Psi_{\mu}$ , although some investigators have identified early hyperpolarization) is a common alteration in apoptosis. A number of lipophilic cationic dyes selectively stain mitochondria in proportion to  $\Delta\Psi_{\mu}$ . Some of the more commonly used probes include: rhodamine 123, tetramethylrosamine, MitoTracker™ rosamine derivatives, DiOC<sub>6</sub> (3), and JC-1 (20). Ratiometric measurements of  $\Delta\Psi_{\mu}$  can be made using the red-emitting  $\Delta\Psi_{\mu}$ -sensitive CMXros in conjunction with the  $\Delta\Psi_{\mu}$ -insensitive dye Mitotracker Green as well as with JC-1, which forms  $\Delta\Psi_{\mu}$ -dependent red-emitting j-aggregates. By normalizing  $\Delta\Psi_{\mu}$  to total mitochondrial mass, ratiometric approaches yield a “unit  $\Delta\Psi_{\mu}$ ,” which can be useful in resolving the apoptotic population, particularly when loss of mitochondrial function is offset by mitochondrial proliferation. Although these

dyes are useful  $\Delta\Psi_{\mu}$ -sensitive probes in living cells, other factors can theoretically alter the fluorescent intensities of these dyes (21) and care should be used both in selecting dyes (especially in multiple dye combinations) and in utilizing appropriate controls.

One mechanism, albeit not the only one, by which mitochondria can undergo a loss in  $\Delta\Psi_{\mu}$  during apoptosis is via an opening of the mitochondrial permeability transition (MPT or PT) pore, a high-conductance channel, allowing nonselective diffusion of small molecules ( $\leq 1.5$  kD) across the inner membrane (22,22a). Although the exact structure and role of this channel in normal physiology remains to be clarified (23), sustained pore opening results in dissipation of the  $H^+$  gradient, uncoupling respiration, large-amplitude swelling of mitochondria and appears to be associated with the release of apoptogenic mitochondrial proteins like cytochrome c. Opening of the pore can be inhibited by a number of compounds including cyclosporin A and bongkrekic acid (24). Low molecular-weight hydrophilic dyes such as calcein are normally excluded from the inner mitochondrial space, but will pass through the opened pore (25). Redistribution of calcein to the inner mitochondrial space, which is blocked by cyclosporin A or other inhibitors of the MPT, appears to represent a true pore-opening event. Bcl 2 family members are thought to exert their pro- or antiapoptotic effects, in part, by interacting with and modulating pore opening (26). In particular, translocation of cytoplasmic BAX to the mitochondrial membrane has been shown to be a key initiating step in apoptosis (27). BAX translocation has been evaluated with confocal microscopy both with immunofluorescence (28) and with expression of BAX-GFP fusion proteins (29,30).

Loss of cytochrome c from the mitochondria and redistribution to the cytoplasm has been shown in many settings to be a key event in initiating apoptosis through activating cytoplasmic caspase cascades and may result from the opening of the PT-pore or in the absence of any evidence of pore opening. Similar to the case with BAX localization, immunohistochemistry/immunofluorescence (31) and cytochrome C-GFP fusion proteins (32) have been employed to assess cytochrome c release from mitochondria. Whereas BAX translocation results in diffuse cytoplasmic fluorescence becoming punctate mitochondrial fluorescence, cytochrome c translocation shows the reverse pattern.

From the aforementioned description of mitochondrial physiology and the MPT, it is clear that pore opening and dissipation of the proton gradient will result in relative alkalization of the inner mitochondrial space and acidification of the cytoplasm. Fluorescence-based assays to detect altered cellular pH and their use in apoptosis will be addressed below, as will alterations in intracellular calcium concentrations. Similarly, although the mitochondrial electron-transport chain is an important source of reactive oxygen

species (ROS) in the cell, discussion of methods to detect apoptosis-associated oxidative stress will be deferred to the following section on cytoplasmic alterations in apoptosis.

Cardiolipin is an important component of the mitochondrial inner membrane. It is a diacidic phospholipid synthesized in the mitochondria and reported to be essential as an important structural component modulating the function of numerous mitochondrial proteins, including cytochrome c and the MPT (33). Recently, cardiolipin has been shown to mediate mitochondrial targeting of caspase 8-cleaved BID to mitochondria in apoptosis (34). Nonyl acridine orange is a fluorescent dye with a high affinity for cardiolipin. When single molecules of NAO are excited (488 nm), they emit yellow-green fluorescence. However, Petit et al. (35) have shown that 2 molecules of NAO bind 1 molecule of cardiolipin with resultant red fluorescence, presumably due to excimer formation. Red NAO fluorescence, as a consequence of the diacidic structure of cardiolipin, has proven to be more specific for cardiolipin than its green fluorescence. NAO fluorescence has been shown to decrease in cells treated with menadione, a mitochondrial redox cycling compound that produces mitochondrial ROS (36). During tumor necrosis factor (TNF)-induced apoptosis in hepatocytes, loss of red NAO fluorescence was shown to occur and to be blocked by antioxidant treatment, thought to reflect oxidative stress-induced catabolism of cardiolipin (37). In the past, NAO fluorescence has been used to measure mitochondrial mass because its fluorescence is  $\Delta\Psi_m$ -insensitive (a feature recently called into question (38)), but given this dye's sensitivity as a measure of cardiolipin loss, its utility as a measure of mitochondrial mass must be restricted.

### 1.3. Cytoplasmic Alterations in Apoptosis

#### 1.3.1. Intracellular Acidification

Cytoplasmic acidification has been shown to be an important feature in apoptotic cells and may be necessary for optimal activation of caspases and execution of the apoptotic pathway. In some systems, concurrent alkalinization of mitochondria is identified, suggesting PT-opening with diffusion of protons into the cytoplasm (18). On the other hand, in somatostatin-induced apoptosis of MCF-7 cells, a nonmitochondrial source of  $H^+$  was implicated in the development of caspase 8-independent cytoplasmic acidification and this acidification was shown to be necessary for the induction of mitochondrial alterations (39). SNARF-1 is the dye most commonly employed in cells to assess alterations in pH in the near-physiologic range (7.0–8.0). It can be excited by the 488 nm line of the argon ion laser and the

acetoxymethyl ester of carboxy SNARF-1 is readily loaded into cells. The emission peak of SNARF-1 shifts from yellow-orange (measured at ~580 nm) in an acidic milieu to deep red (measured at ~640 nm) in a basic one, allowing for sensitive ratiometric analysis of intracellular pH. Tsien and coworkers recently developed a GFP-based ratiometric method of assessing pH that exploits differential pH sensitivity of genetically engineered spectrally altered GFP variants (“cyan” GFP vs “yellow” GFP) (40). Although initially employed to assess mitochondrial pH, by altering the leader sequence these GFP reagents can be targeted to other organelles as well.

#### **1.4. Intracellular Redox Status**

Apoptosis has been correlated with a variety of changes in cellular redox status including loss of glutathione (41), total cellular thiols, and reduced NAD species (22,42,43). In rodent cells, monochlorobimane fluorescence (ex = 340 nm; em = 480 nm) is a good glutathione-S-transferase substrate and has been shown to be proportional to intracellular GSH concentrations (44). Monobromobimane fluorescence, on the other hand, is proportional to total intracellular thiol concentration. Oxidative stress as measured by loss of these thiol-reactive fluorochromes have been associated with apoptosis in a variety of experimental settings. UV-excited blue autofluorescence (ex = 340 nm; em = 480 nm) has been shown to result from reduced NAD (i.e., NADPH and NADH) (45) and loss of blue autofluorescence can be a useful marker of apoptosis-induced oxidative stress (37). Because some cells have significant levels of NAD(P)H and resultant UV-excited blue autofluorescence, care should be taken to assess the contribution of autofluorescence when utilizing other UV-excited blue fluorochromes such as monochloro- and monobromobimane.

Other measures of apoptosis-induced oxidative stress include a variety of fluorochromes that react either directly with ROS to change from a reduced nonfluorescent or low fluorescence state to a highly fluorescent one or vice versa. Among the most commonly used reduced, nonfluorescent probes are: dichlorofluorescein diacetate (DCFDA), dihydrorhodamine 123, hydroethidine, and reduced CMXRosamine. Interestingly, because of its lipophilic cationic structure, reduced CMXRosamine selectively accumulates in mitochondrial membranes and appears to be sensitive to the activity of electron transport. Less commonly used are dyes that lose fluorescence upon reaction with ROS. *cis*-Parinaric acid has been found to be useful, although it requires an excitation source (ex = 325 nm), which is uncommon. Fluorescein has been shown to be quenched upon reacting with ROS and by using a highly lipophilic fluorescein conjugate (C11-fluor), an assay specific for lipid peroxidation was reported (46).

This same group has also used BODIPY-conjugated lipids and fluoresceinated phosphoethanolamine for similar studies (47,48). As discussed earlier, loss of NAO fluorescence can reflect oxidative stress-induced cardiolipin loss, which is often associated with apoptosis.

### **1.5. Alterations in Free Intracellular Calcium Concentration $[Ca^{2+}]_i$**

Increased  $[Ca^{2+}]_i$  has been implicated as an important regulator of cell death both in apoptosis and necrosis. Studies using pharmacologic inhibitors of specific calcium channels indicate that the source of the free calcium varies with the specific experimental model and can include both an increased influx from the extracellular environment or release from internal stores, which are usually sequestered in the endoplasmic reticulum. A number of calcium-dependent fluorochromes are available that serve as useful tools to measure  $[Ca^{2+}]_i$  including Fura-2, Indo-1, Fluo-3, Fluo-4, Fura-red, Rhod-2, and their derivatives (20). In addition to these dyes, investigators have utilized aequorin, a calcium-sensitive bioluminescent protein to measure alterations in  $Ca^{2+}$  concentrations (49). In a fashion analogous to the GFP-based studies of mitochondrial pH, aequorin can be selectively targeted to mitochondria or other organelles by utilizing the appropriate leader sequence.

Many of these dyes and their applications have been reviewed in detail elsewhere (50). Of note, probes are available for both UV and 488 nm excitation and many of these calcium probes (Fura-1, Indo-1, Calcium Green-2) have the advantage of utilizing a ratiometric fluorescence read-out. These dyes have been successfully used in multiparametric analyses, using both flow cytometry and confocal microscopy, which has led to an enhanced understanding of the role of  $[Ca^{2+}]_i$  in apoptosis. Burchiel et al. (51) have recently published a review of multiparametric flow cytometric  $Ca^{2+}$  analysis.

Because flow cytometry measures total cellular fluorescence, most flow cytometric methods of assessing total  $[Ca^{2+}]_i$  may not be sensitive to apoptosis-induced redistribution of  $[Ca^{2+}]_i$ . In 32D cells induced to undergo apoptosis through interleukin-3 (IL-3) withdrawal, total  $[Ca^{2+}]_i$  remained unaltered, although a significant subcellular redistribution of  $Ca^{2+}$  from the cytoplasm to the mitochondria occurred, which could be inhibited by Bcl-2 expression (52). Some  $Ca^{2+}$ -sensitive fluorochromes (Rhod-2 and derivatives) are reported to selectively partition into mitochondria and may be capable of detecting a local change in mitochondrial calcium. Fluorescence microscopy can determine the specific subcellular compartment in which an alteration of  $[Ca^{2+}]_i$  takes place through co-localization of calcium probe fluorescence with the appropriate organelle-specific markers.

### 1.6. Caspase Activation

Recognition of the importance of caspase activation in apoptosis has led to the development of fluorescence caspase substrates that indicate caspase activation. These substrates usually contain peptides that represent the preferred consensus amino acid sequence for a particular caspase. Two methods are generally employed. In the first, a fluorescent dye (usually rhodamine 110) is linked to a peptide substrate; caspase cleavage results in the release of the fluorescent dye resulting in an increase in fluorescence intensity (53–57). The second approach assesses the degree to which fluorescence resonance energy transfer (FRET) occurs between two dye molecules attached to the same peptide substrate (58,59). In the intact state, one dye molecule is excited by the incident light, but instead of emitting a photon, it instead transfers energy to a second dye whose excitation maximum is near that of the emission maximum of the first dye molecule. This second dye molecule then emits a lower-energy (longer-wavelength) photon. With caspase cleavage, the two fluorescent dye molecules are no longer within the distance required for FRET, and instead the first dye molecule now emits a photon. Thus, by examining the ratio of fluorescence emission of the first and second dye molecule, one can gauge the amount of caspase cleavage of the target substrate.

### 1.7. Cytoskeletal Alterations

Several assays are available that detect apoptosis-associated alterations in cytoskeletal components. Studies have characterized actin cytoskeletal reorganization consisting of early transient polymerization, and later depolymerization in a variety of different models of apoptosis (60–62). The most widely used technique for visualization of these changes involves fluorescent microscopy with FITC-labeled phalloidin, which binds F-actin with high affinity. These changes result in punctate staining indicating disorganization of the actin cytoskeleton (60), or overall decreased fluorescence amenable to detection by both fluorescence microscopy and flow cytometry (63).

Intermediate filaments have been shown to be caspase cleavage targets, including cytokeratin 18, which is cleaved principally by activated caspase 3. M30 (Boehringer-Mannheim), an antibody that specifically recognizes the cleaved fragment of cytokeratin 18, has been utilized in both immunofluorescence and flow cytometric analysis to demonstrate caspase activity (64,65).

### **1.8. Cytoplasmic Membrane Alterations in Apoptosis**

Annexin V has also been used to reveal apoptotic cells by both flow and laser cytometry (66,67). This technique takes advantage of the observation that phosphatidyl serine (PS) is transposed to the outer leaflet of the plasma membrane in apoptotic cells (68), and that this can be visualized by staining with Annexin V, which has an affinity for negatively charged phospholipids such as phosphatidylserine (PS). This technique has been used mostly for *in vitro* assays of apoptosis, but it can be used in settings that require demonstration of apoptosis *in vivo* as well. For instance, van Heerde et al. (69) have shown that injection of biotinylated Annexin V, can be useful in identifying cells in the heart that are undergoing apoptosis subsequent to ischemia/reperfusion injury. Advantages to using annexin V are that it can be used on live cells, and that it can be a relatively early event associated with the execution phase of apoptosis (66). Disadvantages to using annexin V are that some cell types (e.g., platelets, syncytiotrophoblasts) naturally express high levels of PS on their outer leaflet (reviewed in ref. 70).

Merocyanine 540 is a red-emitting fluorescent dye that appears to be a sensitive measure of apoptosis-induced alterations in cytoplasmic membrane lipid structure (68). In apoptotic cells, the fluorescence increases; in some models increased fluorescence correlates well with increased annexin V binding (68,71). Merocyanine 540 staining has been successfully used together with Hoechst 33342 to identify cell-cycle specific apoptotic events (72).

Loss of cytoplasmic membrane function occurs early in necrosis and late in apoptosis (so-called “apoptotic necrosis”). If, in a given experimental system, the mode of death has been adequately characterized morphologically and the assay timepoint judiciously chosen, loss of dye exclusion can serve as a useful, easy to quantify measure of cell death in either apoptotic or necrotic model systems. Commonly used dyes for this type of analysis include propidium iodide, 7-AAD, Sytox green, and ethidium homodimer.

### **1.9. Plate Reader Assays**

Since all the assays outlined previously involve an increase or a decrease in fluorescence emission, it should be possible to perform these assays with multiwell fluorescence plate readers. The key advantage of this format is that it allows analysis of large numbers of samples in a short time period, making the fluorescence plate reader platform an ideal format for high-throughput assays. A disadvantage of fluorescence plate reader assays is that the response measured is the average of all responding or not respond-



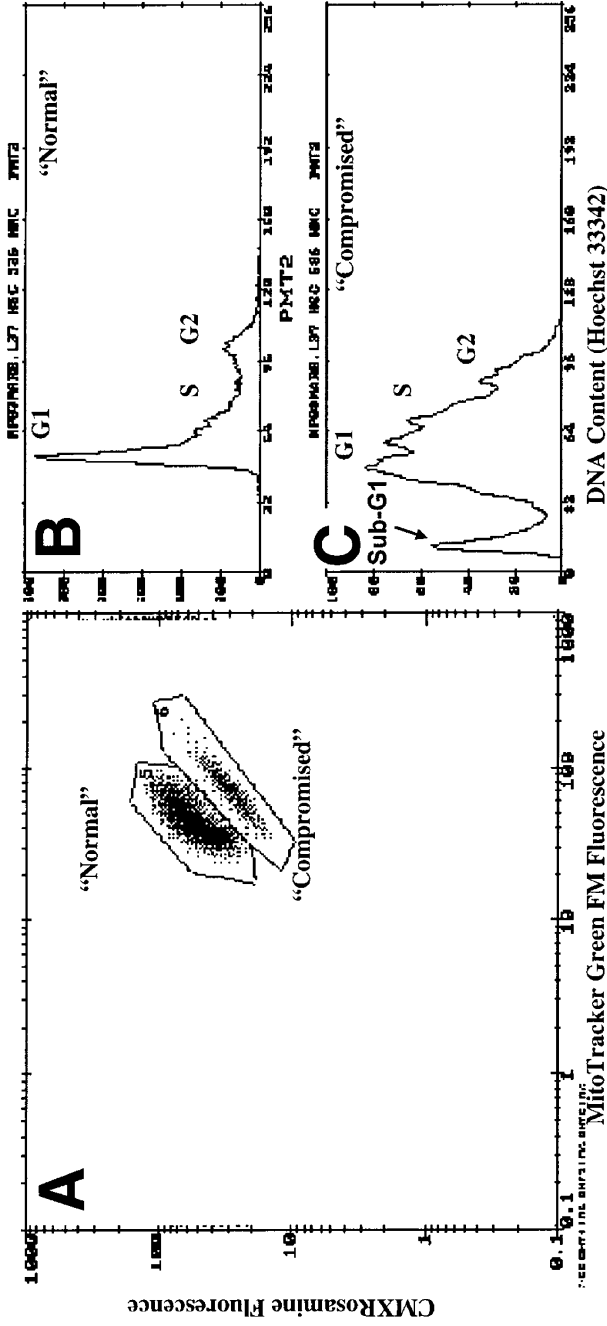


Fig. 1. Cytogram of MitoTracker Green FM and CMXRosamine fluorescence (A) and cell-cycle histograms of "normal" (B) and "compromised" (C) cells from a culture of human lymphoblastoid cells that were treated with 1 mg/mL mitomycin C for 8 h at 37°C, harvested and stained according to Protocol 1. Apoptotic cells show a lower CMXRosamine and a higher MitoTracker Green FM fluorescence (A). The two right hand panels show the cell-cycle distributions, based on Hoechst 33342 fluorescence, of the "normal" and "compromised" cells.

ing cells in the sample. In cases where only a small subset of cells respond or when the magnitude of the response in each cell is small, little or no response may be detected. This severely limits the sensitivity, and thus the applicability, of fluorescence plate reader assays in apoptosis research.

## 2. FUTURE DEVELOPMENTS

Advances in instrumentation, particularly the advent of multiphoton excitation confocal microscopy, has opened up many possibilities including better imaging of living cells and tissues, decreased photobleaching, and increased resolution of fluorescent signals (73). New and improved dyes will likely be manufactured, including photoactivatable fluorochromes (20) (so called “caged probes”). The uses and limitations of currently available dyes will be better understood. Some investigators have already employed advanced techniques such as FRET (59), fluorescent anisotropy (74–76), fluorescence correlation spectroscopy (77–79), and fluorescence lifetime imaging microscopy (80,81) to investigate cell structure and function. The utilization of these powerful methods will undoubtedly contribute to the study of apoptosis in the future.

### 2.1. Examples of Flow Cytometric Detection of Apoptosis

Figure 1 shows a typical result of cells stained with Hoechst 33342 (blue emitting DNA dye), MitoTracker Green FM (green emitting; proportional to mitochondrial mass), and CMXRosamine (red emitting; proportional to mitochondrial membrane potential) and analyzed by flow cytometry. By simultaneous staining with MitoTracker Green FM and CMXRosamine, an enhanced resolution between cells with “normal” and with “compromised” mitochondrial membrane potential is obtained (43). This condition of compromised mitochondrial membrane potential generally correlates with an early stage of apoptosis (82,83). The experiment shown in Fig. 1 allows direct investigation of this correlation. Cells with compromised and normal mitochondrial membrane potential are identified by electronic gating. Their respective DNA profiles, based on Hoechst 33342 fluorescence, are displayed in the panels on the right hand side of the figure. Cells with normal MitoTracker Green FM and CMXRosamine fluorescence (Panel B) show a regular distribution among the G1, S, and G2 compartments of the cell cycle. Cells with compromised MitoTracker Green FM and CMXRosamine fluorescence, in contrast, show cells with G1, S, G2, and Sub-G1 DNA content (Panel C). Sub-G1 DNA content is evidence of apoptosis (*see above*). A protocol for this assay is detailed in Subheading 3.

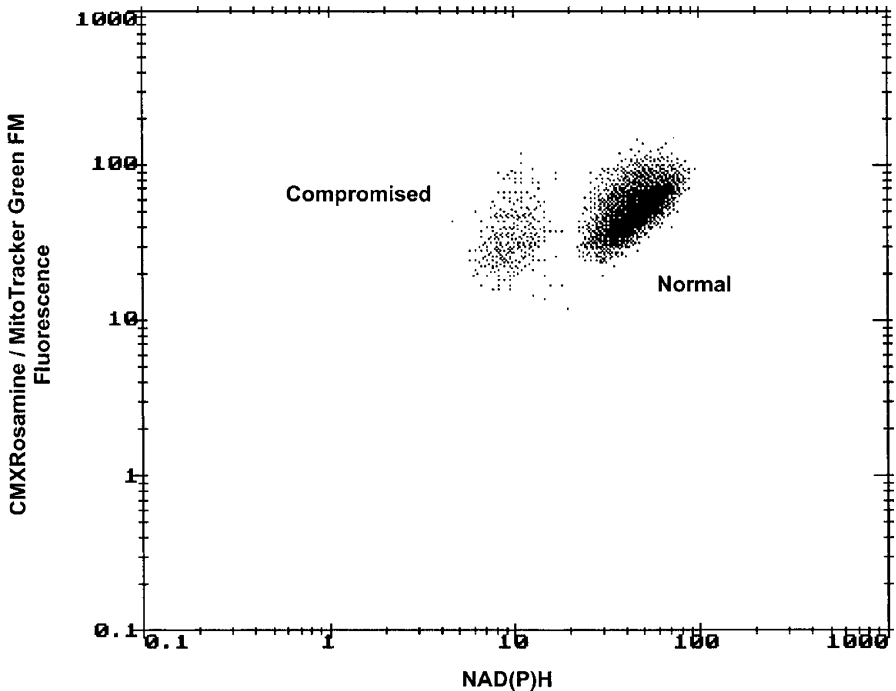


Fig. 2. Cytogram of a combined assay for NAD(P)H levels (UV-excited blue autofluorescence) and mitochondrial membrane potential (CMXRosamine/MitoTracker Green FM fluorescence). Signals representing “normal” and “compromised” cells are labeled.

Since “normal” and “compromised” cells can be distinguished after staining with MitoTracker Green FM and CMXRosamine, the blue region of the visible spectrum is still available for analysis of an additional biochemical parameters. Two parameters that can be readily quantitated are NAD(P)H and thiol content. Blue autofluorescence of cells excited with UV-light (around 360 nm) reflects cellular NAD(P)H levels (45) and as shown in Fig. 2, can easily be quantified by flow cytometry (43). Cellular reduced thiol levels can be quantified by staining with monobromobimane (84). It should be noted, however, that the blue fluorescence generated in proportion to reduced thiol levels covers the same wavelength region as does NAD(P)H, which is relatively weak compared to monobromobimane fluorescence. As a result, the blue fluorescence corresponding to cellular NAD(P)H levels can be a source of background fluorescence in thiol analyses. Therefore, when assaying for cellular reduced thiol levels it is necessary to split all

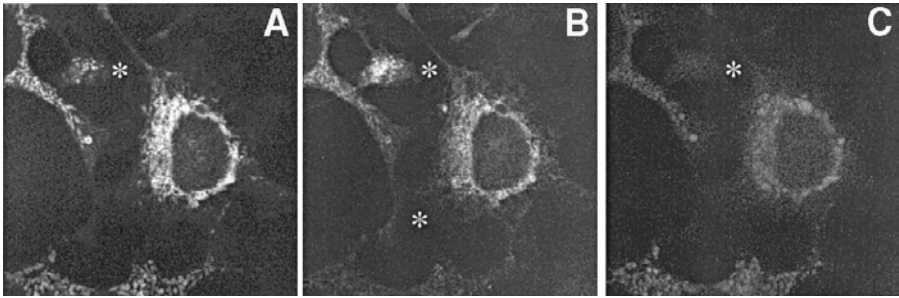


Fig. 3. Confocal laser scanning microscope images obtained on Hepa-1 cells exposed to tumor necrosis factor- $\alpha$  (TNF- $\alpha$ ) and actinomycin D to induce apoptosis. Hepa-1 mouse hepatoma cells were treated with TNF- $\alpha$ /ActD, 12 h later stained with CMX Rosamine and Mitotracker Green, and then analyzed by CLSM. (A) shows light collected with a 605 nm long pass (red) filter (showing CMX Rosamine fluorescence), (B) shows light collected with a 530/30 nm band pass (green) filter (showing Mitotracker Green fluorescence), and (C) shows light collected with a 460/40 nm band pass (blue) filter (showing NAD(P)H autofluorescence). In an apoptotic cell (adjacent to \*), both CMX rosamine and NAD(P)H fluorescence are dramatically reduced. Conversely, MTG fluorescence is significantly enhanced in this same cell.

samples and to use the fluorescence from an “unstained” (NADP(P)H) control for quantification (84). A protocol for measuring these parameters in conjunction with mitochondrial membrane potential is given in Subheading 4.

## 2.2. Examples of Detection of Apoptosis with a Confocal Microscope

As with flow cytometry, multiparameter apoptosis assays may also be performed by confocal laser scanning microscopy (CLSM). Using the approach similar to that detailed above for flow cytometry, we have examined NADPH content, mitochondrial membrane potential (CMX Rosamine fluorescence), and mitochondrial mass (Mitotracker Green), by CLSM. Figure 3 shows an example of a typical multiparameter assay performed by confocal microscopy.

One advantage to examining apoptotic cells by laser-scanning cytometry is that subcellular structure may be examined. For instance, individual mitochondria may be examined for correlations among different parameters. Similarly, nuclear structure may also be examined in apoptotic cells. An example of the complementarity of flow cytometry and CLSM is given in Fig. 4. TNF- $\alpha$ /ActD treated Hepa-1 cells were stained with CMX Rosamine

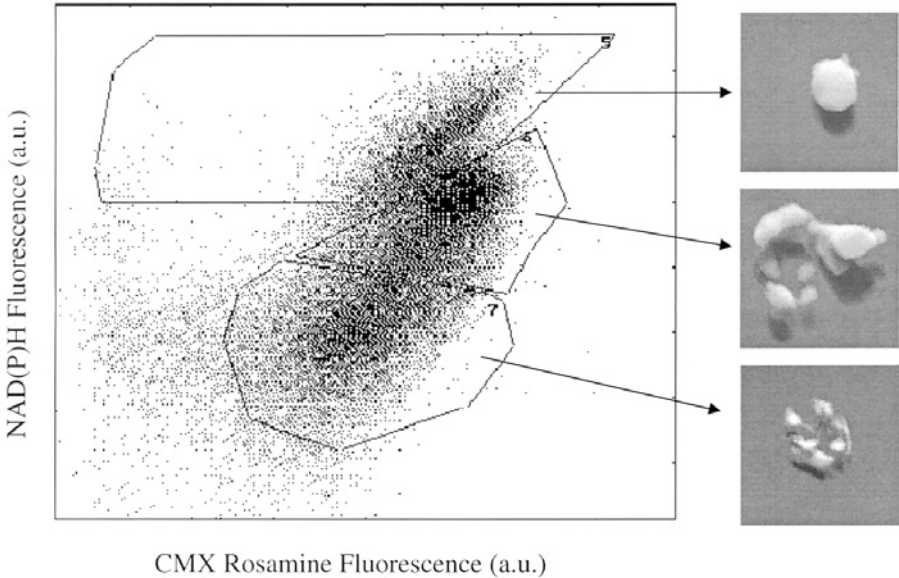


Fig. 4. Combined use of flow cytometry/cell sorting and confocal laser scanning microscopy. TNF- $\alpha$ /ActD treated Hepa-1 cells were stained with CMX Rosamine and then analyzed for mitochondrial membrane potential and NAD(P)H fluorescence (**A**). Cells in different regions of the cytogram were then sorted, and subsequently stained with the DNA fluorochrome Hoechst 33342. These cells were then examined by CLSM. (**B**), (**C**), and (**D**) show three-dimensional reconstructions of nuclei from cells sorted from healthy, early apoptotic, and late apoptotic populations. Whereas healthy cells show normal round nuclei, early and late apoptotic cells show progressive chromatin condensation/margination and nuclear fragmentation.

and then analyzed for mitochondrial membrane potential and NAD(P)H fluorescence (panel A). Cells in different regions of the cytogram were then sorted, and subsequently stained with the DNA fluorochrome Hoechst 33342. These cells were then examined by CLSM. Panels B, C, and D show three-dimensional reconstructions of nuclei from cells sorted from healthy, early apoptotic, and late apoptotic populations. Whereas healthy cells show normal round nuclei, early and late apoptotic cells show progressive chromatin condensation/margination and nuclear fragmentation.

### **2.3. Example Protocols for Measuring Apoptosis by Flow Cytometry**

As indicated earlier, there are many different parameters that can be used to measure apoptosis by flow cytometry. We have chosen two assays of

apoptosis that are readily performed on many cell types, and detailed protocols for carrying them out are given below. Researchers without significant flow cytometry experience are encouraged to contact their institutional flow cytometry centers for specific details of laser tuning and filter sets required for the particular instrumentation available in their centers.

### 3. PROTOCOL 1: ASSAY FOR CELL-CYCLE STAGE SPECIFIC APOPTOSIS

In this protocol the UV excited blue fluorescence of Hoechst 33342 dye, which resolves cells according to the G1, S, and G2 stage of the cell cycle, is combined with the green and red fluorescence of MitoTracker Green FM and CMXRosamine.

#### 3.1. Materials

1. Cells in suspension.
2. Cell-culture medium supplemented with 10% fetal bovine serum (FBS).
3. Dimethyl sulfoxide (DMSO; Sigma).
4. Stock solutions of MitoTracker Green FM<sup>TM</sup> (200  $\mu$ M in DMSO) and CMXRosamine (200  $\mu$ M in DMSO); store at  $-20^{\circ}\text{C}$  in the dark.
5. Stock solution of Hoechst 33342 dye (1 mM in double distilled water; store at  $4^{\circ}\text{C}$  in the dark; do not freeze) (*see* Note 1).
6. 15 mL Screw-capped centrifuge tubes.
7.  $2 \times 75$  mm Polypropylene tubes.
8.  $37^{\circ}\text{C}$  Water bath with cover (or a sheet of aluminum foil).
9. Flow cytometer with either a mercury arc lamp or two argon lasers (one tuned to ultraviolet and the other to 488 nm) as excitation sources.
10. Computer for data collection and processing.

#### 3.2. Procedure

1. Harvest cultured cells by standard procedures and place in 15 mL screw-capped centrifuge tubes. Centrifuge for 5 min at 200g at room temperature. Resuspend the cell pellet at  $0.5\text{--}1.0 \times 10^6$  cells mL in prewarmed  $37^{\circ}\text{C}$  cell-culture medium. Leave cell suspensions in the water bath at  $37^{\circ}\text{C}$  for at least 5 min (*see* Note 2).
2. Thaw out dye solutions at room temperature, keeping them protected from light (e.g., in a drawer) (*see* Note 3).
3. Aliquot cell suspensions into  $12 \times 75$  mm polypropylene tubes. Add 20  $\mu$ L of 1  $\mu$ M Hoechst 33342 and 1  $\mu$ L each of 200  $\mu$ M MitoTracker Green FM and CMXRosamine dye stock solutions into 1 mL of prewarmed cell suspension. Mix immediately by briefly vortexing at maximal speed. Incubate for 30 min. at  $37^{\circ}\text{C}$  in the dark or at subdued light. After staining, place tubes with cell suspensions in a melting ice bath (*see* Note 4).

4. Set up and optimize the flow cytometer as in Basic Protocol 1. UV-excited (360 nm) blue fluorescence (collected with a 450 nm centered bandpass filter) from the Hoechst 33342 dye is proportional with cellular DNA content. To excite MitoTracker Green FM and CMXRosamine stained samples, the argon-ion laser should be tuned to the 488 nm line. To collect fluorescence from MitoTracker Green FM, use a bandpass filter centered around 530 nm; for CMXRos use a longpass filter above 630 nm (*see* Notes 5–8).

## 4. PROTOCOL 2: COMBINED ASSAY FOR REDUCED THIOL AND NAD(P)H LEVELS AND MITOCHONDRIAL MEMBRANE POTENTIAL

This protocol takes advantage of the fact that NAD(P)H emits blue fluorescence upon excitation with UV light. NAD(P)H fluorescence can thus be simultaneously measured with the green and red fluorescence of MitoTracker Green FM and CMXRosamine, respectively. The combination of MitoTracker Green FM and CMXRosamine allows one to better resolve apoptotic cells than does staining with CMXRosamine alone.

### 4.1. Materials

1. Cells in suspension.
2. Cell-culture medium supplemented with 10% FBS.
3. DMSO (Sigma).
4. Stock solutions of MitoTracker Green FM<sup>TM</sup> (200  $\mu$ M in DMSO) and CMXRosamine (200  $\mu$ M in DMSO); store at  $-20^{\circ}\text{C}$  in the dark.
5. Stock solution of monobromobimane (10  $\mu$ M in absolute ethanol).
6. 15 mL Screw-capped centrifuge tubes.
7. 12  $\times$  75 mm Polypropylene tubes.
8. 37 $^{\circ}\text{C}$  Water bath with cover (or a sheet of aluminum foil).
9. Flow cytometer with either a mercury arc lamp or two argon lasers (one tuned to UV and the other to 488 nm) as excitation sources.
10. Computer for data collection and processing.

### 4.2. Procedure

1. Harvest cultured cells by standard procedures in 15 mL screw-capped centrifuge tubes and centrifuge for 5 min at 200g at room temperature. Resuspend the cell pellet at  $0.5\text{--}1.0 \times 10^6$  cells/mL in prewarmed cell-culture medium. Leave cell suspensions in water bath at 37 $^{\circ}\text{C}$  for at least 5 min (*see* Note 9).
2. Thaw out dye solutions at room temperature, keeping them protected from light (e.g., in a drawer) (*see* Note 10).
3. Aliquot cell suspensions into 12  $\times$  75 mm polypropylene tubes such that for each sample two replicate tubes are obtained. Add 1  $\mu$ L of each of the 200  $\mu$ M MitoTracker Green FM and CMXRosamine dye stock solutions to each tube with 1 mL of prewarmed cell suspension. Add 5  $\mu$ L of monobromobimane stock

solution to half of the samples. Mix immediately by briefly vortexing at maximal speed. Incubate for 30 min. at 37°C in the dark or at subdued light. After staining, put tubes with cell suspensions in a melting ice bath (*see* Note 11).

4. Set up and optimize the flow cytometer. UV-excited (360 nm) blue autofluorescence (collected with a 450 nm centered bandpass filter) is proportional with cellular NAD(P)H and to cellular reduced thiol content (in the samples stained with monobromobimane). To excite MitoTracker Green FM and CMXRosamine stained samples, the argon-ion laser should be tuned to the 488 nm line. To collect fluorescence from MitoTracker Green FM use a bandpass filter centered around 530 nm; for CMXRos use a longpass filter above 630 nm. Due to the wide variation in cellular contents of mitochondria, it is advisable to use logarithmic signal amplification for the signal channels collecting mitochondria-related fluorescence. Carefully resuspend the cell sample by gently pipetting up and down a few times immediately before analysis (*see* Note 12).

## 5. NOTES

1. Do not use phosphate-containing buffers, since Hoechst dyes precipitate in the presence of phosphates.
2. Because the functional state of the mitochondria is to be monitored, it is advisable to keep cell suspensions at their optimal temperature (37°C) and to allow them to recover for a brief moment after harvesting.
3. Dye solutions decompose rapidly if exposed to room light.
4. MitoTracker Green FM and CMXRosamine dye concentrations in the range of 100–200 nM are recommended, because at higher concentrations nonmitochondrial staining may occur. A Hoechst 33342 dye concentration of 20 μM to saturate cellular DNA is recommended. Some cell types may have multidrug resistance-like membrane resident dye pumping mechanisms, which will lower the actual dye concentration inside the cell. When using a novel cell type, it may be useful to titrate the Hoechst 33342 dye concentration to determine optimal staining conditions.
5. Due to the wide variation in cellular contents of mitochondria, it is advisable to use logarithmic signal amplification for the signal channels collecting mitochondria-related fluorescence. Carefully resuspend the cell sample by gently pipetting up and down a few times immediately before analysis.
6. All protocols described have been performed on cultured animal cells; limited data exist regarding the use of these methods for plant cells and in yeast.
7. *Caution:* DMSO and dyes solutions are potentially toxic to humans. Use (nitrile) gloves and wear eye protection at all stages of handling. Seek medical advice if dye or dye solutions are ingested or inhaled. The dyes mentioned are for in vitro use only; do not administer either externally or internally.
8. Disposal: All staining solutions should be poured through a funnel with a filter containing activated charcoal in a fume hood. When the passing solution becomes fluorescent, the filter should be incinerated or disposed of according to applicable rules for environmental hygiene, and a fresh filter should be installed.



9. Since the functional state of the mitochondria is to be monitored, it is advisable to keep cell suspensions at their optimal temperature (37°C) and to allow them to recover for a brief moment after harvesting.
10. Dye solutions decompose rapidly if exposed to light.
11. Dye concentrations in the range of 100–200 nM are recommended, because at higher concentrations nonmitochondrial staining may occur.
12. Cells stained with MitoTracker Green FM show maximal emission at 516 nm; cells stained with CMXRosamine show maximal absorption at 594 nm and emit maximally at 608 nm; they also exhibit significant absorption in the UV region of the spectrum and may be excitable with a mercury arc lamp. During the staining period cells tend to clump; to obtain meaningful data on a per cell-basis, it is essential to resuspend cells by briefly and gently vortexing immediately before analysis.

## REFERENCES

1. Levin, S. (1998) Apoptosis, necrosis, or oncosis: what is your diagnosis? A report from the Cell Death Nomenclature Committee of the Society of Toxicologic Pathologists. *Toxicol. Sci.* **41(2)**, 155–156.
2. Portera-Cailliau, C, Price, D. L., and Martin, L. J. (1997) Non-NMDA and NMDA receptor-mediated excitotoxic neuronal deaths in adult brain are morphologically distinct: further evidence for an apoptosis-necrosis continuum. *J. Comp. Neurol.* **378(1)**, 88–104.
3. Lemasters, J. J. (1999) V. Necrapoptosis and the mitochondrial permeability transition: shared pathways to necrosis and apoptosis. *Am. J. Physiol.* **276(1 Pt 1)**, G1–G6.
4. Warny, M. and Kelly, C. P. (1999) Monocytic cell necrosis is mediated by potassium depletion and caspase-like proteases. *Am. J. Physiol.* **276(3 Pt 1)**, C717–C724.
5. Raffray, M. and Cohen, G. M. (1997) Apoptosis and necrosis in toxicology: a continuum or distinct modes of cell death? *Pharmacol. Ther.* **75(3)**, 153–177.
6. Cotran, R. S., Kumar, V., Collins, T., and Robbins, S. L. (1999) *Robbin's Pathological Basis of Disease*. W. B. Saunders, Philadelphia.
7. Green, D., and Kroemer, G. (1998) The central executioners of apoptosis: caspases or mitochondria? *Trends Cell Biol.* **8(7)**: 267–271.
8. Green, D. R. and Reed, J. C. (1998) Mitochondria and apoptosis. *Science* **281(5381)**, 1309–1312.
9. Afanas'ev, V. N., Korol, B. A., Mantsygin Yu, A., Nelipovich, P. A., Pechatnikov, V. A., and Umansky, S. R. (1986) Flow cytometry and biochemical analysis of DNA degradation characteristic of two types of cell death. *FEBS Lett.* **194(2)**, 347–350.
10. Telford, W. G., King, L. E., and Fraker, P. J. (1992) Comparative evaluation of several DNA binding dyes in the detection of apoptosis-associated chromatin degradation by flow cytometry. *Cytometry* **13(2)**, 137–143.

11. Gong, J., Traganos, F., and Darzynkiewicz, Z. (1994) A selective procedure for DNA extraction from apoptotic cells applicable for gel electrophoresis and flow cytometry. *Anal. Biochem.* **218(2)**, 314–319.
12. Darzynkiewicz, Z., Juan, G., Li, X., Gorczyca, W., Murakami, T., and Traganos, F. (1997) Cytometry in cell necrobiology: analysis of apoptosis and accidental cell death (necrosis). *Cytometry* **27(1)**, 1–20.
13. Hotz, M. A., Gong, J., Traganos, F., and Darzynkiewicz, Z. (1994) Flow cytometric detection of apoptosis: comparison of the assays of in situ DNA degradation and chromatin changes. *Cytometry* **15(3)**, 237–244.
14. Gorczyca, W., Gong, J., Ardelt, B., Traganos, F., and Darzynkiewicz, Z. (1993) The cell cycle related differences in susceptibility of HL-60 cells to apoptosis induced by various antitumor agents. *Cancer Res.* **53(13)**, 3186–3192.
15. Jacotot, E., Costantini, P., Laboureaux, E., Zamzami, N., Susin, S. A., and Kroemer, G. (1999) Mitochondrial membrane permeabilization during the apoptotic process. *Ann. NY Acad. Sci.* **887**, 18–30.
16. Mancini, M., Anderson, B. O., Caldwell, E., Sedghinasab, M., Paty, P. B., and Hockenbery, D. M. (1997) Mitochondrial proliferation and paradoxical membrane depolarization during terminal differentiation and apoptosis in a human colon carcinoma cell line. *J. Cell Biol.* **138(2)**, 449–469.
17. Gross, A., Jockel, J., Wei, M. C., and Korsmeyer, S. J. (1998) Enforced dimerization of BAX results in its translocation, mitochondrial dysfunction and apoptosis. *EMBO J.* **17(14)**, 3878–3885.
18. Matsuyama, S., Llopis, J., Deveraux, Q. L., Tsien, R. Y., and Reed, J. C. (2000) Changes in intramitochondrial and cytosolic pH: early events that modulate caspase activation during apoptosis. *Nat. Cell Biol.* **2(6)**, 318–325.
19. Saraste, M. (1999). Oxidative phosphorylation at the fin de siècle. *Science* **283(5407)**, 1488–1493.
20. Haugland, R. (1999) *Handbook of Fluorescent Probes and Research Chemicals*. Molecular Probes, Inc., Eugene, OR.
21. Poot, M. and Pierce, R. H. (1999) Detection of changes in mitochondrial function during apoptosis by simultaneous staining with multiple fluorescent dyes and correlated multiparameter flow cytometry. *Cytometry* **35(4)**: 311–317.
22. Lemasters, J. J., Qian, T., Bradham, C. A., Brenner, D. A., Cascio, W. E., Trost, L. C., et al. (1999) Mitochondrial dysfunction in the pathogenesis of necrotic and apoptotic cell death. *J. Bioenerg. Biomembr.* **31(4)**: 305–319.
- 22a. Lemasters, J. J., Qian, T., Trost, L. C., Herman, B., Cascio, W. E., Bradham, C. A. (1999) Confocal microscopy of the mitochondrial permeability transition in necrotic and apoptotic cell death. *Biochem. Soc. Symp.* **66**, 205–222.
23. Halestrap, A. P. (1999) The mitochondrial permeability transition: its molecular mechanism and role in reperfusion injury. *Biochem. Soc. Symp.* **66**, 181–203.
24. Zamzami, N., Marchetti, P., Castedo, M., Hirsch, T., Susin, S. A., Masse, B., and Kroemer, G. (1996) Inhibitors of permeability transition interfere with

- the disruption of the mitochondrial transmembrane potential during apoptosis. *FEBS Lett.* **384(1)**, 53–57.
25. Lemasters, J. J., Nieminen, A. L., Qian, T., Trost, L. C., Elmore, S. P., Nishimura, Y., et al. (1998) The mitochondrial permeability transition in cell death: a common mechanism in necrosis, apoptosis and autophagy. *Biochim. Biophys. Acta* **1366(1-2)**, 177–196.
  26. Shimizu, S., Narita, M., and Tsujimoto, Y. (1999) Bcl-2 family proteins regulate the release of apoptogenic cytochrome c by the mitochondrial channel VDAC [see comments]. *Nature* **399(6735)**, 483–487.
  27. Finucane, D. M., Bossy-Wetzel, E., Waterhouse, N. J., Cotter, T. G., and Green, D. R. (1999) Bax-induced caspase activation and apoptosis via cytochrome c release from mitochondria is inhibitable by Bcl-xL. *J. Biol. Chem.* **274(4)**, 2225–2233.
  28. Bedner, E., Li, X., Kunicki, J., and Darzynkiewicz, Z. (2000) Translocation of bax to mitochondria during apoptosis measured by laser scanning cytometry. *Cytometry* **41(2)**, 83–88.
  29. Wolter, K. G., Hsu, Y. T., Smith, C. L., Nechushtan, A., Xi, X. G., and Youle, R. J. (1997) Movement of Bax from the cytosol to mitochondria during apoptosis. *J. Cell Biol.* **139(5)**, 1281–1292.
  30. Mahajan, N. P., Linder, K., Berry, G., Gordon, G. W., Heim, R., and Herman, B. (1998) Bcl-2 and Bax interactions in mitochondria probed with green fluorescent protein and fluorescence resonance energy transfer [see comments]. *Nat. Biotechnol.* **16(6)**, 547–552.
  31. Qin, Z. H., Wang, Y., Kikly, K. K., Sapp, E., Kegel, K. B., Aronin, N., and DiFiglia, M. (2000) Pro-caspase-8 is Predominantly localized in mitochondria and released into cytoplasm upon apoptotic stimulation. *J. Biol. Chem.* **276(11)**, 8079–8086.
  32. Goldstein, J. C., Waterhouse, N. J., Juin, P., Evan, G. I., and Green, D. R. (2000) The coordinate release of cytochrome c during apoptosis is rapid, complete and kinetically invariant. *Nat. Cell Biol.* **2(3)**, 156–162.
  33. Bobyleva, V., Bellei, M., Paziienza, T. L., and Muscatello, U. (1997) Effect of cardiolipin on functional properties of isolated rat liver mitochondria. *Biochem. Mol. Biol. Int.* **41(3)**, 469–480.
  34. Lutter, M., Fang, M., Luo, X., Nishijima, M., Xie, X., and Wang, X. (2000) Cardiolipin provides specificity for targeting of tBid to mitochondria. *Nat. Cell Biol.* **2(10)**, 754–761.
  35. Petit, J. M., Maftah, A., Ratinaud, M. H., and Julien, R. (1992) 10N-nonyl acridine orange interacts with cardiolipin and allows the quantification of this phospholipid in isolated mitochondria. *Eur. J. Biochem.* **209(1)**, 267–273.
  36. Polyak, K., Xia, Y., Zweier, J. L., Kinzler, K. W., and Vogelstein, B. (1997). A model for p53-induced apoptosis [see comments]. *Nature* **389(6648)**, 300–305.
  37. Pierce, R. H., Campbell, J. S., Stephenson, A. B., Franklin, C. C., Chaisson, M., Poot, M., et al. (2000) Disruption of redox homeostasis in tumor necrosis factor-induced apoptosis in a murine hepatocyte cell line. *Am. J. Pathol.* **157(1)**, 221–236.

38. Keij, J. F., Bell-Prince, C., and Steinkamp, J. A. (2000) Staining of mitochondrial membranes with 10-nonyl acridine orange, MitoFluor Green, and MitoTracker Green is affected by mitochondrial membrane potential altering drugs. *Cytometry* **39(3)**, 203–210.
39. Liu, D., Martino, G., Thangaraju, M., Sharma, M., Halwani, F., Shen, S. H., et al. (2000) Caspase-8-mediated intracellular acidification precedes mitochondrial dysfunction in somatostatin-induced apoptosis. *J. Biol. Chem.* **275(13)**, 9244–9250.
40. Llopis, J., McCaffery, J. M., Miyawaki, A., Farquhar, M. G., and Tsien, R. Y. (1998) Measurement of cytosolic, mitochondrial, and Golgi pH in single living cells with green fluorescent proteins. *Proc. Natl. Acad. Sci. USA* **95(12)**, 6803–6808.
41. Shenker, B. J., Guo, T. L., and Shapiro, I. M. (1998) Low-level methylmercury exposure causes human T-cells to undergo apoptosis: evidence of mitochondrial dysfunction. *Environ. Res.* **77(2)**: 149–159.
42. Scarlett, J. L., Packer, M. A., Porteous, C. M., and Murphy, M. P. (1996) Alterations to glutathione and nicotinamide nucleotides during the mitochondrial permeability transition induced by peroxynitrite. *Biochem. Pharmacol.* **52(7)**, 1047–1055.
43. Poot, M. and Pierce, R. C. (1999) Detection of apoptosis and changes in mitochondrial membrane potential with chloromethyl-X-rosamine [letter]. *Cytometry* **36(4)**: 359–360.
44. Ublacker, G. A., Johnson, J. A., Siegel, F. L., and Mulcahy, R. T. (1991) Influence of glutathione S-transferases on cellular glutathione determination by flow cytometry using monochlorobimane. *Cancer Res.* **51(7)**, 1783–1788.
45. Thorell, B. (1983) Flow-cytometric monitoring of intracellular flavins simultaneously with NAD(P)H levels. *Cytometry* **4(1)**, 61–65.
46. Makrigiorgos, G. M., Kassis, A. I., Mahmood, A., Bump, E. A., and Savvides, P. (1997) Novel fluorescein-based flow-cytometric method for detection of lipid peroxidation. *Free Radic. Biol. Med.* **22(1-2)**, 93–100.
47. Makrigiorgos, G. M. (1997) Detection of lipid peroxidation on erythrocytes using the excimer-forming property of a lipophilic BODIPY fluorescent dye. *J. Biochem. Biophys. Methods* **35(1)**, 23–35.
48. Maulik, G., Kassis, A. I., Savvides, P., and Makrigiorgos, G. M. (1998) Fluoresceinated phosphoethanolamine for flow-cytometric measurement of lipid peroxidation. *Free Radic. Biol. Med.* **25(6)**, 645–653.
49. Rizzuto, R., Simpson, A. W., Brini, M., and Pozzan, T. (1992) Rapid changes of mitochondrial Ca<sup>2+</sup> revealed by specifically targeted recombinant aequorin [published erratum appears in Nature 1992 Dec 24–31; 360(6406):768]. *Nature* **358(6384)**, 325–327.
50. Nuccitelli, R., (Ed.) (1994) *A Practical Guide to the Study of Calcium in Living Cells*. Academic Press, San Diego.
51. Burchiel, S. W., Edwards, B. S., Kuckuck, F. W., Lauer, F. T., Prossnitz, E. R., Ransom, J. T., and Sklar, L. A. (2000) Analysis of free intracellular calcium by flow cytometry: multiparameter and pharmacologic applications. *Methods* **21(3)**, 221–230.

52. Baffy, G., Miyashita, T., Williamson, J. R., and Reed, J. C. (1993) Apoptosis induced by withdrawal of interleukin-3 (IL-3) from an IL-3- dependent hematopoietic cell line is associated with repartitioning of intracellular calcium and is blocked by enforced Bcl-2 oncoprotein production. *J. Biol. Chem.* **268(9)**, 6511–6519.
53. Klingel, S., Rothe, G., Kellermann, W., and Valet, G. (1994) Flow cytometric determination of cysteine and serine proteinase activities in living cells with rhodamine 110 substrates. *Methods Cell Biol.* **41**, 449–459.
54. Hug, H., Los, M., Hirt, W., and Debatin, K. M. (1999) Rhodamine 110-linked amino acids and peptides as substrates to measure caspase activity upon apoptosis induction in intact cells. *Biochemistry* **38(42)**, 13,906–13,911.
55. Liu, J., Bhalgat, M., Zhang, C., Diwu, Z., Hoyland, B., and Klaubert, D. H. (1999) Fluorescent molecular probes V: a sensitive caspase-3 substrate for fluorometric assays. *Bioorg. Med. Chem. Lett.* **9(22)**, 3231–3236.
56. Komoriya, A., Packard, B. Z., Brown, M. J., Wu, M. L., and Henkart, P. A. (2000) Assessment of caspase activities in intact apoptotic thymocytes using cell-permeable fluorogenic caspase substrates. *J. Exp. Med.* **191(11)**, 1819–1828.
57. Los, M., Walczak, H., Schulze-Osthoff, K., and Reed, J. C. (2000) Fluorogenic substrates as detectors of caspase activity during natural killer cell-induced apoptosis. *Methods Mol. Biol.* **121**, 155–162.
58. Xu, X., Gerard, A. L., Huang, B. C., Anderson, D. C., Payan, D. G., and Luo, Y. (1998) Detection of programmed cell death using fluorescence energy transfer. *Nucleic Acids Res.* **26(8)**, 2034–2035.
59. Mahajan, N. P., Harrison-Shostak, D. C., Michaux, J., and Herman, B. (1999) Novel mutant green fluorescent protein protease substrates reveal the activation of specific caspases during apoptosis. *Chem. Biol.* **6(6)**, 401–409.
60. Korichneva, I. and Hammerling, U. (1999) F-actin as a functional target for retro-retinoids: a potential role in anhydroretinol-triggered cell death. *J. Cell Sci.* **112(Pt 15)**, 2521–2528.
61. Rao, J. Y., Jin, Y. S., Zheng, Q., Cheng, J., Tai, J., and Hemstreet, G. P., 3rd. (1999) Alterations of the actin polymerization status as an apoptotic morphological effector in HL-60 cells. *J. Cell Biochem.* **75(4)**, 686–697.
62. Bursch, W., Hohegger, K., Torok, L., Marian, B., Ellinger, A., and Hermann, R. S. (2000) Autophagic and apoptotic types of programmed cell death exhibit different fates of cytoskeletal filaments. *J. Cell Sci.* **113(Pt 7)**, 1189–1198.
63. Endresen, P. C., Prytz, P. S., and Aarbakke, J. (1995) A new flow cytometric method for discrimination of apoptotic cells and detection of their cell cycle specificity through staining of F-actin and DNA. *Cytometry* **20(2)**, 162–171.
64. Leers, M. P., Kolgen, W., Bjorklund, V., Bergman, T., Tribbick, G., Persson, B., et al. (1999) Immunocytochemical detection and mapping of a cytokeratin 18 neo- epitope exposed during early apoptosis. *J. Pathol.* **187(5)**, 567–572.
65. Morsi, H. M., Leers, M. P., Radespiel-Troger, M., Bjorklund, V., Kabarity, H. E., Nap, M., and Jager, W. (2000) Apoptosis, bcl-2 expression, and proliferation in benign and malignant endometrial epithelium: An approach using multiparameter flow cytometry. *Gynecol Oncol.* **77(1)**, 11–17.

66. van Engeland, M., Ramaekers, F. C., Schutte, B., and Reutelingsperger, C. P. (1996) A novel assay to measure loss of plasma membrane asymmetry during apoptosis of adherent cells in culture. *Cytometry* **24(2)**, 131–139.
67. Bedner, E., Li, X., Gorczyca, W., Melamed, M. R., and Darzynkiewicz, Z. (1999) Analysis of apoptosis by laser scanning cytometry. *Cytometry* **35(3)**, 181–195.
68. Fadok, V. A., Voelker, D. R., Campbell, P. A., Cohen, J. J., Bratton, D. L., and Henson, P. M. (1992) Exposure of phosphatidylserine on the surface of apoptotic lymphocytes triggers specific recognition and removal by macrophages. *J. Immunol.* **148(7)**, 2207–2216.
69. van Heerde, W. L., Robert-Offerman, S., Dumont, E., Hofstra, L., Doevendans, P. A., Smits, J. F., et al. CP (2000). Markers of apoptosis in cardiovascular tissues: focus on Annexin V. *Cardiovasc. Res.* **45(3)**, 549–559.
70. van Engeland, M., Nieland, L. J., Ramaekers, F. C., Schutte, B., and Reutelingsperger, C. P. (1998) Annexin V-affinity assay: a review on an apoptosis detection system based on phosphatidylserine exposure. *Cytometry* **31(1)**, 1–9.
71. Callahan, M. K., Williamson, P., and Schlegel, R. A. (2000) Surface expression of phosphatidylserine on macrophages is required for phagocytosis of apoptotic thymocytes. *Cell Death Differ.* **7(7)**, 645–653.
72. Reid, S., Cross, R., and Snow, E. C. (1996) Combined Hoechst 33342 and merocyanine 540 staining to examine murine B cell cycle stage, viability and apoptosis. *J. Immunol. Methods* **192(1-2)**, 43–54.
73. Xu, C., Zipfel, W., Shear, J. B., Williams, R. M., and Webb, W. W. (1996) Multiphoton fluorescence excitation: new spectral windows for biological non-linear microscopy. *Proc. Natl. Acad. Sci. USA* **93(20)**, 10,763–10,768.
74. Scalettar, B. A., Abney, J. R., and Hackenbrock, C. R. (1991) Dynamics, structure, and function are coupled in the mitochondrial matrix. *Proc. Natl. Acad. Sci. USA* **88(18)**, 8057–8061.
75. Ricchelli, F., Gobbo, S., Moreno, G., and Salet, C. (1999) Changes of the fluidity of mitochondrial membranes induced by the permeability transition. *Biochemistry* **38(29)**, 9295–9300.
76. Benderitter, M., Vincent-Genod, L., Berroud, A., and Voisin, P. (2000) Simultaneous analysis of radio-induced membrane alteration and cell viability by flow cytometry. *Cytometry* **39(2)**, 151–157.
77. Brock, R., Hink, M. A., and Jovin, T. M. (1998) Fluorescence correlation microscopy of cells in the presence of autofluorescence. *Biophys. J.* **75(5)**, 2547–2557.
78. Schwille, P., Haupts, U., Maiti, S., and Webb, W. W. (1999) Molecular dynamics in living cells observed by fluorescence correlation spectroscopy with one- and two-photon excitation. *Biophys. J.* **77(4)**, 2251–2265.
79. Schwille, P., Korfach, J., and Webb, W. W. (1999) Fluorescence correlation spectroscopy with single-molecule sensitivity on cell and model membranes. *Cytometry* **36(3)**, 176–182.
80. Ng, T., Squire, A., Hansra, G., Bornancin, F., Prevostel, C., Hanby, A., et al. (1999) Imaging protein kinase Calpha activation in cells. *Science* **283(5410)**, 2085–2089.

81. Verveer, P. J., Wouters, F. S., Reynolds, A. R., and Bastiaens, P. I. (2000) Quantitative imaging of lateral ErbB1 receptor signal propagation in the plasma membrane. *Science* **290**(5496), 1567–1570.
82. Cossarizza, A., Kalashnikova, G., Grassilli, E., Chiappelli, F., Salvioli, S., Capri, M., et al. (1994) Mitochondrial modifications during rat thymocyte apoptosis: a study at the single cell level. *Exp. Cell Res.* **214**(1), 323–330.
83. Macho, A., Decaudin, D., Castedo, M., Hirsch, T., Susin, S. A., Zamzami, N., and Kroemer, G. (1996) Chloromethyl-X-Rosamine is an aldehyde-fixable potential-sensitive fluorochrome for the detection of early apoptosis [see comments]. *Cytometry* **25**(4), 333–340.
84. Poot, M., Verkerk, A., Koster, J. F., and Jongkind, J. F. (1986) De novo synthesis of glutathione in human fibroblasts during in vitro ageing and in some metabolic diseases as measured by a flow cytometric method. *Biochim. Biophys. Acta* **883**(3), 580–584.

# Analysis of Apoptosis by Laser-Scanning Cytometry

---

Zbigniew Darzynkiewicz, Elzbieta Bedner,  
and Piotr Smolewski

## 1. INTRODUCTION

One of the major goals in applications of cytometry in analysis of apoptosis is to identify and quantify dead cells and often to discriminate between apoptosis and necrosis. Recognition of dead cells relies on the presence of a particular biochemical or molecular marker that is characteristic for apoptosis, necrosis, or both. A variety of methods have been developed, especially for the identification of apoptotic cells (*see* reviews in refs. 1–3). These methods were initially designed to be used by flow cytometry. The drawback of flow cytometric methods stems from the fact that identification of apoptotic or necrotic cells relies on a single attribute that is assumed to represent a characteristic feature (hallmark) of apoptosis or necrosis. However, this attribute may often be absent, particularly in the case of “atypical apoptosis,” which is common in the case of cells of epithelial or fibroblast lineage (e.g., refs. 4–6). The apoptotic attribute may also be absent when apoptosis is induced by the agents that directly or indirectly suppress the appearance of this attribute. The characteristic changes in cell morphology (7), therefore, still remain the gold standard for recognition of apoptotic cell death.

The laser scanning cytometer (LSC) is a microscope-based cytofluorometer that combines advantages of flow cytometry and image analysis and is finding wide applicability in many disciplines of biology and medicine (*see* reviews in refs. 8,9). LSC measures cell fluorescence rapidly and with similar accuracy as flow cytometer. However, since the *xy* coordi-



nates of cell location on the slide are recorded in a list-mode fashion together with other measured cell parameters, cells can be relocated after the measurement. They can be then examined visually or subjected to image analysis to correlate the observed change in the measured parameter with the change in their morphology. The possibility of cell relocation and other attributes of LSC which are presented further in this chapter, has contributed to this instrument's usefulness in numerous applications in analysis of apoptosis (10). The most common methods for identification of apoptotic and necrotic cells that have been adapted to LSC as well as the specifics of sample preparation for LSC are described below. In the Notes section, we address for each method discussed some potential pitfalls and problems arising with data interpretation. Because LSC is a relatively new, not yet a widely known instrument, its scheme, unique features, and principles of fluorescence measurement are presented as well.

## 2. CELL MEASUREMENT BY LSC

Figure 1 presents a diagrammatic view of the LSC. The base of the instrument is the standard research microscope (Olympus Optical Co.). The specimen on the microscope slide is placed on the microscope stage and its fluorescence is excited by the laser beams that rapidly scan the slide. In the current instruments, the spatially merged beams from two lasers (argon and He-Ne) are directed onto the oscillating (350 Hz) mirror, which in turn directs the beams through the epi-illumination port of the microscope and images them through the objective lens onto the slide. Depending on the lens magnification, the beam spot size varies from 2.5 (at 40 $\times$ ) to 10.0  $\mu\text{m}$  (at 10 $\times$  magnification). The position of the slide ( $xy$  coordinates) is located on the computer-controlled motorized microscope stage is monitored by sensors, and the slide is moved with the stage perpendicular to the scan at 0.5  $\mu\text{m}$  steps per each scan. Light scattered by the cells is imaged by the condenser lens and recorded by scatter sensors. A portion of the fluorescence emitted by the specimen is collected by the objective lens and directed to a CCD camera for imaging. Another portion of emitted fluorescence is directed through the scan lens to the scanning mirror. Upon reflection, it passes through a series of dichroic mirrors and optical interference filters to reach one of the four photomultipliers. Each photomultiplier records fluorescence at a specific wavelength range, defined by the combination of filters and dichroic mirrors. An additional light source provides transmitted illumination that is used to visualize the specimen through an eyepiece or CCD camera. The measurement of cell fluorescence (or light scatter) is computer-controlled and triggered by setting a desired threshold contour for

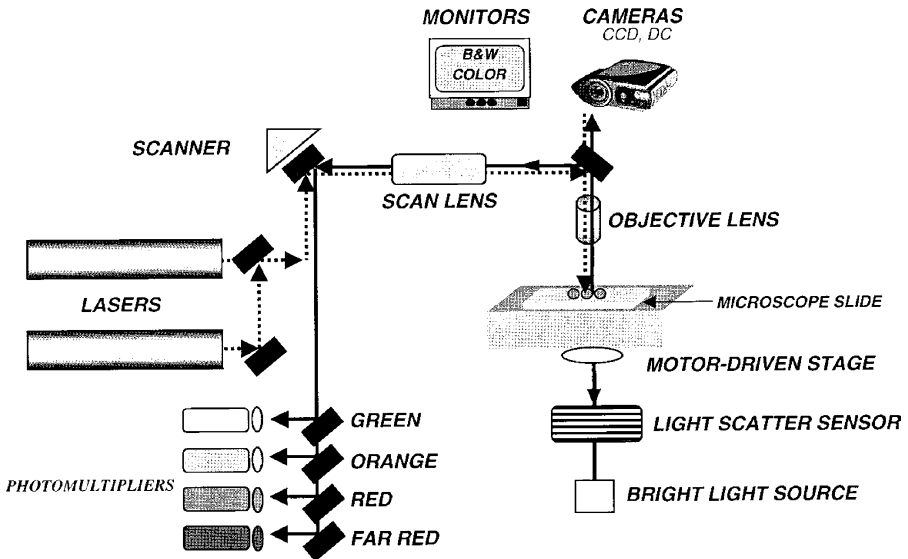


Fig. 1. Scheme representing major components of the LSC. See text for explanation.

the cell above background level of emission. For each measured object, the following parameters are recorded by LSC:

1. Integrated fluorescence intensity within the integration contour, which can be adjusted to a desired width with respect to the threshold contour;
2. Maximal pixel intensity within this area, so called "peak-," or "max pixel-value."
3. The area within the integration contour.
4. The perimeter of the contour (in micrometers).
5. Integrated fluorescence intensity within the area of a torus of a desired width defined by the peripheral contour located around (outside) the primary integration contour. Thus, if the integration contour is set for the cell nucleus based on, e.g., red fluorescence (DNA stained by propidium), then the integrated (or maximal pixel) green fluorescence of fluorescein isothiocyanate (FITC)-stained cytoplasm can be measured separately, within the integration contour (i.e., over the nucleus) and within the peripheral contour (i.e., over the rim of cytoplasm of desired width outside the nucleus). It should be noted that all the aforementioned values of integrated fluorescence are automatically corrected for background, measured locally outside the cell.
6. The  $xy$  spatial coordinates of the maximal pixel.
7. The computer clock time at the moment of individual cell measurement.

The measurements by LSC are rapid and with optimal cell density on the slide up to 5000 cells can be measured per min. The accuracy and sensitivity of cell fluorescence measurements by LSC are similar as with advanced

flow cytometers (8). Unlike flow cytometry, LSC measures individual pixel values and records the value of the maximum intensity pixel. This parameter reflects homogeneity of the fluorochrome distribution within the cell and was shown to be particularly useful in studies of translocation of Bax from cytosol to mitochondria during induction of apoptosis (11). The possibility of differential analysis of fluorescence emitted from nucleus vs cytoplasm is another feature provided by LSC that is not available with flow cytometry. This feature allows one to study a change in localization of cell constituents from nucleus to cytoplasm or vice versa and was useful to detect activation of NF- $\kappa$ B also during induction of apoptosis (12).

The most characteristic feature of LSC that distinguishes it from flow cytometry is that cell analysis is performed on a slide. This allows visual cell examination to assess morphology and correlate it with the measured parameters. It also allows cell image capture, analysis, and/or display. Furthermore, additional cytofluorometric analysis of the same cells is possible using new sets of markers or other contouring thresholds. The results of the sequential measurements can be then integrated in the list-mode form into a single file, using the “file merge” capability of the instrument. This allows one then to directly correlate, within the same cells, the results of functional assays such as collapse of mitochondrial transmembrane potential ( $\Delta\Psi_m$ ), change in pH, or generation of reactive oxygen intermediates (ROIs) with cell attributes that can be measured only after cell fixation and permeabilization (e.g., the presence of DNA strand breaks, cell-cycle position, and so on (13)). The data can be used to map the sequence of both functional and structural changes occurring during apoptosis to determine whether a particular death-associated event is a prerequisite for the latter steps. Applications for studies of apoptosis that descend from these unique features of LSC are presented further in this chapter.

### 3. ATTACHMENT OF CELLS TO MICROSCOPE SLIDES FOR ANALYSIS BY LSC

Many assays of apoptosis by LSC are performed on fixed cells. For these assays the cells are attached to microscope slides by standard methods that include smear films, tissue sections, “touch” preparations from freshly transected tissues, or cytocentrifuging cell suspensions. Cytocentrifugation (*see* below) is often preferred over “touch” or smear preparations because it flattens cells on the slides so that their geometry is favorable, and therefore more morphological details can be revealed.

Some assays of apoptosis by LSC require the cells to be alive with their vital functions preserved. Such assays include analyses of plasma membrane

transport function, detection of phosphatidylserine on cell surface (14), probing  $\Delta\Psi_m$  (6), intracellular pH, oxidative stress, activation of caspases, or intracellular level of ionized calcium. Suspensions of live cells in appropriately prepared reaction media are generally used when such analyses are performed by flow cytometry, and such suspensions may also be measured by LSC. It is often desired, however, that the measured cells be attached to a microscope slide or coverglass. Attachment is required if one intends to relocate the measured cells for their subsequent morphologic examination or to probe additionally by another fluorochrome(s). The relocation allows correlation of the initial measurement with cell morphology or with the secondary analysis involving another fluorochrome.

### 3.1. Attachment of Cells by Cyto centrifugation

1. Prepare cell suspension in tissue-culture medium (with serum) at density  $5\text{--}10 \times 10^3$  cells 1 mL.
2. Transfer 300  $\mu\text{L}$  of this suspension into a cytospin chamber (e.g., Shandon Scientific, Pittsburgh, PA).
3. Cyto centrifuge at 1000 rpm (115g) for 6 min. The speed and time of centrifugation may be extended (to 1500 rpm (173g) and 10 min, respectively) to additionally flatten the cells for their more favorable geometry that may be useful to detect variation in local density of fluorochrome, e.g., when studying translocation of certain some molecules.
4. Fix cells by immersing the slides in a Coplin jar containing fixative (e.g., 1% formaldehyde in PBS or 70% ethanol). For most applications (e.g., immunocytochemistry; see Subheadings 8. and 9.) the cells may be fixed in 1% formaldehyde at 0–4°C for 15–30 min, then rinsed in PBS and postfixed and/or stored for up to several days in 70% ethanol at –20°C. Postfixation in ethanol makes the cells more permeable to the immunocytochemical reagents. Avoid complete cell drying in air following cyto centrifugation and prior to fixation if the cells are being subsequently subjected to immunocytochemical analysis.

### 3.2. Attachment of Live Cells

A variety of cells grow attached to flasks in culture. Such cells can be attached to microscope slides by culturing them on the slides or coverslips. Culture vessels that have a microscope slide at the bottom of the chamber are commercially available (e.g., “Chamberslide,” Nunc, Inc., Naperville, IL). The cells growing in these chambers spread and attach to the slide surface in a few hours after suspending them in full culture medium (with serum) and incubation at 37°C. Glass rather than plastic slides are preferred as the latter often have high autofluorescence that interferes with measurements by LSC. Alternatively, the cells can be grown on coverslips, e.g., placed on the bottom of Petri dishes. The coverslips are then inverted over shallow (<1 mm) wells on the microscope slides. The wells can be pre-

pared by constructing the well walls ( $\sim 2 \times 1$  cm square) with either a pen that deposits a hydrophobic barrier (Isolator, Shandon Scientific), nail polish, or melted paraffin. Alternatively the wells can be made by preparing a strip of Parafilm "M" (American National Can, Greenwich, CT) of the size of the slide, cutting a hole  $\sim 2 \times 1$  cm in the middle of this strip, placing the strip on the microscope slide, and heating the slide on a warm plate until the Parafilm starts to melt. It should be stressed, however, that because the cells detach during late stages of apoptosis, these cells may be selectively lost if the analysis is limited to attached cells.

Cells that normally grow in suspension can be attached to glass slides by electrostatic forces. This is due to the fact that sialic acid on the cell surface has net negative charge while the glass surface is positively charged. Incubation of cells on microscope slides in the absence of any serum or serum proteins (which otherwise neutralize the charge), thus, leads to their attachment. The cells taken from culture should be rinsed in PBS in order to remove serum proteins and then resuspended in PBS at a concentration of  $2 \times 10^5$ – $10^6$  cells/mL. An aliquot (50–100  $\mu$ L) of this suspension should be deposited within a shallow well (prepared as described above) on the horizontally placed microscope slide. To prevent drying, a small piece ( $\sim 2 \times 2$  cm) of a thin polyethylene foil or Parafilm may be placed atop of the cell suspension drop. A short (15–20 min) incubation of such cell suspension at room temperature in a closed box containing wet tissue or filter paper that provides 100% humidity is adequate to ensure that most cells will firmly attach to the slide surface. Cells attached in this manner remain viable for several hours and can be subjected to surface immunophenotyping, viability tests, or intracellular enzyme kinetics assays (15). Such preparations can be fixed (e.g., in formaldehyde) without a significant loss of cells from the slide. However, as in the case of cell growth on glass, late apoptotic cells have a tendency not to attach or may even detach after the initial attachment.

It should be stressed that the microscope slide to which the cells are going to be attached electrostatically should be extra clean; the surface should never be hand-touched. To remove possible contamination of the glass surface that may interfere with cell attachment it is advised to rinse the microscope slides in a household detergent, then thoroughly in water, finally in 100% ethanol, then completely air dry and use the same day.

#### 4. DETECTION OF CHROMATIN CONDENSATION

One of the hallmarks of apoptosis is condensation of nuclear chromatin (7). DNA in condensed chromatin stains with many dyes with greater intensity

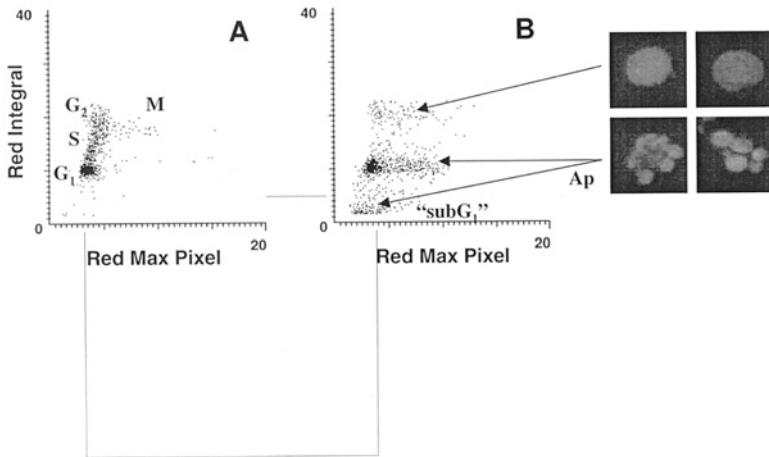


Fig. 2. Identification of apoptotic cells by LSC based on high values of maximal pixel detecting red fluorescence or fractional DNA content of propidium iodide (PI) stained cells. Exponentially growing human leukemic HL-60 cells, untreated (A) or induced to undergo apoptosis by treatment with camptothecin (B) (refs. 26,28), were stained with PI in the presence of RNase as described in the protocol. The scatterplots represent bivariate distributions of cells with respect to their integrated red fluorescence (proportional to DNA content) vs maximal red fluorescence pixel value. Only mitotic cells (M) have high maximal pixel value in the untreated culture. Apoptotic cells (Ap) that are present in the CPT treated cultures, are characterized either by the increased intensity of maximal pixel of red fluorescence or by a low (sub-G<sub>1</sub>) DNA content. The relocation feature of LSC allows one to observe morphology of the cells selected from particular regions of the bivariate distributions. Upon the relocation, the cells with high maximal pixel value or with fractional DNA content show chromatin condensation and nuclear fragmentation, typical of apoptosis (panels on right).

per unit of the projected area (hyperchromasia). The hyperchromasia of DNA in apoptotic cells can be detected by the increased value of the maximal pixel of the DNA-associated fluorescence (10,16). Propidium iodide (PI) is used as the DNA fluorochrome in the method described below and apoptotic cells can be identified by high values of the maximal pixel of DNA-associated PI fluorescence (Fig. 2).

#### 4.1. Materials

1. 1% Formaldehyde in phosphate-buffered saline (PBS). **Caution:** Formaldehyde is a health hazard: wear gloves and do not inhale its vapors.
2. Stock solution of PI: Dissolve 1 mg of PI (Molecular Probes, Eugene, OR) in 1 ml of distilled water. It can be stored for several months at 4°C in the dark. **Caution:** PI is a suspected carcinogen: wear gloves and observe caution.

3. Stock solution of RNase: Dissolve 2 mg of DNase-free RNase A (Sigma Chemical Co., St Louis, MO) in 1 mL of distilled water. If DNase-free RNase is unavailable, DNase activity is destroyed by boiling the stock RNase solution for 5 min. Aliquots can be stored at  $-20^{\circ}\text{C}$ .
4. Staining solution of PI: Add 10  $\mu\text{L}$  of the stock solution of PI to 1 mL of PBS to obtain 10  $\mu\text{g}/\text{mL}$  final PI concentration.
5. Working solution of RNase: Add 100  $\mu\text{L}$  of RNase stock solution to 1.9 mL of PBS to obtain 0.1  $\text{mg}/\text{mL}$  final concentration.
6. Specimen mounting solution: Add 1 part of PI staining solution to 9 parts of glycerol.

#### 4.2. Cell Staining and Measurement

1. Deposit cells on the microscope slide by cyto centrifugation, electrostatically, or by growing them on the slide, as described in Subheading 3.
2. Fix cells by immersing the slides in a Coplin jar containing 1% formaldehyde in PBS on ice for 15 min.
3. Wash the slides briefly by immersing in PBS and transfer them into Coplin jars containing 70% ethanol. The cells may be stored in ethanol indefinitely at  $4^{\circ}\text{C}$ .
4. Rinse slides briefly ( $\sim 1$  min) in 50%, then in 30% ethanol, and finally in distilled water.
5. Transfer slides to a Coplin jar containing RNase working solution and incubate at room temperature for 60 or at  $37^{\circ}\text{C}$  for 30 min. Alternatively, to save the reagent, a small volume ( $\sim 0.5$  mL) of RNase staining solution may be deposited onto the horizontally placed slide at the area containing the cells, covered with a  $\sim 2 \times 4$  cm strip of Parafilm and the slide kept in the box containing wet tissue of filter paper to ensure 100% humidity for 60 min at room temperature or for 30 min at  $37^{\circ}\text{C}$ .
6. Immerse slides in a Coplin jar containing the PI staining solution. Keep slides immersed in PI solution for 10 min at room temperature in the dark.
7. Mount the stained cells under a coverslip in a drop of the mounting medium and seal the preparation with melted paraffin or nail polish. The slides should be kept in the dark until measurement on LSC.
8. Measure cell fluorescence by LSC using argon ion laser (488 nm) to excite the emission. Use red fluorescence signal for contouring. Record integrated and maximal pixel values of red fluorescence ( $>600$  nm).

#### 4.3. Notes

1. This staining procedure is simple and can be combined with analysis of other constituents of the cell when they are probed with fluorochromes of another color.
2. Apoptotic cells are identified either as the cells with high maximal pixel values of the PI fluorescence or as the cells with fractional (sub- $G_1$ ) DNA content as shown in Fig. 2.
3. Because cellular DNA content also is measured cell ploidy and/or cell cycle position of nonapoptotic cells can be determined at the same time.
4. DNA in late apoptotic cells is fragmented and low MW may be extracted during the staining procedure. Some DNA may also be lost as a result of shedding

of apoptotic bodies that contain fragments of nuclear chromatin. Thus, DNA content of apoptotic cells may not be a reliable marker of their cell-cycle position or ploidy. The loss of DNA may also be reflected by the decreased DNA-associated fluorescence including maximal pixel. Therefore, such cells or nuclear fragments can be detected only based on their fractional DNA content (sub- $G_1$ '' cell subpopulation) but not based on the increase of maximal pixel.

5. The drawback of this approach is that it cannot discriminate between mitotic and apoptotic cells. Early  $G_1$  (postmitotic) cells also have high fluorescence intensity of the maximal pixel (17). The distinction between apoptotic and mitotic cells is critical after treatment with agents such as taxol or other mitotic blockers, i.e., when mitotic cells undergo apoptosis. The visual examination of the cells, or analysis of other morphometric features such as nucleus to cytoplasm ratio, nuclear or cellular area or circumference, forward light scatter, and so on, as offered by LSC, however, can be helpful in these instances.
6. Although individual nuclear fragments of the late apoptotic cells are within the same cell they may be completely separated from each other. Therefore, they may be separately contoured and each fragment identified as a whole individual nucleus of an apoptotic cell with a fractional (sub- $G_1$ ) DNA content. This may lead to an overestimate of a frequency of apoptotic cells (apoptotic index).

## 5. COLLAPSE OF MITOCHONDRIAL TRANSMEMBRANE POTENTIAL ( $\Delta\Psi_m$ )

Dissipation (collapse) of mitochondrial transmembrane potential ( $\Delta\Psi_m$ ) occurs early in most models of apoptosis and is often considered as a marker of apoptosis (6,18). Permeable lipophilic cationic fluorochromes such as rhodamine 123 (Rh 123) or 3,3'-dihexyloxa-dicarbocyanine [DiOC<sub>6</sub> (3)] can serve as probes of ( $\Delta\Psi_m$ ) (19). When live cells are incubated with Rh 123 the probe accumulates in mitochondria and the extent of its uptake as measured by intensity of cellular fluorescence, reflects ( $\Delta\Psi_m$ ). A combination of either Rh 123 or DiOC<sub>6</sub> (3) with PI can be used as a viability assay that discriminates between live cells that only stain with them (green fluorescence) vs dead or dying cells whose plasma membrane integrity is compromised (cells with damaged plasma membrane, late apoptotic, and necrotic cells) that stain only with PI (red fluorescence), vs early apoptotic cells that show somewhat increased staining with PI but still take up Rh 123 or DiOC<sub>6</sub> (3) (19). The protocol below presents a combination of DiOC<sub>6</sub> (3) and PI.

### 5.1. Materials

1. Stock solution of PI: Described in Subheading 4.1.2.
2. Stock solution of DiOC<sub>6</sub> (3): Prepare 0.1 mM solution of DiOC<sub>6</sub> (3) (Molecular Probes) by dissolving 5.7 mg of the dye in 10 mL of dimethyl sulfoxide



(DMSO). Store in small aliquots at  $-20^{\circ}\text{C}$  in the dark. Prior to use dilute 10-fold with PBS to obtain  $10\ \mu\text{M}$  concentration.

3. Staining solution of DiOC<sub>6</sub>(3): Add  $5\ \mu\text{L}$  of the diluted DiOC<sub>6</sub>(3) solution to  $1\ \text{mL}$  of PBS to obtain the final concentration of  $50\ \text{nM}$ .
4. Staining solution of PI: To  $10\ \text{mL}$  of the culture medium that is normally used to grow the studied cells add  $100\ \mu\text{L}$  of the PI stock solution.

## 5.2. Cell Staining and Fluorescence Measurement

1. Attach live cells to microscope slides as described in Subheading 3.2.
2. With Pasteur pipet gently remove the culture medium in which the cells were growing (or PBS if they were attached electrostatically) and immediately (without allowing cells to dry) replace it with the staining solution of DiOC<sub>6</sub>(3). Cover with a  $\sim 2 \times 4\ \text{cm}$  strip of Parafilm and place the slide in the box containing wet tissue or filter paper to ensure 100% humidity.
3. Incubate at room temperature for 20 min.
4. With Pasteur pipet gently remove the staining solution of DiOC<sub>6</sub>(3) and immediately mount the cells under a coverslip in a drop of the staining solution of PI.
5. Measure cell fluorescence by LSC within the next 10 min. Excite fluorescence of PI and DiOC<sub>6</sub>(3) with the argon ion laser (488 nm) and measure intensity of red ( $>400\ \text{nm}$ ) and green ( $530 \pm 20\ \text{nm}$ ) fluorescence. Contour the cells on light-scatter signal.

## 5.3. Notes

1. Cells that were growing attached to microscope slides may be incubated with  $50\ \text{nM}$  DiOC<sub>6</sub>(3) in the same culture medium in which they are normally maintained, with full serum content. Thus, the staining solution of DiOC<sub>6</sub>(3) (Subheading 5.3.) may contain serum. The electrostatically attached cells however, have a tendency to detach if maintained for longer time in the presence of serum. Therefore, it is preferred to incubate them with DiOC<sub>6</sub>(3) in a serum-free medium.
2. Live nonapoptotic cells have only green fluorescence, the cells with collapsed  $\Delta\Psi_{\text{m}}$  at early stage of apoptosis have very dim green and still no red fluorescence and late apoptotic (necrotic stage of apoptosis) and necrotic cells have only red fluorescence.
3. Because collapse of  $\Delta\Psi_{\text{m}}$  not always is a prerequisite for a release of cytochrome c from mitochondria and activation of caspases (20), in these instances apoptotic cells may still have strong DiOC<sub>6</sub>(3) fluorescence (Fig. 3).
4. DiOC<sub>6</sub>(3) is rapidly removed from the cells that have active efflux pump (P glycoprotein), such as stem cells or multi-drug resistant tumor cells, which may simulate collapse of  $\Delta\Psi_{\text{m}}$ .
5. DiOC<sub>6</sub>(3) may be substituted by Rh 123 in this protocol, at a final concentration  $100\text{--}200\ \text{nM}$ .
6.  $\Delta\Psi_{\text{m}}$  is sensitive to any change in cell environment. The samples to be compared, therefore, should be incubated and measured under identical conditions,

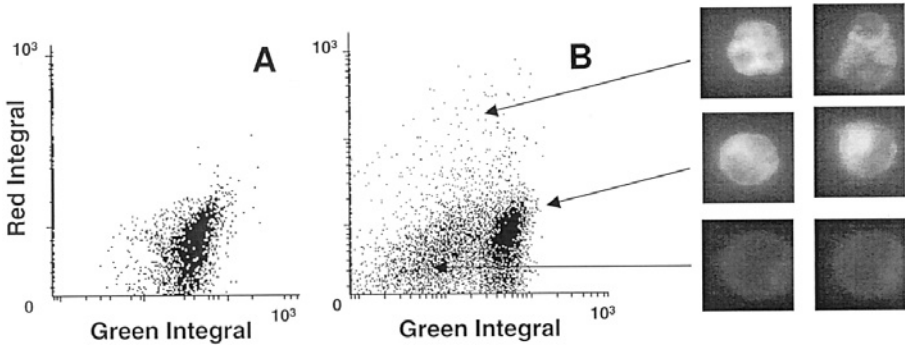


Fig. 3. Detection of the collapse of mitochondrial electrochemical potential ( $\Delta\Psi_m$ ) by LSC after cell staining with DiOC<sub>6</sub> (3) and PI. Human histiomonocytic lymphoma U937 cells untreated (A) or to induce apoptosis by treatment treated with tumor necrosis factor- $\alpha$  (TNF- $\alpha$ ) and cycloheximide (B; refs. 26,28), were stained according to the protocol. The bivariate green vs red fluorescence distribution (scatterplot) represents  $\Delta\Psi_m$  vs uptake of PI, respectively. Nonapoptotic cells fluoresce only green, early apoptotic cells show decreased green fluorescence but no red fluorescence while late apoptotic cells stain cannot exclude PI and thus have red fluorescence. After relocation their stainability with DiOC<sub>6</sub> (3) and PI can be correlated with morphology.

taking into an account temperature, pH, time elapsed between the onset of incubation and actual fluorescence measurement, and other potential variables. If possible (e.g., the microscope stage of LSC is thermostatically controlled), the measurements should be performed at 37°C. Otherwise, the samples should be equilibrated to ambient temperature.

## 6. ANNEXIN V BINDING

Phosphatidylserine, which normally is on the inner leaflet of the plasma membrane, early during apoptosis becomes exposed on the outside cell surface (13). Because the anticoagulant protein annexin V binds with high affinity to phosphatidylserine, fluorochrome-conjugated annexin V can serve as a marker of apoptotic cells (21). During progression of apoptosis, the ability to bind annexin V precedes the loss of the plasma membrane's ability to exclude cationic dyes such as PI.

Therefore, by staining cells with a combination of annexin V-FITC and PI, it is possible to distinguish cells at different stages of apoptosis.

### 6.1. Materials

1. Annexin V-FITC solution: Dissolve annexin V-FITC conjugate (1:1 stoichiometric complex, available from BRAND Applications, The Netherlands) in

binding buffer (10 mM HEPES (N-2-hydroxyethylpiperazine-N-2-ethanesulfonic acid) -NaOH, pH. 7.4, 140 mM NaCl, 2.5 mM CaCl<sub>2</sub>) at a concentration of 1.0 µg/mL. This solution has to be prepared fresh prior to use.

2. Stock solution of PI: described in Subheading 4.1.2.
3. Staining solution of PI: described in Subheading 5.1.4.

## 6.2. Cell Staining and Fluorescence Measurement

1. Attach live cells to microscope slides as described in Subheading 3.2.
2. With a Pasteur pipet, gently remove the culture medium in which the cells were growing (or PBS if they were attached electrostatically) and immediately (without allowing cells to dry) replace it with the Annexin V-FITC solution. Cover with a ~2 × 4 cm strip of Parafilm and place in the box containing wet tissue or filter paper to ensure 100% humidity.
3. Incubate at room temperature for 10 min.
4. With a Pasteur pipet, gently remove the Annexin V-FITC solution and immediately mount the cells under a coverslip in a drop of the staining solution of PI.
5. Measure cell fluorescence by LSC within the next 10 min. Excite fluorescence of FITC and PI with the argon ion laser (488 nm) and measure intensity of red (>400 nm) and green (530±20 nm) fluorescence. Contour the cells on light scatter signal.

## 6.3. Notes

1. Live nonapoptotic cells have minimal green fluorescence and also minimal or undetectable red fluorescence (annexin V negative/PI negative) (Fig. 4). At early stages of apoptosis, cells stain green but still exclude PI and therefore continue to have no significant red fluorescence (annexin V positive/PI negative). Late apoptotic cells show intense green and red fluorescence (both annexin V and PI positive).
2. Isolated nuclei, cells with severely damaged membranes, and very late apoptotic cells stain rapidly and intensely with PI and may not bind annexin V. Stainability of DNA with PI in isolated nuclei is stoichiometric and therefore their frequency histograms of DNA content may have pattern characteristic of the cell-cycle distribution.
3. Interpretation of the data is complicated by the presence of nonapoptotic cells with damaged membranes. Such cells may have phosphatidylserine exposed on plasma membrane and, therefore, similar to apoptotic cells, bind annexin V. Mechanical disaggregation of tissues; to isolate individual cells; extensive use of proteolytic enzymes to disrupt cell aggregates, remove adherent cells from cultures, or to isolate cells from tissue; mechanical removal of the cells from tissue culture flasks (e.g., by a rubber policeman); and cell electroporation, may affect the binding of annexin V. Such treatments, therefore, may introduce experimental bias in subsequent analysis of apoptosis by this method.
4. Because even intact and live cells may take up PI after prolonged incubation fluorescence measurement should be performed rather shortly following addition of the dye.

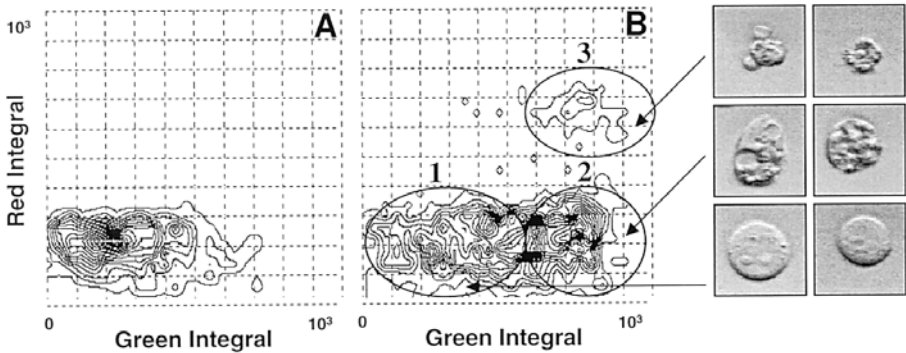


Fig. 4. Detection of early and late apoptotic cells by LSC after staining with annexin V-FITC conjugate and PI. HL-60 cells untreated (A), or to induce apoptosis treated with camptothecin (B; refs. 26,28), were stained with annexin V-FITC and PI as described in the protocol. The bivariate distributions (contour maps) of their green vs red fluorescence represent annexin V-FITC binding vs PI uptake, respectively. Nonapoptotic cells (region 1) show low green no red fluorescence, early apoptotic cells have green but have no red fluorescence (region 2) while late apoptotic cells fluoresce in both red and green wavelength (region 3). Relocation allows one to examine morphology of cells in each region.

## 7. DETECTION OF DNA STRAND BREAKS (TUNEL ASSAY)

Apoptosis-associated DNA fragmentation (22) generates a multitude of DNA strand breaks. The 3' OH ends of the breaks can be detected by attaching to them fluorochrome-labeled deoxynucleotides in a reaction catalyzed by exogenous terminal deoxynucleotidyltransferase (23,24). The assay is commonly known as TUNEL from **T**DT-mediated **d**UTP-biotin **n**ick-**e**nd **l**abeling. Of all the markers used to label DNA breaks, BrdUTP appears to be the most advantageous with respect to sensitivity, low cost and simplicity of the reaction (24). When attached to DNA strand breaks in the form of poly-BrdU, this deoxynucleotide can be detected with an FITC-conjugated anti-BrdU Ab; the same Ab that is commonly used to detect BrdU incorporated during DNA replication. Poly-BrdU attached to DNA strand breaks by TdT, however, is accessible to the Ab without the need for DNA denaturation, which otherwise is required to detect the precursor incorporated during DNA replication.

The detection of DNA strand breaks requires cell prefixation with a crosslinking agent such as formaldehyde to prevent the extraction of low MW DNA during the procedure. Labeling DNA strand breaks with FITC is

combined with staining of DNA with PI. Bivariate analysis of DNA strand breaks vs DNA content allows one to distinguish apoptotic from nonapoptotic cell subpopulations and reveal the cell-cycle distribution in these subpopulations (23).

### **7.1. Materials**

1. Fixatives: primary fixative: 1% methanol-free formaldehyde (available from Polysciences Inc., Warrington, PA) in PBS, pH 7.4. Secondary fixative: 70% ethanol.
2. The TdT reaction buffer (5X concentrated) contains: potassium (or sodium) cacodylate, 1 M 125 mM, Tris-HCl, pH 6.6, 1.25 mg/mL bovine serum albumin (BSA).
3. 10 mM Cobalt chloride (CoCl<sub>2</sub>).
4. TdT in storage buffer, 25 U in 1  $\mu$ L. The buffer, TdT, and CoCl<sub>2</sub> are available from Boehringer Mannheim (Indianapolis, IN).
5. BrdUTP stock solution: BrdUTP (Sigma) 2 mM (100 nmol in 50  $\mu$ L) in 50 mM Tris-HCl, pH 7.5.
6. FITC-conjugated anti-BrdU MAb solution: dissolve 0.3  $\mu$ g of anti-BrdU FITC conjugated MAb (available from Phoenix Flow Systems, San Diego, CA) in 100  $\mu$ L of PBS that contains 0.3% Triton X-100 and 1% (w/v) BSA.
7. Reaction solution: Prepare a solution that in 100  $\mu$ L contains: 20  $\mu$ L of the reaction buffer, 4.0  $\mu$ L of BrdUTP stock solution, 1.0  $\mu$ L (25 U) of TdT in storage buffer, 10  $\mu$ L of CoCl<sub>2</sub> solution, 65  $\mu$ L distilled H<sub>2</sub>O. This solution is prepared just prior to use.
8. Rinsing solution. Dissolve in PBS: Triton X-100, 0.1% (v/v), 5 mg/mL BSA.
9. PI Staining solution: Dissolve in PBS: 5  $\mu$ g/mL PI, 200  $\mu$ g/mL DNase-free RNase A.

### **7.2. Cell Fixation**

1. Deposit cells on the microscope slide by cytocentrifugation, electrostatically, or by growing them on the slide, as described in the Subheading 3.
2. Fix cells by immersing the slides in a Coplin jar containing 1% formaldehyde in PBS, on ice for 15 min.
3. Wash the slides briefly by immersing in PBS and transfer them into Coplin jars containing 70% ethanol. The cells may be stored in ethanol indefinitely at 4°C.

### **7.3. DNA Strand Break Labeling**

1. Remove slides from 70% ethanol and rinse them briefly (~1 min) in 50%, then in 30% ethanol, and finally in distilled water.
2. Place the slide horizontally and deposit 50 or 100  $\mu$ L (depending on the area size) of the reaction solution atop of the area of the slide where the cells are attached. Cover with ~2  $\times$  4 cm strip of Parafilm and place the slide in the box containing wet tissue or filter paper to ensure 100% humidity. Incubate for 40 min at 37°C or overnight at room temperature.

3. With Pasteur pipet (or vacuum suction pipet) remove from the slide the reaction solution and replace it 0.5 mL of the rinsing solution. Repeat the rinsing.
4. Remove from the slide the rinsing solution and replace it with 100  $\mu$ L of the FITC-conjugated anti-BrdU MAb solution. Cover with a strip of Parafilm as described above, place in 100% humidity box and incubate at room temperature for 1 h or at 4°C overnight.
5. Remove the anti-BrdU solution and rinse the slide with PBS.
6. Apply a drop or two of the PI staining solution containing RNase A over the area with cells. Cover with a strip of Parafilm and incubate for 30 min in the 100% humidity box at room temperature in the dark.
7. Replace the PI staining solution with a drop of a mixture of glycerol and PI staining solution (9:1) and mount under the coverslips. To preserve the specimen for longer period of time or transport, seal the coverslip with nail polish or melted paraffin.
8. Measure cell fluorescence by LSC using 488 nm argon ion laser for excitation. Contour on red fluorescence signal and measure intensity (integrated values) of green fluorescence of FITC-anti BrdU MAb at 530 $\pm$ 20 nm and red fluorescence of PI at >600 nm.

#### 7.4. Notes

1. A plethora of kits designed to label DNA strand breaks are available from different vendors. For example, Phoenix Flow Systems, PharMingen Inc., and ALEXIS (all from San Diego, CA) all provide kits to identify apoptotic cells based either on a single-step procedure utilizing TdT and FITC-conjugated dUTP (APO-DIRECT) or TdT and BrdUTP, as described earlier (APO-BRDU<sup>TM</sup>). A description of the method, which is nearly identical to the one presented in this chapter, is included with the kit. Another kit (ApopTag), based on two-step DNA strand break labeling with digoxigenin-16-dUTP by TdT, is provided by Intergen (Purchase, NY).
2. Apoptotic cells are strongly labeled with fluoresceinated anti-BrdU Ab which distinguishes them from the nonapoptotic cells (Fig. 5). Because of the high intensity of their green fluorescence, an exponential scale often must be used for data acquisition and display.
3. Analysis of the bivariate DNA content vs DNA strand break-labeling distributions makes it possible to identify the cell-cycle position of cells in apoptotic and nonapoptotic populations.
4. When apoptosis is more advanced late apoptotic cells may have diminished DNA content because of prior shedding of apoptotic bodies (which may contain nuclear fragments), or due to such massive DNA fragmentation that small DNA fragments cannot be retained in the cell even after fixation with formaldehyde. Such late apoptotic cells, thus may have sub-G<sub>1</sub> DNA content (not shown in Fig. 5).
5. In some instances of apoptosis, DNA fragmentation stops after the initial DNA cleavage to 50–300 kb fragments (4,5). The frequency of DNA strand breaks in nuclei of these cells is low, and therefore they may not be easily detected by the TUNEL method.

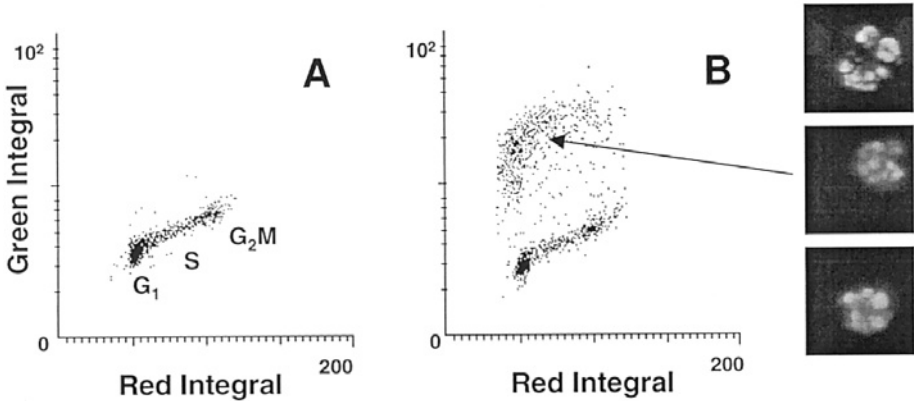


Fig. 5. Detection of apoptotic cells based on the presence of DNA strand breaks. U937 cells were untreated (A) or treated TNF- $\alpha$  in the presence of cycloheximide (B) (refs. 26,28). The cells were then subjected to DNA strand break labeling and DNA staining as described in the protocol. The bivariate distributions (scatterplots) allow one to identify apoptotic cells as the cells with DNA strand breaks, and reveal the cell-cycle position of cells in either apoptotic or nonapoptotic population.

## 8. THE FLUOROCHROME LABELED INHIBITORS OF CASPASES (FLICA) ASSAY

Activation of caspases is the critical event initiating the irreversible steps of apoptosis (25). One assay of their activation relies on the use of fluorochrome-labeled inhibitors (FLICA) that covalently bind to their active centers (26). Each FLICA consists of three functionally distinct parts: (a) the fluorochrome, (b) the recognition peptide, and (c) the halo- (generally fluoro-) methyl ketone moiety. For example, one such ligand, the carboxyfluorescein-(FAM)-valylalanylaspatic acid- (VAD)-fluoromethyl ketone (FMK) has only three amino acid (VAD) recognition sequence, which makes it nonspecific, generic ligand that can detect activation of every caspase. Other inhibitors, such as FAM-DEVD-FMK or FAM-VEID-FMK, are designed to target caspase-3 or caspase-6, respectively, more specifically. These ketone reagents penetrate through the plasma membrane of live cells and are relatively nontoxic to the cell (26). Their irreversible binding to active centers of the caspases ensures that only the cells with the activated enzymes become labeled. The protocol below is given for FAM-VAD-FMK, which is a substrate for all active caspases, but the same protocol can be applied to any other FLICA, such as with DEVD, VEID, YVAD, LETD, or LEHD recognition peptides.

### **8.1. Materials**

1. Dissolve lyophilized FAM-VAD-FMK (available as a component of the CaspaTag™ Fluorescein Caspase Activity kit from Intergen, Cat no. S7300) in DMSO as specified in the kit to obtain 150X concentrated (stock) solution of this inhibitor. Aliquots of this solution may be stored at  $-20^{\circ}\text{C}$  in the dark for several months.
2. Just prior to use prepare a 30X concentrated solution of FAM-VAD-FMK by diluting the stock solution 1:5 in PBS. Mix the vial until becomes transparent and homogenous. This solution should be made fresh. Protect all FAM-VAD-FMK solutions from light.
3. FLICA staining solution: just prior to the use add 3  $\mu\text{L}$  of 30X concentrated FAM-VAD-FMK solution into 100  $\mu\text{L}$  of culture medium.
4. Stock solution of PI: Dissolve 1 mg of PI (Molecular Probes) in 1 mL of distilled water.
5. Rinsing solution: 1% (w/v) BSA in PBS.
6. Staining solution of PI: Add 10  $\mu\text{L}$  of stock solution of PI to 1 mL of the rinsing solution.

### **8.2. Cell Staining and Analysis by LSC**

1. Attach the cells to the microscope slide electrostatically (within the shallow wells), or by growing them on the slide or coverslip, as described in the Sub-heading 3.2. Keep the cells immersed in the culture medium by adding 100  $\mu\text{L}$  of the medium (with 10% serum) into the well on the microscope slide to cover the area with the cells.
2. Remove the medium and replace it with 100  $\mu\text{L}$  of FLICA (FAM-VAD-FMK) staining solution.
3. Place a  $\sim 2 \times 4$  cm strip of Parafilm atop the staining solution to prevent drying. Incubate the slides horizontally for 1 h at  $37^{\circ}\text{C}$  in a closed box with wet tissue or filter paper to ensure 100% humidity, in the dark.
4. Remove the staining solution with Pasteur pipet. Rinse three times with the rinsing solution each time by adding new aliquot, gently mixing, and after 2 min replacing with the next rinse.
5. Apply one or two drops of the PI staining solution atop of the cells deposited on the slide. Cover with a coverslip and seal the edges to prevent drying.
6. Measure cell fluorescence on LSC. Use the argon ion laser (488 nm) to excite fluorescence, contour on light scatter and measure green fluorescence of FAM-VAD-FMK at  $530 \pm 20$  nm and red fluorescence of PI at  $>600$  nm.

### **8.3. Notes**

1. Protect cells from light throughout the procedure.
2. Staining with PI is optional (e.g., Fig. 6). It allows to distinguish the cells that have integrity of plasma membrane compromised to the extent that they cannot exclude PI (necrotic and late apoptotic cells, cells with mechanically damaged membranes, isolated cell nuclei).



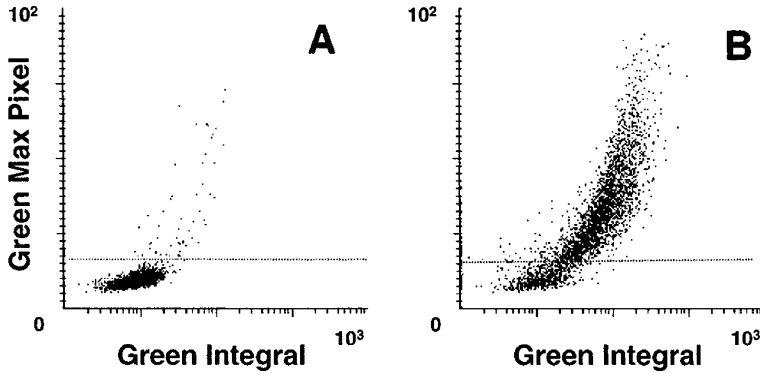


Fig. 6. Activation of caspases detected by the fluorochrome-labeled caspase (FLICA) inhibitors assay. HL-60 cells were untreated (**A**), treated in culture with camptothecin to induce apoptosis (**B**) (ref. 26). The cells were then electrostatically attached to microscope slides, incubated with staining solution of FAM-VAD-FMK as described in the protocol, and their green fluorescence (integrated value and pixel of maximal intensity) measured by LSC. Note the appearance of apoptotic cell subpopulation characterized by the increased green fluorescence (above the marked threshold level of the maximal pixel) reflecting activation of caspases that bind FAM-VAD-FMK.

3. After step 4 the cells may be fixed in 1% formaldehyde followed by 70% ethanol and then subjected to staining with PI in the presence of RNase, e.g., as described in Subheading 7.3., steps 6–8. Analysis of the FLICA vs PI fluorescence by LSC would allow then to correlate activation of caspases with cellular DNA content, i.e., the cell-cycle position or DNA ploidy.

## 9. CLEAVAGE OF POLY(ADP-RIBOSE) POLYMERASE (PARP)

PARP is a nuclear enzyme involved in DNA repair that is activated in response to DNA damage (27). Early during apoptosis, PARP is cleaved by caspases, primarily by caspase-3 (25). The specific cleavage of this protein that results in distinct 89-kDa and 24-kDa fragments (usually detected electrophoretically) is considered one of the hallmarks of apoptosis. Antibodies that recognize the cleaved PARP products were recently developed and they can be used as immunocytochemical markers of apoptotic cells. The antibody to p89 PARP has been adapted to label apoptotic cells for detection by cytometry (28). The protocol below combines the detection of PARP cleavage and cellular DNA content measurement, which allows one not only to identify and score apoptotic cell populations, but also to correlate apoptosis with the cell cycle position or DNA ploidy.

### **9.1. Materials**

1. Fixatives: primary fixative: 1% methanol-free formaldehyde (available from Polysciences Inc., Warrington, PA) in PBS, pH 7.4. Secondary fixative: 70% ethanol.
2. Anti-PARP p89 antibody (Promega Corp., MI; defined by the vendor as anti-PARP-85 fragment, rabbit polyclonal, cat. no. G7341).
3. Fluorescein-conjugated anti-rabbit immunoglobulin Ab (DAKO Corporation, Carpinteria, CA).
4. 0.25% Solution of Triton X-100 (Sigma) in PBS.
5. PBS/BSA solution: 1% (w/v) solution of BSA (Sigma) in PBS.
6. Stock solution of PI: Dissolve 1 mg of PI (Molecular Probes) in 1 mL of distilled water.
7. Stock solution of RNase: Dissolve 2 mg of DNase-free RNase A (Sigma) in 1 mL of distilled water. If RNase is not DNase-free, boil this solution for 3 min. Solutions 4–7 may be stored at 4 °C for several weeks.
8. Staining solution of PI: Add 10  $\mu$ L of stock solution of PI and 100  $\mu$ L of stock solution of RNase to 1 mL of PBS. This solution is made freshly.
9. Mounting solution: Add 100  $\mu$ L of the staining solution of PI to 0.9 mL of glycerol.

### **9.2. Cell Attachment and Fixation**

1. Attach cells to the microscope slide by cytocentrifugation, electrostatically, or by growing them on the slide, as described in the Subheading 3.
2. Fix cells by immersing the slides in a Coplin jar containing 1% formaldehyde in PBS, on ice for 15 min.
3. Wash the slides briefly by immersing in PBS and transfer them into Coplin jars containing 70% ethanol. The cells may be stored in ethanol at  $-20^{\circ}\text{C}$  for several days.

### **9.3. Cell Staining and Analysis by LSC**

1. Remove the slide from 70% ethanol, rinse it sequentially in 50 and 30% ethanol, then in 0.25% Triton X-100/PBS solution for 10 min
2. Place the slide horizontally and deposit atop of the cells on the slide 100  $\mu$ L of anti-PARP p89 pAb diluted 1:200 in PBS/BSA. Cover with  $\sim 2 \times 4$  cm strip of Parafilm and place the slide in the box containing wet tissue or filter paper to ensure 100% humidity. Incubate for 2 h at room temperature, or at  $4^{\circ}\text{C}$  overnight.
3. With Pasteur pipet (or vacuum suction pipet) remove anti-PARP p89 Ab and rinse the cells twice with BSA/PBS.
4. Deposit atop of the cells on the slide 100  $\mu$ L of fluorescein-conjugated secondary Ab (swine anti-rabbit immunoglobulin) diluted 1:30 in PBS/BSA. Incubate 1 h in the dark at room temperature.
5. Remove the secondary Ab and rinse the cells twice with PBS/BSA. Deposit  $\sim 200$   $\mu$ L of the PI staining solution, cover with a strip of Parafilm, and incubate at 100% humidity at room temperature for 30 min.

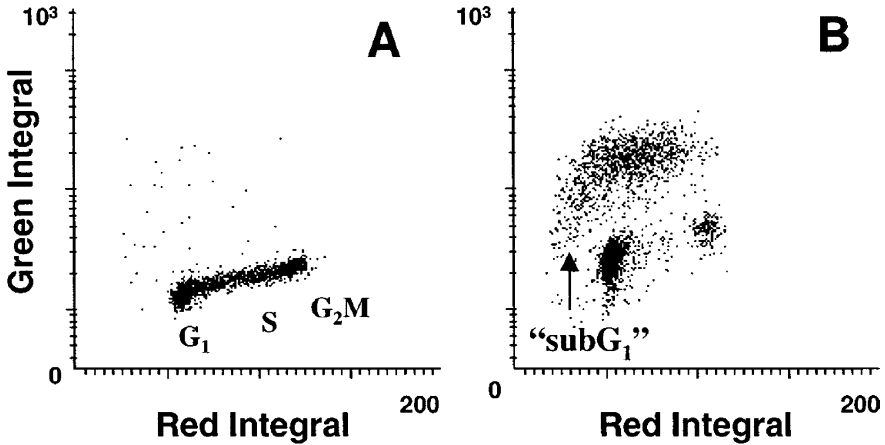


Fig. 7. Identification of apoptotic cells based on the immunocytochemical detection of the 89-kDa PARP cleavage fragment. HL-60 cells untreated (A) or treated with camptothecin (B) (refs. 26,28) were immunostained with FITC-anti-PARP p98 and PI according to the protocol. Note that in the treated culture, S phase cells preferentially were undergoing apoptosis. Some cells have diminished (“sub-G<sub>1</sub>”) DNA content, likely due to shedding of apoptotic bodies and/or extensive DNA fragmentation.

6. Remove the PI staining solution and mount the cells under a coverslip in a drop of the mounting solution. To preserve the specimen for longer period of time seal the coverslip with nail polish or melted paraffin and store at 4°C in the dark.
7. Measure cell fluorescence by LSC using argon ion laser (488 nm) to excite the emission. Use red fluorescence signal for contouring. Record green fluorescence of FITC-anti PARP p89 Ab at 530±20 nm and red fluorescence of PI at >600 nm.

#### 9.4. Notes

1. Bivariate scatterplots of PARP p89 vs DNA content allow one to distinguish subpopulations of apoptotic from nonapoptotic cells (based on the PARP p89 fluorescence) and assess the cell cycle distributions of these subpopulations (Fig. 7).
2. Late apoptotic cells that have lost DNA by fragmentation and/or via shedding of apoptotic bodies are characterized by a fractional (sub-G<sub>1</sub>) DNA content. Compared with early apoptotic cells, they also have diminished PARP p89 immunofluorescence.

#### ACKNOWLEDGMENTS

Supported by NCI grant CA RO1 28704, the Chemotherapy Foundation and This Close Cancer Research Foundation.

## REFERENCES

1. Darzynkiewicz, Z., Bruno, S., Del Bino, G., Gorczyca, W., Hotz, M. A., Lassota, P., and Traganos, F. (1992) Features of apoptotic cells measured by flow cytometry. *Cytometry* **13**, 795–808.
2. Darzynkiewicz, Z., Juan, G., Li, X., Murakami, T., and Traganos, F. (1997a) Cytometry in cell necrobiology: analysis of apoptosis and accidental cell death (necrosis). *Cytometry*, **27**, 1–20.
3. Vermes, I., Haanen, C. and Reutelingsperger, C. (2000) Flow cytometry of apoptotic cell death. *J. Immunol. Meth.* **243**, 167–190.
4. Collins, R. J., Harmon, B. V., Gobe, G. C., and Kerr, J. F. R. (1992) Internucleosomal DNA cleavage should not be the sole criterion for identifying apoptosis. *Int. J. Radiat. Biol.* **61**, 451–453.
5. Zamai, L., Falcieri, E., Marhefka, G., and Vitale, M. (1996) Supravital exposure to propidium iodide identifies apoptotic cells in the absence of nucleosomal DNA fragmentation. *Cytometry*, **23**, 303–311.
6. Finucane D. M., Waterhouse, N. J., Amaranto-Mendes. G.P., Cotter, T. G., and Green, D. R. (1999) Collapse of the inner mitochondrial transmembrane potential is not required for apoptosis of HL-60 cells. *Exp. Cell Res.*, **251**, 166–174.
7. Kerr, J. F. R., Wyllie, A. H., and Curie, A. R. (1972) Apoptosis: a basic biological phenomenon with wide-ranging implications in tissue kinetics. *Br. J. Cancer* **26**, 239–257.
8. Kametsky, L. A. (2001) Laser scanning cytometry. *Methods Cell Biol.* **63**, 51–87.
9. Darzynkiewicz, Z., Bedner, E., Li, X., Gorczyca, W., and Melamed, M.R (1999) Laser scanning cytometry. A new instrumentation with many applications. *Exp. Cell Res.* **249**, 1–12.
10. Bedner, E., Li, X., Gorczyca, W., Melamed, M. R., and Darzynkiewicz, Z. (1999) Analysis of apoptosis by laser scanning cytometry. *Cytometry* **35**, 181–195.
11. Bedner, E., Li, X., Kunicki, J., and Darzynkiewicz, Z. (2000) Translocation of Bax to mitochondria during apoptosis measured by laser scanning cytometry. *Cytometry* **41**, 83–88.
12. Deptala, A., Bedner, E., Gorczyca, W., and Darzynkiewicz, Z. (1998) Activation of nuclear factor kappa B (NF- $\kappa$ B) assayed by laser scanning cytometry. *Cytometry* **33**, 376–382.
13. Li, X. and Darzynkiewicz, Z. (1999) The Schrödinger's cat quandary in cell biology: integration of live cell functional assays with measurements of fixed cells in analysis of apoptosis. *Exp. Cell Res.* **249**, 404–412.
14. Koopman, G., Reutelingsperger, C. P. M., Kuijten, G. A. M., Keehnen, R. M. J., Pals, S. T., and van Oers, M. H. J. (1994) Annexin V for flow cytometric detection of phosphatidylserine expression of B cells undergoing apoptosis. *Blood* **84**,1415–1420.

15. Bedner, E., Melamed, M.R., and Darzynkiewicz, Z. (1998) Enzyme kinetic reactions and fluorochrome uptake rates measured in individual cells by laser scanning cytometry (LSC). *Cytometry*, **33**, 1–9.
16. Furuya, T., Kamada, T., Murakami, T., Kurose, A., and Sasaki, K. (1997) Laser scanning cytometry allows detection of cell death with morphological features of apoptosis in cells stained with PI. *Cytometry* **29**, 173–177.
17. Kawasaki, M., Sasaki, K., Satoh, T., Kurose, A., Kamada, T., Furuya, T., et al. (1997) Laser scanning cytometry (LSC) allows detailed analysis of the cell cycle in PI stained human fibroblasts (TIG-7). *Cell Prolif.* **30**, 139–147.
18. Zamzani, N., Brenner, C., Marzo, I., Susin, S. A., and Kroemer, G. (1998) Subcellular and submitochondrial mode of action of Bcl-2-like oncoproteins. *Oncogene* **16**, 2265–2282.
19. Darzynkiewicz, Z., Traganos, F., Staiano-Coico, L., Kapuscinski, J., and Melamed, M.R. (1982) Interactions of rhodamine 123 with living cells studied by flow cytometry. *Cancer Res.* **42**, 799–806.
20. Li, X., Du, L., and Darzynkiewicz, Z. (2000) During apoptosis of HL-60 and U937 cells caspases are activated independently of dissipation of mitochondrial electrochemical potential. *Exp. Cell Res.* **257**, 290–297.
21. van Engeland, M., Nieland, L. J. W., Ramaekers, F. C. S., Schutte, B., and Reutelingsperger, P. M. (1998) Annexin V -affinity assay: a review on an apoptosis detection system based on phosphatidylserine exposure. *Cytometry* **31**, 1–9.
22. Arends, M. J., Morris, R. G., and Wyllie, A. H. (1990) Apoptosis: The role of endonuclease. *Am. J. Pathol.* **136**, 593–608.
23. Gorczyca, W., Bruno, S., Darzynkiewicz, R. J., Gong, J., and Darzynkiewicz, Z. (1992) DNA strand breaks occurring during apoptosis: their early *in situ* detection by the terminal deoxynucleotidyl transferase and nick translation assays and prevention by serine protease inhibitors. *Int. J. Oncol.* **1**, 639–648.
24. Li, X. and Darzynkiewicz, Z. (1995) Labelling DNA strand breaks with BrdUTP. Detection of apoptosis and cell proliferation. *Cell Prolif.* **28**, 571–579.
25. Alnemri, E. S., Livingston, D. I., Nicholson, D. W., Salvesen, G., Thornberry, N. A., Wong, W. W and Yuan, J. (1996) Human ICE/CED-4 protease nomenclature. *Cell* **87**, 171–173.
26. Bedner, E., Smolewski, P., Amstad, P., and Darzynkiewicz, Z. (2000) Activation of caspases measured *in situ* by binding of fluorochrome-labeled inhibitors of caspases (FLICA): correlation with DNA fragmentation. *Exp. Cell Res.* **259**, 308–313.
27. de Murcia, G. and Menissier-de Murcia, J. M. (1994) Poly(ADP-ribose) polymerase: a molecular nick sensor. *Trends Biochem. Sci.* **19**, 172–176.
28. Li, X. and Darzynkiewicz, Z. (2000) Cleavage of poly(ADP-ribose) polymerase measured *in situ* in individual cells: relationship to DNA fragmentation and cell cycle position during apoptosis. *Exp. Cell Res.* **255**, 125–132.

# Specific Methods for Detection and Quantification of Apoptosis in Tissue Sections

---

Matthew A. Wallig, Curtis M. Chan, and Nancy A. Gillett

## 1. INTRODUCTION

Apoptosis as a distinct pathologic process has been recognized for decades. Its importance in many disease processes has become increasingly appreciated as new techniques for detecting and quantifying it have been developed with almost exponential rapidity. While all these techniques have their advantages and disadvantages, it is surprising how often simple morphologic assessment is overlooked in the rush to develop ever more sophisticated and “glitzy” techniques. With the appropriate training, apoptosis can be evaluated and even semi-quantified by simply examining a standard hematoxylin-and eosin-stained section closely and carefully. Admittedly, apoptosis (also termed apoptotic necrosis) can be harder to detect morphologically than necrosis (also termed oncotic necrosis). Its rapid progression once triggered (usually minutes), the rapid disposition of the apoptotic cells via ingestion by adjacent cells or resident macrophages (often just several hours), and the participation of only small numbers of cells at any one time during the process can make detecting apoptosis challenging. However, there are unique morphologic features associated with the process that an experienced morphologist can easily and rapidly detect to obtain a “global,” if not truly quantitative assessment of the degree of apoptosis occurring in a particular tissue. Simple morphologic assessment offers the advantages of giving the investigator an idea of the distribution of apoptosis within a tissue in the context of “real life” as well as the specific cell types involved within that tissue. It also allows one the advantage of observing the reaction on the

part of surrounding tissue, for example, whether the cells are being ingested by endogenous tissue macrophages, phagocytosed by adjacent tissue cells, or sloughing into the lumen of a hollow organ. Oftentimes simple morphologic assessment is a necessary prelude to other more sophisticated biochemical techniques in order to insure that there is not overinterpretation or misinterpretation of results obtained with the more elaborate, nonspecific (and often more expensive) methodology (1).

When actually observed histologically on slides prepared from tissues fixed and processed in standard fashion (i.e., fixed in 10% neutral buffered formalin, dehydrated in graded alcohols, embedded in paraffin, and sectioned at 3  $\mu\text{m}$  thickness, and stained with hematoxylin and eosin), apoptotic cells have characteristic and readily discernible features (2). One of the most prominent is shrinkage and sometimes fragmentation of *individual* cells within the affected tissue. Whole fields of cells are rarely, if ever, affected. The apoptotic cells or their fragments are shrunken and condensed and round in profile, with well-defined cell borders. Depending on the cell type involved, apoptotic cells can be either hyperbasophilic or hypereosinophilic compared to neighboring unaffected cells. They may also have a “waxy” or hyalin staining quality. The characteristic clearly defined boundaries of the apoptotic bodies may break after ingestion and degradation by a tissue macrophage or a neighboring cell.

Another consistent feature of apoptotic bodies is that a large proportion of them are surrounded by a clear space or “halo,” which usually represents the phagocytic vacuole of an adjacent parenchymal cell or tissue macrophage. Due to the rapidity of ingestion of the apoptotic body once it is formed, it is rare to see an uningested apoptotic body in a tissue section; therefore the halo around the apoptotic body is a consistent feature of the process. Perhaps the most noteworthy morphologic feature of apoptosis, if the affected organelle is in the plane of section, is the dense, *homogeneous* condensation of chromatin along the periphery of the nuclear membrane, often forming a “cap” or “crescent” of uniformly staining, intensely basophilic material at one pole of the nucleus (*see* Fig. 1). The nuclear envelope of apoptotic cells, unlike with necrosis, remains intact (3,4).

Another morphologic feature that aids in the identification of apoptosis in tissue sections is the reaction of surrounding tissues to the dying cells. In tissues in which apoptosis has occurred, there is a distinct lack of inflammatory reaction to the dying cells. Since in apoptosis no biologically active substances to activate neutrophils are generated or released by the dying cells, neutrophils are not present, even when widespread apoptosis is observed. However, the biochemical changes in the membranes of the

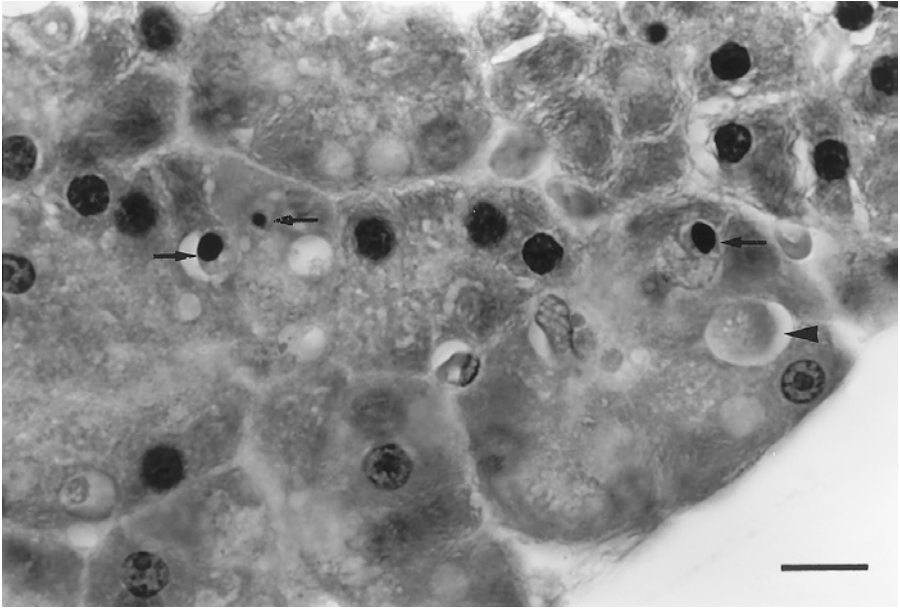


Fig. 1. Exocrine pancreas from a rat treated with 1-cyano-2-hydroxy-3-butene, a naturally occurring phytochemical that induces widespread pancreatic apoptosis within 12 h of a 200 mg/kg oral dose. Arrows point to pancreatic acinar cells with the typical apoptotic nuclear morphology (i.e., homogeneous chromatin crescents or caps with intact nuclear membrane). The arrowhead indicates an apoptotic body in which the nucleus is not in the plane of section. Hematoxylin and eosin, bar = 25  $\mu$ m.

apoptotic cells are stimulatory to neighboring tissue cells and macrophages, prompting rapid ingestion. Furthermore, release of intracellular enzymes does not occur and hence there is no activation of endothelium to activate inflammation.

The proportion of apoptotic cells present in a particular tissue section is usually quite low, oftentimes only 1–2% of the total cell population even in a tissue in which widespread and massive apoptotic necrosis is known to be occurring. In normal tissues, for example liver, the “background” of apoptotic cells is as low as 0.1%, which may be a problem if semi-quantification via counting is desired (*see* below). The rapidity of formation and the rapid degradation of the bodies by adjacent cells or phagocytes are major factors behind the low number of identifiable apoptotic bodies in a histologic sections and hence may lead the observer to underestimate the actual proportion of cells that are or have undergone the process. If the peak of the apoptotic response has passed, it may be almost impossible to determine if



apoptosis has even occurred. However, atrophy without scarring may be a primary change that could lead an investigator to deduce that apoptosis has occurred. Since true activation of the inflammatory reaction has not occurred, there may be collapse of stroma but no scarring in the usual sense of the word. Macrophages containing dark basophilic, or occasionally hypereosinophilic, round “tingible bodies” may be present, providing a further clue that apoptosis has indeed occurred. These bodies represent the partially degraded remnants of apoptotic cells within the phagolysosomes of the macrophage. Care must be taken to distinguish these digested bodies from secretory droplets that can also accumulate in these cells.

Although fairly stereotypical histomorphologically, some investigators have observed enough variation to subclassify apoptosis into at least two categories, Type I and Type II (5). While this is by no means standard across laboratories, the classification system has some merit in attempting to link specific morphologic manifestations with some of the functional differences in tissue or cellular apoptotic responses. The classification is not based on the “end stage” apoptotic body, which is basically the same in both types, but rather on differences in the sequence of cytosolic and nuclear changes that occur among various cell types. “Type I” (heterophagic) apoptosis is most consistent with “classic” apoptosis, and is most common in cell types with high mitotic activity or the potential for high mitotic activity. In Type I apoptosis, nuclear condensation of chromatin is an early event and participation by resident tissue macrophages in disposal of the apoptotic bodies is the typical response. The lysosomal content of cells involved in Type I apoptosis is generally low, and hence the apoptotic bodies are more stable. Thymocyte apoptosis after corticosteroid exposure is the classic example of this type.

With “Type II” (autophagic) apoptosis, by contrast, chromatin condensation often does not occur until after the cell has fragmented. Vacuolation of the apoptotic body may be prominent, coincident with internal lysosomal degranulation, which may even begin before fragmentation has been completed. Phagocytosis of the apoptotic bodies by adjacent cells in the tissue is often observed in this type. Apoptosis in renal tubular epithelium after exposure to okadaic acid could be considered the prototype for Type II apoptosis.

Although this type of classification has not been used by many investigators, it can provide insights at a qualitative level into mechanistic differences between various cell types in the genesis of apoptosis. However, the classification scheme has severe limitations, in part because a mixture of the two morphologic types can be readily observed, for example, in prostatic epithelium after castration.

Another means of dealing with the limitations of standard histopathology is to combine standard histologic examination with evaluation utilizing a molecular pathology technique such as immunohistochemistry or one of the molecular end-labeling techniques. These techniques can provide another layer of information with regard to the apoptotic status of a particular cell or cells. Each technique is able to examine one particular aspect of the apoptotic pathway from detection of pre-apoptotic associated proteins such as initiator caspases to detection of DNA fragmentation events. Since no single molecular event is a hallmark of apoptosis, information from multiple techniques should be utilized or at a minimum, an investigator should be aware of the limitations of each assay.

The morphologic features typically associated with apoptosis such as cellular shrinkage and membrane blebbing are the culmination of a complex biochemical cascade of molecular events. There are a number of fairly unique proteins associated with this apoptotic cascade and many of them can be detected immunohistochemically using specific antibodies. Though provide a brief overview of many of the immunohistochemical apoptosis assays is provided here, investigators who are interested in using immunohistochemistry to evaluate apoptosis should also read the very thorough review by Huppertz et al (6).

Those interested in using immunohistochemistry to study apoptosis need to consider the method of tissue preparation and fixation. Since many antibody epitopes do not survive formalin/glutaraldehyde fixation or paraffin embedding, investigators should determine under what conditions the antibody of interest will work prior to sample collection. There are antibodies that will successfully bind to formalin-fixed, paraffin-embedded material, but if the investigator is unsure, fresh snap-frozen samples can be used to optimize conditions for success since freezing generally will not alter epitopes.

## **2. USE OF CASPASE IMMUNOCYTOCHEMISTRY TO DETECT APOPTOSIS**

The caspases are a family of intracellular proteases responsible for the disassembly of the cell into apoptotic bodies. They are a popular target for immunohistochemical evaluation of apoptosis since these proteins are major components of the apoptotic cascade. Caspases are typically present in normal cells as inactive pro-enzymes that are activated in apoptotic cells by proteolytic cleavage into the active form. Active caspases contain a cysteine at their catalytic site and cleave target proteins adjacent to aspartate residues,

hence their name (cysteine **aspartases**). To date, 14 different caspases have been identified and are generally differentiated into two basic types, initiator (initiates cell death cascade) or effector (effects cell death disassembly).

The initiator caspases such as caspase-8, caspase-9, and caspase-10 are activated by external apoptosis inducers (Fas ligand, tumor necrpsos [TNF- $\alpha$ ], Granzyme B) or internal apoptosis inducers (release of cytochrome c in response to cellular damage) and initiate the apoptotic cascade. Caspase-8 has been shown by immunohistochemistry to have differential expression after apoptotic stimuli in rat cortical neurons following focal stroke (7) and in human lymphomas (8,9). Using immunohistochemistry, immunoelectron microscopy, and confocal immunofluorescence microscopy, caspase-9 (a member of the cytochrome-c apoptosis pathway) has been demonstrated to migrate in response to apoptotic stimuli (causing release of cytochrome-c) from inside of the mitochondria to the nucleus in several cell types (10). There are a number of commercially available antibodies that are capable of detecting specific initiator caspases in tissue sections, but it should be noted that although the detection of the initiator caspases in cells may be indicative of their expression, only the active forms of these caspases are associated with apoptosis. Many of the antibodies available against the caspases (both initiator and effector types) recognize an epitope that is present on both the inactive and active forms of the enzymes and cannot differentiate between the two forms. There are a few antibodies available that are directed against epitopes either in the pro-domain (capable of detecting the inactive pro-enzyme) or directed specifically against an epitope generated by the cleavage activation of the enzyme (detects only the active form). In general, use of anti-cleavage site specific antibodies is a more relevant marker of apoptosis than use of antibodies against epitopes present on both the active and inactive forms of the enzyme, especially in cell types where high levels of procaspases are normally present.

The effector caspases (caspase-3, caspase-6, caspase-7) are responsible for the morphological and biochemical changes that mark apoptosis. Activation of the effector caspases occurs via cleavage of the proform by activated initiator caspases and often marks the "point of no return" for cell death. Substrates for effector caspases include the caspases themselves (autoactivation), cytoskeletal components (i.e., actin, fodrin, and cytokeratins), poly (ADP-ribose) polymerase (PARP), and nuclear matrix proteins like Lamin B. Detection of caspase-3 expression by immunohistochemistry has been studied extensively due to its apical position in the effector caspase cascade (7-9,11-16). As with the initiator caspases, it is important to determine which form of the enzyme is recognized by the spe-

cific caspase antibody since antibodies against the cleaved (activated) form of caspase-3 are now available.

### **3. USE OF OTHER APOPTOSIS-REGULATED PROTEINS AND EVENTS IN DETECTION OF APOPTOSIS**

There are a number of other apoptosis-related proteins such as the apoptosis-inducing ligands such as Fas ligand (FasL) and TNF-related apoptosis-inducing ligand (TRAIL) and their receptors, which have been used as targets for immunohistochemistry. FasL has been shown by immunohistochemistry to be expressed in normal kidney in tubular epithelium and in glomeruli following glomerular injury suggesting that FasL plays a role in normal kidney cell homeostasis and in glomerular cell apoptosis following injury (17). Antibodies against the apoptosis-inducer FasL and its receptor, Fas, have been examined in a number of studies of human cancers, but expression of these proteins has been used more to attempt to predict tumor aggressiveness rather than as markers of apoptosis (18–21).

The bcl-2 family of proteins represent both repressors (bcl-2, bcl-x1) and inducers (bax, bak) of apoptosis. The ratio of bcl-2/bax expression as determined by immunohistochemical evaluation in pediatric acute lymphoblastic leukemia (22) and in nonlactating human mammary gland epithelium (23) may determine whether or not a cell becomes apoptotic. Levels of bcl-2 and bcl-x1 expression detected by immunohistochemistry appear to increase with the progression of malignant melanoma consistent with the idea that there is an increased malignant potential caused by inhibition of apoptosis by an increase in expression of apoptosis repressors (24). However, bcl-2 overexpression has been correlated with a lower risk of metastases and death in patients with infiltrating breast carcinoma (25) and has also been shown to have no prognostic significance with human colon carcinoma (26) so the relationship between bcl-2 and cancer progression is not clear.

One of the early apoptotic events is exposure of phosphatidylserine normally present in the inner leaflet of the plasma membrane to the outer leaflet otherwise known as the phosphatidylserine flip (PS-flip) (27,28). Detection of the PS-flip is possible using annexin V, a 35 kDa protein with a high affinity for phosphatidylserine. Because of the nature of the PS-flip, annexin V is most useful in studying intact cells such as in flow cytometry or confocal microscopy. Cells in fixed tissue sections are not intact and use of labeled annexin V would not be able to differentiate between internal and external phosphatidylserine, though at least one investigator has attempted to circumvent this problem (29).

The cleavage substrates for the execution caspases have also been targets for immunohistochemical detection of apoptosis. The intermediate filament cytokeratin 18 is cleaved by caspases 3, 6, and 7 following activation and can be detected by immunohistochemistry (30,31). PARP is a nuclear protein that is activated in response to DNA damage to repair DNA strand breaks and is a prominent caspase cleavage target during apoptosis. Lamin B is a nuclear envelope structural protein whose cleavage by activated effector caspases causes structural changes in the nucleus and ultimately leads to fragmentation and collapse of the nucleus associated with apoptosis. Both PARP and lamin B can be used as targets for immunohistochemistry and are indicative of effector caspase activity in tissue sections (32–34).

#### 4. MEASUREMENT OF DNA FRAGMENTATION IN DETECTION OF APOPTOSIS

Extensive DNA fragmentation is a characteristic event that often occurs early in cells undergoing apoptosis. Fragmentation of the DNA can result in double-stranded low molecular weight DNA fragments or in single-strand breaks or “nicks” in high molecular-weight DNA. The DNA strand breaks can be detected in tissue sections by labeling the 3<sup>1</sup>-OH ends with modified nucleotides such as X-dUTP (X = biotin, digoxigenin, or fluorescein). There are essentially two different approaches to labeling/staining fragmented DNA in tissue sections with modified nucleotides, *in situ* nick translation (ISNT) and *in situ* end labeling (ISEL). ISNT utilizes the repair mechanism of DNA polymerase I to catalyze the template-dependent addition of labeled nucleotides when one strand of a double-stranded DNA molecule is nicked (35). The ISEL techniques utilize a DNA polymerase to label the blunt ends of double-stranded DNA breaks independent of a template (36–38). Terminal deoxynucleotidyl transferase-mediated dUTP nick end-labeling (TUNEL, Fig. 2) is the most popular of the ISEL techniques and has been the most widely used histochemical marker for apoptosis (39). In either method, incorporation of the labeled nucleotides can be detected through a number of standard techniques on both formalin-fixed and frozen samples, a common approach being the use of an antibody directed against the nucleotide label.

Of the two techniques, it is commonly accepted that the ISEL techniques are more sensitive than the ISNT techniques since the ISNT technique theoretically labels not only apoptotic DNA, but also the random nicking of DNA occurring in cellular necrosis. Thus, in early stages of apoptosis, the ISEL techniques should preferentially label apoptotic cells while ISNT identifies

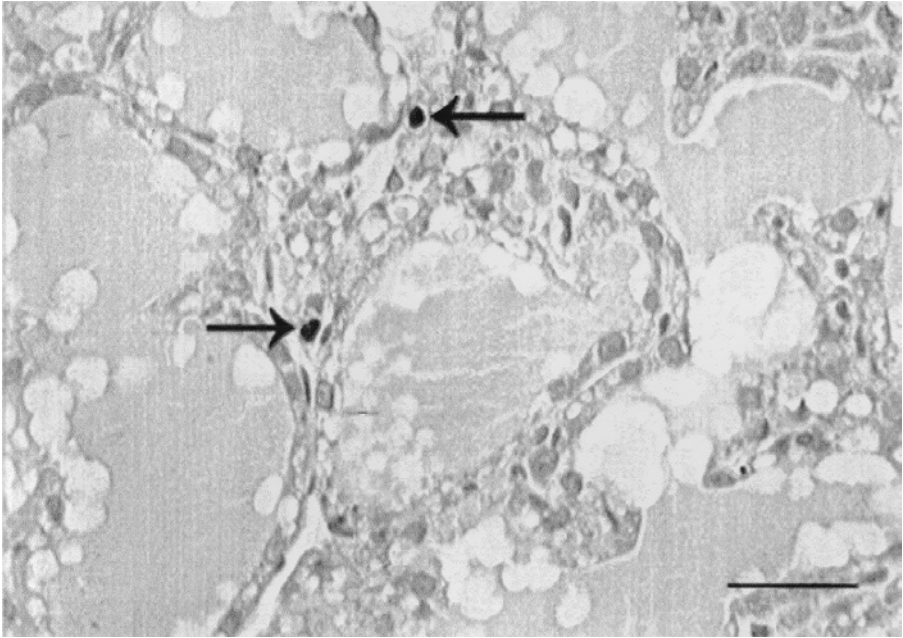


Fig. 2. Rat mammary gland, 3–4 d postweaning, stained by terminal deoxynucleotidyl transferase-mediated dUTP nick end-labeling (TUNEL) assay. The nuclei of the apoptotic cells are stained dark. Nonapoptotic cell nuclei are counterstained with hematoxylin (pale).

both apoptotic and necrotic cells. Though the TUNEL technique was initially heralded as the “definitive” technique for detecting apoptosis in tissue sections, subsequent studies have shown that the TUNEL techniques may also identify necrotic cells (but at a lower sensitivity or frequency than ISNT), and that with both the ISNT and ISEL techniques, false-positives may occur due to mechanical damage of the DNA during sampling. Also, it must be remembered that the use of ISNT or ISEL assays eliminates identification of those apoptotic cells in which the nucleus is absent or not in the plane of section and hence will “undercount” the number of apoptotic cells by as much as two-thirds (40), although there is a consistent correlation between the incidence of apoptotic bodies visualized histologically and the incidence of TUNEL positive cells. That being said, however, the ISEL techniques can still be one of the most valuable weapons in the arsenal of a trained morphologist studying apoptosis in tissue sections.

Antibodies directed against single-stranded DNA have been reported to be more specific than the TUNEL assay in differentiating apoptotic cells

from necrotic cells. DNA from apoptotic cells is less stable than DNA in nonapoptotic cells (including necrotic cells) due to action of activated proteases on DNA-stabilizing histones in the apoptotic cascade. Using a selective *in situ* thermal denaturation technique, it is possible to cause DNA denaturation in apoptotic cells but leave the DNA in nonapoptotic cells intact. Detection of the denatured single-stranded conformation DNA in apoptotic cells is then achieved by immunohistochemistry with a single-stranded DNA specific monoclonal antibody (MAb) (41–43).

Another possible adjunct to standard histologic examination is fluorescence microscopy, for example examining very thin (1–2  $\mu\text{m}$  thick) sections in which the highly condensed eosin-stained cytoplasm of the apoptotic cells will fluoresce intensely under UV light (44). This methodology has the advantage of counting those apoptotic cells in which the nucleus may be absent or out of the plane of section but it has the drawback of staining hyalin droplets, condensed microfilaments and other nonapoptotic structures.

## 5. QUANTIFICATION AND CLASSIFICATION OF APOPTOSIS IN TISSUE SECTIONS

Many investigators have attempted to semi-quantify or quantify apoptosis observed in histologic sections using a variety of counting methods. At the simplest level, one can grade histologic sections on a number scale, for example, 0–4+, with each degree indicating a percentage range of apoptotic cells per 400 $\times$  fields (0 = no lesions, 1+ = a mean of 1–5 apoptotic cells per 400 $\times$  field, 2+ = a mean of 5–10 apoptotic cells per 400 $\times$  field, etc.), with anywhere from 10–50 400 $\times$  fields examined. One can then list the findings in a table and allow the reader to draw his own conclusions or perform the appropriate statistical analysis (e.g., Student's *t*-test, analysis of variance) to compare the mean values of the rankings between treatment groups. Ranking is another semi-quantitative method that can be utilized when viewing histologic sections. In this case, the slides are evaluated subjectively in blind or double-blind fashion for the degree of apoptosis and ranked numerically in order from least severe to most severe, each slide receiving a number. Nonparametric statistical assessments, such as the Wilcoxon-Mann-Whitney or Wilcoxon rank sum tests can then be used to determine differences of significance between treatment groups.

Alternatively, one can count a set number of cells (e.g., 100) in a set number of 400 $\times$  fields (e.g., 10, 20, or 50), identifying and recording both normal and apoptotic cells to obtain a mean value, either a percentage or a ratio (e.g., 15 apoptotic cells per 1000–3000 total cells). This is probably the

more common method of quantifying apoptosis in tissue section. Counts can be performed either manually or through automated image analysis to determine apoptotic index, defined as the number of apoptotic bodies divided by the total number of nuclei counted (45,46). In order to estimate the rate of cell loss due to apoptosis, one can calculate the overall incidence of apoptosis for the duration of the study, multiply this figure by a factor to correct for the formation of more than one body by an apoptotic cell, (calculated as 0.5 for liver [3]) and divide the product by the duration of the visible manifestations of an apoptotic event (47). This, of course, necessitates evaluation of apoptosis at several time points in order to make the appropriate calculations. More complicated, precise, and predictive models for estimating the incidence of apoptosis using exponential equations have been developed for use (48).

In attempting to quantify apoptosis in tissue sections, an investigator should be cognizant of several factors. First of all quantification of microscopic samples represents a “snapshot” in time, which records the number of apoptotic cells at any one time; however, it is much less useful in determining rates of apoptosis over time. Sampling bias is always a concern, more so if the apoptotic lesions are not uniformly distributed within the particular tissue of interest. For example, does the gastric lobe of the exocrine pancreas have a higher incidence of apoptosis than the duodenal lobe, or are apoptotic bodies more frequent in the centrilobular portions of the hepatic lobule and virtually absent in periportal regions? Situations such as these might require separate counts for each lobe, lobule, or portion of lobule in order to get an unbiased estimate of the number of apoptotic cells present. Another consideration related to this is whether the apoptosis is confined to a particular lesion within the tissue yet absent from the unaffected portion of the tissue, such as enhanced apoptosis in a preneoplastic hepatic nodule. In this case, an investigator might consider counting all the cells in the nodule, both apoptotic and nonapoptotic, as well as the number of apoptotic and nonapoptotic cells in the surrounding “normal” tissue.

## **6. CONSIDERATION OF “CELL VOLUME” IN QUANTIFICATION OF APOPTOSIS**

Perhaps the biggest difficulty with microscopic quantification is the issue of bias associated with quantifying a three-dimensional structure in a two-dimensional section. In essence, investigators are quantifying nuclear profiles, rather than nuclei, and this terminology should be reflected in the published reports. Because the process of apoptosis leads to condensation of the nucleus, the size of the apoptotic nucleus is smaller than that of normal



nuclei. In tissue sections, the counts are based on nuclear profiles, and the condensation of the nuclei then results in an under-representation of the number of apoptotic cells as compared to normal nuclei. Ideally, unbiased counts would utilize proper stereologic techniques that count objects in a three dimensional volume, rather than a two-dimensional area. Within stereology, optical- or physical-dissector methods have been developed to count in an unbiased manner, different sized structures within a defined volume (49). However, for quantification of apoptotic nuclei, we are limited by the techniques available to identify apoptosis. Optical dissector methods are employed on sections much thicker than those normally used to identify apoptosis. New methodologies are available that have simplified physical dissector techniques, however, they are not yet widely used. The individual using morphologic sections for quantification of apoptosis should be aware of the limitations and mathematical bias in counting nuclear profiles in two-dimensional sections. If there is a dramatic difference between the groups, this probably appropriately reflects a change in numbers of apoptotic cells. However, if the numbers are quite close, a true three-dimensional quantification, or nonmorphologic quantification should be done.

A further consideration that is very important in whole animal studies is the inter-individual variation in response to treatment. This variation can be quite high between animals and it has been recommended that at least 10 animals per treatment be used if one wishes to quantify apoptosis in a tissue (4). A final item that can become a concern is those situations where the basal apoptotic index is very low (<0.1%), in which case counting sufficient apoptotic bodies to obtain an index of sufficient confidence may warrant the counting of far more cells than originally intended, perhaps as many as 6000 (3,44).

While histopathologic examination may be a relatively quick, inexpensive way to screen for apoptosis, in some cases the morphologic changes may be rare or subtle enough that distinguishing apoptotic cells from degenerate cells undergoing autophagy or from individual cells actually undergoing necrosis may be difficult. Discerning chromatin crescents or caps within an intact nuclear membrane may be difficult if the tissue is poorly fixed, autolytic, or sectioned too thickly, but methyl green pyronin may be used to aid in discernment of chromatin crescents (3). However, ultrastructural examination of the tissue may be necessary at some point to confirm histologic findings. Furthermore, it is virtually impossible to determine organellar morphology in standard formalin-fixed, paraffin-embedded tissues and usually difficult even in glutaraldehyde fixed, plastic embedded tissues sectioned at 1  $\mu\text{m}$  and stained with toluidine blue. Therefore, when initially defining a lesion as "apoptotic," it is often worthwhile to do at least one ultrastructural evaluation of the tissue being studied.

## 7. ULTRASTRUCTURAL EVALUATION OF APOPTOSIS

Ultrastructural examination of tissues is, in many minds, the “gold standard” for confirming that a suspected tissue change is indeed apoptosis. With minor changes, the criteria outlined by Kerr et al. (50) still stand as the essential features of apoptosis. While the methodology for standard ultrastructural examination is fairly routine, care should be taken in selecting a fixative (e.g., if one wants to perform immunohistochemistry one must determine if the antigen is glutaraldehyde sensitive), fixative buffer (e.g., dextran instead of sucrose to minimize shrinkage or swelling), method of fixation (immersion vs perfusion), and embedding medium (epoxides for morphology, acrylates for immunohistochemistry).

Among the earliest and most apparent change in tissue sections is the detachment of the dying cell from its neighbors and its rapid transformation into a “round” (i.e., spherical) morphology with a smooth plasma membrane and loss of specialized surface structures (Fig. 3). If the cell is a secretory cell, there is usually an initial degranulation that occurs prior to its assuming a rounded configuration. Initial dilation of the endoplasmic reticulum may also be present but careful examination will reveal that ribosomes are intact and that little membrane degradation has occurred. As the cells round up, the cytosol becomes denser and organelles cluster closer together. “Zeiosis,” a rapid process in which the cell “pinches off” into numerous round (i.e., spherical) membrane bound fragments is frequently observed in many cell types, being a very prominent feature in cells of lymphoid or hematopoietic origin. Despite the rounding and fragmentation, the plasma membrane is preserved until after the apoptotic body is ingested and a phagolysosome is formed around it.

Organelle morphology is generally well-preserved in apoptosis, even though substantial biochemical changes are happening. In recent ultrastructural studies, however, subtle changes within mitochondria have been detected. These consist of minute “herniations” of the inner mitochondrial membrane through the outer mitochondrial membrane, with focal swelling of the matrix, and loss of cristae in the vicinity of the breach in the outer membrane. In the remaining portions of the mitochondria, the ultrastructural arrangement of inner and outer membrane, cristae, and matrix remain intact. Furthermore, this change is not uniform among all mitochondria, with usually only a few mitochondria in an apoptotic cell having visible evidence of this localized microherniation and swelling. This is in marked contrast to cells undergoing necrosis, where mitochondrial swelling, loss of cristae, and rarefaction of matrix is a prominent and consistent feature affecting almost

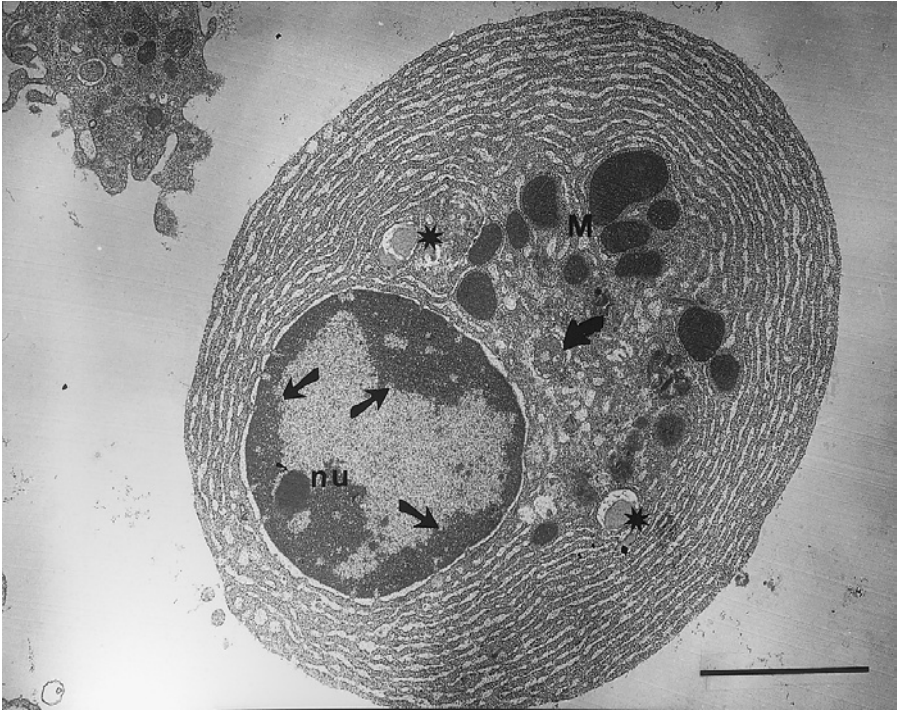


Fig. 3. An apoptotic pancreatic acinar cell from a rat treated with 1-cyano-2-hydroxy-3-butene. The cell has a rounded morphology and has lost all but a few of its zymogen granules (\*). There is early condensation of nuclear chromatin (small arrows) around the margins of the nuclear envelope and the nucleolus (nu) is partially segregated from the chromatin. Most mitochondria (M) are normal in morphology, although one swollen one (large arrow) with microherniation is present. Bar = 5  $\mu$ m.

all mitochondria in the dying cell. Interestingly, in the affected mitochondria, free cytochrome oxidase within the swollen portion of the organelle can be identified by immunochemical methods (51).

The nuclear changes that are unique to apoptosis may occur prior to, during, or even some time after the cytoplasmic changes, depending on cell type. Characteristically, there is preservation of the nuclear envelope, segregation of the nucleolus from chromatin, and the uniform condensation of chromatin into crescents or smooth-edged clusters along the inner margins of the intact nuclear envelope. Zeiosis may also occur in the nucleus, but, as with the cytoplasm, the nuclear membranes surrounding the fragments remain intact. The formation and condensation of uniformly dense compact chromatin masses allows for unequivocal determination of apoptosis since

in necrosis, chromatin clumping will not be uniformly electron-dense, regular, or compact (52). Nucleolar segregation away from the chromatin into the relatively clear, electron-lucent nucleoplasm is often easily discerned by electron microscopy even though this is usually hard to detect histologically.

Although ultrastructural examination of dying cells provides unequivocal evidence of apoptosis, this methodology is time-consuming and can be expensive. In addition, quantification is difficult if not impossible to the vast number of thin sections that would have to be examined, the large amount of time it would take to examine these sections, and obvious sampling bias in selecting sections for examination. Nevertheless, ultrastructural examination remains the ultimate qualitative methodology for confirming the presence of apoptosis in tissues with dying cells.

## REFERENCES

1. Renvoize, C., Biola, A., Pallardy, M., and Breard, J. (1998) Apoptosis: identification of dying cells. *Cell Biol. Toxicol.* **14** (2), 111–120.
2. Wyllie, A. H., Kerr, J. F. R., and Currie, A. R. (1980) Cell death: the significance of apoptosis. *Int. Rev. Cytol.* **68**, 251–307.
3. Bursch, W., Tuper, H. S., Lauer, B., and Schulte-Harmann, R. (1985) Quantitative histological and histochemical studies on the occurrence and stages of controlled cell death (apoptosis) during regression of rat liver hyperlasia. *Virchows Arch. [Cell Pathol.]* **50**, 153–166.
4. Goldsworthy, T. L., Franssen-Steen, R., and Maronpot, R. R. (1996) Importance of and approaches to quantification of hepatocyte apoptosis. *Toxicol. Pathol.* **24**(1), 24–35.
5. Majno, G., and Joris, I. (1995) Apoptosis, oncosis and necrosis: an overview of cell death. *Amer. J. Pathol.* **146**, 3–15.
6. Huppertz, B., Frank, HG, Kauffmann, P. (1999) The apoptosis cascade: morphological and immunohistochemical methods for its visualization. *Anat. Embryol.* **200**, 1–18.
7. Velier, J., Ellison, J., Kikly, K., Spera, P., Barone, F., Feuerstein, G. (1999) Caspase-8 and Caspase-3 are expressed by different populations of cortical neurons undergoing delayed cell death after focal stroke in the rat. *J. Neurosci.* **19**(14), 5932–5941.
8. Soini, Y., and Paakko, P. (1999) Apoptosis and expression of caspases 3, 6 and 8 in malignant non-Hodgkin's lymphomas. *APMIS* **107**(11), 1043–1050.
9. Xerri, L., Palmerini, F., Devilard, E., Defrance, T., Bouabdallah, R., Hassoun, J., and Birg, F. (2000) Frequent nuclear localization of ICAD and cytoplasmic co-expression of caspase-8 and caspase-3 in human lymphomas. *J. Pathol.* **192**, 194–202.
10. Krajewski, S., Krajewska, M., Ellerby, L., Welsh, K., Xie, Z., Deveraux, Q., et al. (1999) Release of caspase-9 from mitochondria during neuronal apoptosis and cerebral ischemia. *Proc. Natl. Acad. Sci. USA* **96**, 5752–5757.

11. Krupinski, J., Lopez, E., Marti, E., and Ferrer, I. (2000) Expression of caspases and their substrates in the rat model of focal cerebral ischemia. *Neurobio. Dis.* **7**, 332–342.
12. Tanaka, M., Momoi, T., and Marunouchi, T. (2000) In situ detection of activated caspase-3 in apoptotic granule neurons in the developing cerebellum in slice cultures and in vivo. *Brain Res. Dev. Brain Res.* **121(2)**, 223–228.
13. Hartmann, A., Hunot, S., Michel, P., Muriel, P., Vyas, S., Faucheux, B., et al. (2000) Caspase-3: a vulnerability factor and final effector in apoptotic death of dopaminergic neurons in Parkinson's disease. *Proc Natl. Acad. Sci. USA* **97(6)**, 2875–2880.
14. Urase, K., Fujita, E., Miho, Y., Kouroku, Y., Mukasa, T., Yagi, Y., et al. (1998) Detection of activated caspase-3 (CPP32) in the vertebrate nervous system during development by a cleavage site-directed antiserum. *Brain Res. Dev. Brain Res.* **111(1)**, 77–87.
15. Pompeiano, M., Blaschke, A. J., Flavell, R. A., Srinivasan, A., and Chun, J. (2000) Decreased apoptosis in proliferative and postmitotic regions of the Caspase 3-deficient embryonic central nervous system. *J. Comp. Neurol.* **423(1)**, 1–12.
16. Mukasa, T., Momoi, T., and Momoi, M. Y. (1999) Activation of caspase-3 apoptotic pathways in skeletal muscle fibers in laminin alpha2-deficient mice. *Biochem. Biophys. Res. Commun.* **260(1)**, 139–142.
17. Lorz, C., Ortiz, A., Justo, P., Gonzalez-Cuadrado, S., Duque, N., Gomez-Guerrero, C., and Egido, J. (2000) Proapoptotic fas ligand is expressed by normal kidney tubular epithelium and injured glomeruli. *J. Am. Soc. Nephrol.* **11**, 1266–1277.
18. Basolo, F., Fiore, L., Baldanzi, A., Giannini, R., Dell'Omodarme, M., Fontanini, G., et al. (2000) Suppression of Fas expression and down-regulation of Fas ligand in highly aggressive human thyroid carcinoma. *Lab. Invest.* **80(9)**, 1413–1419.
19. Herrnring, C., Reimer, T., Jeschke, U., Makovitzky, J., Kruger, K., et al. (2000) Expression of the apoptosis-inducing ligands FasL and TRAIL in malignant and benign human breast tumors. *Histochem. Cell Biol.* **113**, 189–194.
20. Ito, Y., Takeda, T., Sasaki, Y., Sakon, M., Yamada, T., Ishiguro, S., et al. (2000) Expression of fas and fas ligand reflects the biological characteristics but not the status of apoptosis of intrahepatic cholangiocellular carcinoma. *Int. J. Mol. Med.* **6(4)**, 581–586.
21. Nakamura, M., Rieger, J., Weller, M., Kim, J., Kleihues, P., and Ohgaki, H. (2000) APO2L/TRAIL expression in brain tumors. *Acta Neuropathol.* **99**, 1–6.
22. Srinivas, G., Kusumakumary, P., Nair, M. K., Panicker, K. R., and Pillai, M. R. (2000) Mutant p53 protein, Bcl-2/Bax ratios and apoptosis in paediatric acute lymphoblastic leukaemia. *J. Cancer Res. Clin. Oncol.* **126(1)**, 62–67.
23. Feuerhake, F., Sigg, W., Hofter, E. A., Dimpfl, T., Welsch, U. (2000) Immunohistochemical analysis of Bcl-2 and Bax expression in relation to cell turnover and epithelial differentiation markers in the non-lactating human mammary gland epithelium. *Cell Tissue Res.* **299**, 47–58.
24. Leiter, U., Schmid, R., Kaskel, P., Peter, R., and Krahn, G. (2000) Antiapoptotic bcl-2 and bcl-xL in advanced malignant melanoma. *Arch. Dermatol. Res.* **292**, 225–232.

25. Le, M. G., Mathieu, M. C., Douc-Rasy, S., Le Bihan, M. L., Adb El All, H., Spielmann, M., and Riou, G. (1999) c-myc, p53 and bcl-2, apoptosis-related genes in infiltrating breast carcinomas: evidence of a link between bcl-2 protein over-expression and a lower risk of metastasis and death in operable patients. *Int. J. Cancer* **84**(6), 562–567.
26. Bukholm, I. and Nesland, J. (2000) Protein expression of p53, p21 (WAF1/CIP1), bcl-2, Bax, cyclin D1 and pRb in human colon carcinomas. *Virchows Arch.* **436**, 224–288.
27. Martin, S. J., Reutelingsperger, C. P., McGahon, A. J., Rader, J. A., van Schie, R. C., LaFace, D. M., and Green, D. R. (1995) Early redistribution of plasma membrane phosphatidyl serine is a general feature of apoptosis regardless of the initiating stimulus: inhibition by overexpression of Bcl-2 and Abl. *J. Exp. Med.* **182**(5), 1545–1556.
28. Martin, S. J., Finucane, D. M., Amarante-Mendes, G. P., O'Brien, G. A., and Green, D. R. (1996) Phosphatidylserine externalization during CD95-induced apoptosis of cells and cytoplasts requires ICE/CED-3 protease activity. *J. Biol. Chem.* **271**(46), 28,753–28,756.
29. Bronckers, A. L. J. J., Goei, S. W., Dumont, E., Lyaruu, D. M., Woltgens, J. H. M., van Heerde, W. L., et al. (2000) In situ detection of apoptosis in dental and periodontal tissues of the adult mouse using annexin-V-biotin. *Histochem. Cell Biol.* **113**, 293–301.
30. Carr, N. J. (2000) M30 expression demonstrates apoptotic cells correlates with in situ end-labeling, and is associated with Ki-67 expression in large intestinal neoplasms. *Arch. Pathol. Lab. Med.* **124**(12), 1768:1772.
31. Leers, M. P., Kolgen, W., Bjorklund, V., Bergman, T., Tribbick, G., Persson, B., et al. (1999) Immunocytochemical detection and mapping of a cytokeratin 18 neo-epitope exposed during early apoptosis. *J. Pathol.* **187**(5), 567–572
32. Mandir, A. S., Przedborski, S., Jackson-Lewis, V., Wang, A., Simbulan-Rosenthal, C. M., Smulson, M. E., et al. (1999) Poly(ADP-ribose) polymerase activation mediates 1-methyl-4-phenyl-1,2,3,6-tetrahydropyridine (MPTP)-induced parkinsonism. *Proc. Natl. Acad. Sci. USA* **96**, 5774–5779.
33. Davis, R. E., Mysore, V., Browning, J. C., Hsieh, J. C., Lu, Q., and Katsikis, P. D. (1998) In situ staining for poly(ADP-ribose) polymerase activity using an NAD analogue. *J. Histochem. Cytochem.* **46**(11), 1279–1289.
34. Hytioglou, P., Choi, S. W., Theise, N. D., Chaudhary, N., Worman, H. J., and Thung, S. N. (1993) The expression of nuclear lamins in human liver: an immunohistochemical study. *Hum. Pathol.* **24**(2), 169–172.
35. Hashimoto, S., Koji, T., Niu, J., Kanematsu, T., and Nakane, P. K. (1995) Differential staining of DNA strand breaks in dying cells by non-radioactive in situ nick translation. *Arch. Histol. Cytol.* **58**(2), 161–170.
36. Chun, J. (1998) Detection of cells undergoing programmed cell death using in situ end-labeling plus, in *Apoptosis Detection and Assay Methods* (Zhu, L. and Chun, J. M., eds.), Biotechniques Books, Natick, MA, pp. 7–14.
37. Wijmsman, J. H., Jonker, R. R., Keijzer, R., van de Velde, C. J., Cornelisse, C. J., and van Dierendonck, J. H. (1993) A new method to detect apoptosis in paraffin sections: in situ end labeling of fragmented DNA. *J. Histochem. Cytochem.* **41**(1), 7–12.

38. Wood, K. A., Diapsquale, B., and Youle, R. J. (1993) In situ labeling of granule cells for apoptosis-associated DNA fragmentation reveals different mechanisms of cell loss in developing cerebellum. *Neuron* **11(4)**, (Zhu, L. and Chun, J. M., eds.) 621–632.
39. Gavrieli, Y., Sherman, Y., and Ben-Sasson, S. A. (1992) Identification of programmed cell death in situ via specific labeling of nuclear DNA fragmentation. *J. Cell Biol.* **119(3)**, 493–501.
40. Wheeldon, E. B., Williams, S. M., Soanes, A. R., James, N. H., Roberts, R. A. (1995) Quantitation of apoptotic bodies in rat liver by *in situ* end labelling (ISEL): Correlation with morphology. *Toxicol. Pathol.* **23(3)**, 410–415.
41. Frankfurt, O. S., Robb, J. A., Sugarbaker, E. V., and Villa, L. (1997) Apoptosis in breast carcinomas detected with monoclonal antibody to single-stranded DNA: relation to bcl-2 expression, hormone receptors, and lymph node metastases. *Clin. Cancer Res.* **3(3)**, 465–471.
42. Frankfurt, O. S., Robb, J. A., Sugarbaker, E. V., and Villa, L. (1996) Monoclonal antibody to single-stranded DNA is a specific and sensitive cellular marker of apoptosis. *Exp. Cell Res.* **226(2)**, 387–397.
43. Frankfurt, O. S. (1998) Detection of apoptotic cells with monoclonal antibodies to single-stranded DNA, in *Apoptosis Detection and Assay Methods* (Zhu, L. and Chun, J. M., eds.) Biotechniques Books, Natick, MA, pp.47–62.
44. Stinchcombe, S., Buchmann, A., Bock, K. E., and Schwarz, M. (1995) Inhibition of apoptosis during 2,3,7,8-tetrachlorodibenzo-*p*-dioxin-mediated tumour promotion in rat liver. *Carcinogenesis* **16(6)**, 1271–1275.
45. Kong, J., and Ringer, D. P. (1995) Quantitative in situ image analysis of apoptosis in well and poorly differentiated tumor from rat liver. *Am. J. Pathol.* **147(6)**, 1626–1632.
46. Fujita, K., Ohyama, H., and Yamada, T. (1997) Quantitative comparison of in situ methods for detecting apoptosis induced by X-ray irradiation in mouse thymus. *Histochem. J.* **29**, 823–830.
47. Bursch, W., Patte, S., Putz, B., Barthel, G., and Schulte-Hermann, R. (1990) Determination of the length of the histological stages of apoptosis in normal liver and in altered hepatic foci of rats. *Carcinogenesis* **11(5)**, 847–853.
48. Moolgavkar, S. H., Luebeck, E. G. (1992) Interpretation of labeling indices in the presence of cell death. *Carcinogenesis* **13(6)**, 1007–1010.
49. Howard, C. V., Reed, M. G. (1998) *Unbiased Stereology: Three Dimensional Measurement in Stereology*. Springer-Verlag, New York, New York.
50. Kerr, J. F. R., Wyllie, A. H., and Currie, A. R. (1972) Apoptosis: A basic biological phenomenon with wide-ranging implications in tissue kinetics. *Br. J. Cancer.* **68**, 239–257.
51. Angermuller, S., Schuman, J., Fahimi, H. D., Tiege, G. (1999) Ultrastructural alterations of mitochondria in pre-apoptotic and apoptotic hepatocytes of TNF-alpha-treated galactosamine-sensitized mice. *Ann NY Acad. Sci.* **887**, 12–1748.
52. Payne C. M., and Cromey, D. W. (1991) Ultrastructural analysis of apoptotic and normal cells using digital imaging techniques. *J. Comp.-Assisted Microscopy* **3(1)**, 33–50.

## DNA Microarrays

### *An Overview of Technologies and Applications*

---

**Helmut Zarbl**

#### **1. INTRODUCTION**

The Genome Project and the technological innovations that it spawned have dramatically altered the future course of all biological research. The Genbank database already harbors billions of base pairs of DNA sequences derived from millions of individual sequence entries (<http://www.ncbi.nlm.nih.gov/WEB/Genbank/index.html>). The first complete genomic sequence to be completed was that of *Haemophilus influenzae* (1). Since then, the genomes of more than 30 additional organisms have been completed and made available to the research community (<http://www.ncbi.nlm.nih.gov/Entrez/Genome/org.html>). Continued improvements in high-throughput DNA sequence technology made it possible to complete 90% of the reference human genome sequence in 2000, several years ahead of schedule. To utilize the enormous potential of genome-wide sequence information will require the development of a battery of new tools for high-throughput and highly parallel molecular analyses and commensurate bioinformatics tools to analyze data sets of unprecedented depth and complexity.

An increasing number of molecular techniques for high-throughput analyses of gene expression and genetic polymorphisms continue to be developed in both academic and commercial settings. Examples of high-throughput analytical methodologies include automated DNA sequencing, serial analysis of gene expression (2), denaturing high-performance liquid chromatography (HPLC) (3), differential display (4), high density filter hybridization (5), and highly sensitive mutation assays coupled with iterative sample re-pooling strategies (6). While each of these approaches has advantages and limita-



tions, none possess the versatility or potential of DNA microarrays, also known as DNA “chips.” The unprecedented capacity of DNA chips for highly parallel detection of RNA expression and/or DNA variation at the genomic level ensure a major role for microarrays in functional genomics, the study of how genome-wide genetic variation and patterns of gene expression interact to produce complex biological responses, including apoptosis.

The response of cells or organisms to morphogens, toxic stimuli, DNA damage, or inappropriate expression of oncogenes can range from the induction of a specific xenobiotic-metabolizing enzyme to the induction of a program of cellular suicide or apoptosis. Except in the case where a toxin induces immediate cellular destruction, toxins invariably induce an altered pattern of gene expression in exposed cells. Moreover, it is now well-understood that polymorphisms in genes comprising the toxic-response pathways can have a major effect on toxicity, while also effecting the pattern of gene expression in cells with variant genotypes. The availability of DNA sequence data and DNA microarray technologies affords the unique opportunity to study complex cellular responses to biological or environmental stimuli on a genomic scale, simultaneously observing effects on all cellular components and the effect of genetic polymorphisms. The purpose of this article is to provide an overview the currently available, state-of-the-art DNA microarray technology for analysis of gene expression. More detailed discussions can be found in previous reviews (7–17). In this chapter, we will discuss potential applications to the study of apoptosis, with emphasis on present limitations and potential pitfalls associated with use of these technologies, and whenever suggest possible mitigating experimental approaches.

## 2. OLIGONUCLEOTIDE ARRAYS

Allele-specific oligonucleotide (ASO) hybridization for detection of specific DNA sequence was developed in the early 1980s (18,19). Subsequently, several groups of investigators independently proposed the use of ASO hybridization on a large scale as a method for sequencing DNA. The first strategy proposed involved arraying individual sequences of interest (targets) onto membrane filters, which would then be sequentially hybridized with a large number of individual oligonucleotide probes (20). Since each target molecule will hybridize specifically to its complementary oligonucleotide probe, this approach could in theory allow for highly parallel extraction of sequence information from a single hybridization. Nonetheless, this strategy requires the synthesis of a large number of oligonucleotides for use as probes, each of which would then be individually labeled and sequentially hybridized the array.

The alternative approach was to arrange a large number of oligonucleotide probes on a solid support, and then hybridize the array with labeled genomic DNA (target) from cells of interest (21–23). Some of the approaches developed to array probes on a solid matrix included microinjection of synthesized oligomers into patches of activated polyacrylamide (22) and the coupling of synthesized oligomers to surface modified glass, gold, or polypropylene (24,25). However, arraying a large number of individual oligonucleotide sequences to a solid support represents a formidable technical challenge as the number of oligonucleotides increases. The limitations imposed by arraying individual probes mitigated by the *in situ* synthesis of the individual oligonucleotides at spatially addressable sites on the solid support. *In situ* synthesis of oligonucleotides benefited from the availability of established methods for solid phase chemical synthesis. The *in situ* approach requires the precise and sequential delivery of chemical reagents to individual positions on the solid support. These prerequisites are satisfied by using “masks,” which allow the sequential protection and de-protection of specific areas of the surface from reaction synthetic reagents (21,23,26). By sequential masking of the reactive surface, it is possible to synthesize large numbers of oligonucleotide sequences using a limited number of nucleotide coupling reactions. Using the four possible nucleotides at any position in an oligonucleotide, the number of sequences that can be generated increases as a function of  $4^n$ , where  $n$  is the number of nucleotides the sequence. It is theoretically possible to synthesize  $4^n$  sequences using  $n$  coupling reactions.

One method for *in situ* synthesis of oligonucleotides makes use of channels formed by sealing the surface with a chemical mask, guiding the precursor molecules to the appropriate areas on the surface (23). An alternative approach being developed is the use of modified inkjet printer heads to, in effect, spray the reagents onto a designated address on the surface (27). In this approach, the “masks” are defined by the two-dimensional displacement of the printer head. Using the inkjet technology, reagents can be applied with high spatial precision, making it possible to synthesize thousands of oligonucleotides per  $\text{cm}^2$ . By utilizing the chemistry of solid-phase organic synthesis, the inkjet technology permits efficient synthesis of oligonucleotides over 25 base pairs in length. The longer probe lengths allow for more complete hybridization with target sequences, with a commensurate increase in sensitivity and specificity. The inkjet technology has the further advantage of flexibility, in that the pattern of reagents applied to the surface can be easily adapted to generate probes for different genes or applications.

Photolithography methods developed by the semiconductor industry to produce computer chips have been adapted for the synthesis of high-density oligonucleotide arrays (21,28). A comprehensive description of the technology for production of these arrays can be viewed on the World Wide Web at the Affymetrix (Santa Clara) URL (<http://www.Affymetrix.com/technology/index.html>). The feasibility of the photolithography approach was contingent upon the availability of nucleotide precursors with chemical protecting groups that can be cleaved by exposure to light of a specific wavelength. By shining high-intensity light through openings in a light impermeable, chromium mask, it is possible to de-protect and chemically activate specific regions of the chip. Only the deprotected precursors on the surface of the array are available to react with the next nucleotide precursor washed across the entire surface of the chip. Sequential application of several masks permits the synthesis of any nucleotide sequence at a given site or feature on the surface of the chip. Microarrays produced by photolithography are typically comprised of tiles or features that are 20–50  $\mu\text{m}^2$  in size, each with a specific oligonucleotide sequence of 25 nucleotides in length. It is therefore possible to synthesize ~65,000 separate probes using 50  $\mu\text{m}$  tiles, or as many as ~400,000 different probes using 20  $\mu\text{m}$  tiles, on a single 1.28-cm chip, with a probe density of  $10^7$ – $10^8$  molecules per feature.

High-density oligonucleotide arrays represented a momentous leap forward in our capacity to analyze DNA sequences present in biological specimens. Allele-specific hybridization of the individual oligonucleotide probes to target sequences allows for the application of these arrays to a variety of sequence-based assays including detection of single nucleotide polymorphisms (SNPs) (29), loss of heterozygosity (LOH) analysis, constitutive and somatic allelotyping, genetic linkage analysis, mRNA expression analysis, gene mapping, and so on.

### **3. ANALYSIS OF GENE EXPRESSION PATTERNS USING NUCLEIC ACID ARRAYS**

The fundamental determinant of cell phenotype, growth, and differentiation is the pattern of gene expression. The amounts of each gene expressed in a cell at any given time are a function of the genetic and epigenetic constitution of the cell, and how the cells integrate response to environmental stimuli. The pattern of gene expression thus provides a snapshot of the cell's physiological state. By hybridizing arrays (the probe) with labeled cDNA or in vitro transcribed cRNA from cells (the target), one can simultaneously compare the levels of thousands of mRNAs between any two cell types or physiological states. The ability to detect and decipher the meaning of these

altered patterns of gene expression will lead to a better understanding of the biochemical mechanisms and hence predictions of cellular responses associated with complex biological processes including, apoptosis.

#### 4. OLIGONUCLEOTIDE ARRAYS

Analysis of gene-expression patterns can be performed using either oligonucleotide arrays or printed cDNA arrays (Fig. 1). Oligonucleotide arrays produced by *in situ* chemical synthesis of probes directly on a matrix (30,31) have several advantages over printed arrays. The amount of each probe synthesized on the chip surface using *in situ* synthesis techniques is highly reproducible (21,32). This reproducibility allows for direct comparison of expression data obtained among chips. In practice, this means the target nucleic acid from each cell studied is hybridized to a separate chip. The latter is an important consideration when multiple comparisons are to be made using samples with limited cell numbers.

Another advantage of the oligonucleotide array is the higher probe density makes it possible to include multiple probes representing different regions of each transcript. The GeneChip™ Expression analysis system produced by Affymetrix (Santa Clara) is comprised of a set of chips that collectively can compare the levels of up to ~40,000 separate human transcripts. The design of the arrays is such that the level of each transcript is interrogated by at least 10 separate perfectly matched probes (PM). In addition, a probe with a mismatched base (MM) relative to each PM probe is included on the chip. By comparing the amount of hybridization between the PM and the MM probes, it is possible to differentiate signal from noise and to distinguish among signals from hybridization with transcripts from gene family members. Moreover, the fluorescent signal generated by hybridization with the fluorescent target yields linear data over three to four orders of magnitude and the arrays can reproducibly detect changes in mRNA levels that are as low as two- to threefold. Transcripts that are present at a frequency as low as 1:300,000 in the target cells.

To monitor gene expression using the GeneChip Expression™ arrays, mRNA extracted from cells is reverse-transcribed using a primer comprised of a T7 Polymerase start site at its 5' end and an oligo dT sequence at its 3' end. Following second-strand synthesis, the purified double stranded cDNA is used as a template for *in vitro* transcription using T7 Polymerase. Biotinylated ribonucleotides are incorporated into the cRNA during the *in vitro* transcription reaction. After purification and fragmentation to an optimal size, the labeled target cRNA is hybridized to the array. Hybridization requires ~10 µg of labeled, *in vitro* transcribed cRNA that can be generated

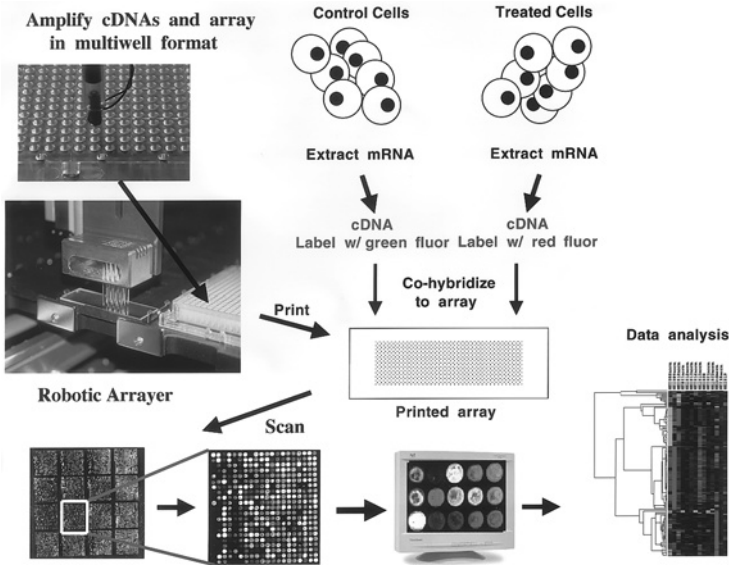


Fig. 1. Expression analysis using cDNA microarrays. To produce cDNA microarrays, individual cDNA clones are amplified by PCR and arrayed in a multiwell format with or without purification. The upper left panel shows samples being arrayed with a piezo-ceramic fluid-dispensing system (Engineering Arts, Seattle, WA). The multiwell plates with cDNA clones are then placed on a robotic printer such as the Gene Machines (Redwood City, CA) system shown in the second panel. The software that drives the robot is used to assign each clone to a specific address on the surface of a polylysine coated or chemically derivatized microscope slide. Spotting of individual clones is accomplished using a series of pins or quills that are dipped into each well to take up a sufficient volume of the cDNA solution to spot or print each clone onto all of the slides. Printing is accomplished by rapid displacement of the robot head and the microscope stage using precision micro-manipulation technologies. After each round of printing, the pins are washed and the process repeated until all clones have been printed on each slide to produce a microarray. Microarrays can then be used to compare expression levels of the each represented gene under two sets of experimental conditions, such as before and after exposure to an inducer of apoptosis. Messenger RNA is extracted from the cell types and cDNA is produced by reverse transcription in the presence of a different fluorescence-labeled dNTP precursors for each mRNA, in this case Cy3-dUTP for the reference sample and Cy5-dUTP for the test sample. The labeled cDNAs are then co-hybridized to the microarray such that each target molecule will form a stable duplex with its corresponding probe on the array. The amount of each labeled target molecule hybridized to the probe spot is a function of how much of each target was present in each cell type. Each spot on the array is then scanned for fluorescence at the optimal wavelength for the Cy3 and Cy5 fluors using lasers, or high-intensity light and monochromatic filters. Expression

from as little as 0.1  $\mu\text{g}$  of poly A+ mRNA, or  $\sim 5 \times 10^5$  cells. Following hybridization, the target molecules are stained with streptavidin-phycoerythrin or fluorescently labeled antibodies using proprietary protocols (Affymetrix). Fluorescence associated with each tile is then analyzed using a Hewlett-Packard Gene Array™ Scanner. The amount of each target cRNA molecule synthesized depends on the original number of mRNA molecules present in the poly A+ mRNA preparation, and the signal emitted by each tile should reflect the relative amounts of each target mRNA. Following the image acquisition, the software algorithms compute the average fluorescence intensity for each PM and MM probe. Statistical analyses are then used to estimate fold changes in the expression of each gene in a test sample relative to the levels in the reference sample.

## 5. cDNA MICROARRAYS

The simplest expression arrays consist of individual cDNA clones manually or robotically spotted onto nitrocellulose or nylon filters. Replicates of the clone arrays are then hybridized sequentially or in parallel with different radioactively labeled target cDNAs, and hybridization to each clone measured by Phosphor Imager or similar technologies (33–36). Our own laboratory used this simple approach to assess the efficacy of protocols to generate subtracted cDNA libraries (37). Filters with thousands of arrayed human or murine genes and the requisite analysis software have been commercially available for the past several years.

---

Fig. 1. (*continued from opposite page*) data for each gene represented on the array is expressed as a ratio of fluorescence intensities normalized to the reference sample (i.e., Cy3/Cy5). Shown in the figure is an array with the entire set of yeast genes printed and hybridized in our facility at the Fred Hutchinson Cancer Research Center. If the expression of a gene is unchanged, the ratio will remain close to unity (yellow color on computer generated false image). Any significant deviation from unity indicates either an increase ( $>1$ , image becomes more red) or a decrease ( $<1$ , image becomes more green) in the level of expression between the test and the reference sample, and the magnitude of the change is indicative of the fold difference in the expression levels. Fluorescence intensity data are collected in the form of a spread sheet, which is merged with a database that contains the identity of the gene at each position on the array. The complete set of specific alterations defines the expression signature for the given experimental condition relative to the reference condition. Expression signatures can be compared using a variety of statistical and visual tools such as gene clustering algorithms, which group genes showing similar responses as function of time, dose, genotype, etc. Data from multiple experiments can also be compared using appropriate “data mining” software.

One of the most significant limitations of these spotted arrays is the variability in the amount of probe that is applied to each spot or feature, which increases the variance in the data and limits the sensitivity when comparing gene-expression levels results among samples or experiments. The variance is particularly problematic for low copy-number mRNAs that give a weak signal-to-noise ratio. A second limitation derives from the use of radioactively labeled target cDNA. Although the scattering of the signal resulting from radioactive decay can be mitigated by using  $^{33}\text{P}$ -labeled hybridization probes, the tendency of filters to warp during experimental manipulation, and high background noise limit the density at which probes can be arrayed and still retain the ability to resolve individual signals.

A major advance in cDNA microarray technology was the introduction of fluorescently labeled nucleotide precursors into the target nucleic acid (38–40). As for oligonucleotides, target mRNA purified from cells of interest is reverse-transcribed into cDNA. Fluorescently labeled nucleotides that can be efficiently incorporated into the cDNA by reverse transcriptase, typically Cy3-dUTP and Cy5-dUTP, are used to label target RNA from two cell types being compared for expression profiles. A more efficient labeling protocol involves the incorporation of amino-allyl derivatives of dNTPs, followed by chemical coupling of amino allyl groups with reaction with NHS-esters of Cy3 or Cy5 (complete protocol can be found at the following URL:<http://cmgm.stanford.edu/pbrown/protocols/aadUTPCouplingProcedure.htm>). In either labeling protocol, the amount of label associated with each target mRNA is a function of the amount of each in the cell from which the mRNA was extracted. The differentially labeled targets are then co-hybridized to the array under conditions that allow each target mRNA to hybridize to its corresponding probe. Hence, the ratio Cy3 to Cy5 of fluorescence associated with each probe is a measure of the fold change in the level of expression of each gene represented on the probe array (Fig. 1).

The use of fluorescently labeled probes required the development of alternative solid supports, as such glass, with a low inherent fluorescence. Techniques for automated transfer of cDNAs by spotting onto coated glass supports were pioneered by Pat Brown and his colleagues and the complete plans for the inexpensive assembly of the robotic arrayer are available at the following URL: <http://www.cmgm.stanford.edu/pbrown/array.html>. Robotic arrayers are also commercially available from numerous suppliers for a range of prices. Confocal imaging of the fluorescence signal emitted from each feature following hybridization with labeled target provided a significant increase in the performance of parallel gene-expression assays. Detection by fluorescence does not suffer from the spatial restraints encoun-

tered using radioactive probes and generally yield a higher signal-to-noise ratio. More importantly, the ability to label target sequences from different sources (e.g., treated or untreated cells) with fluors with different light-emission spectra makes it possible to co-hybridize different targets to the same array. The latter approach not allows for direct comparison of gene-expression levels on one chip, but by expressing the data as the ration of fluorescence intensities, also permits the comparison of data among arrays or experiments (40).

The lower cost of hardware and chip production make cDNA microarrays more attractive and accessible to academic researchers than the commercially fabricated oligonucleotide arrays. Nonetheless, it is important to remember that cDNA arrays still require the production, purification, and handling of a large number individual cDNAs that are to be spotted onto the matrix. Printing of chips with more than a few hundred probes will therefore require a substantial investment of effort, hardware, and software to produce and amplify the individual cDNAs. Typically the cDNA clones or genomic DNAs of interest are obtained and amplified using the polymerase chain reaction (PCR). The amplified probes, which should ideally be between 500 and 2500 nucleotides in length, are then arrayed onto the matrix with or without further purification. The advantage of using clones from cDNA libraries is that one pair of vector primers can be used to amplify coding sequences from all of the clones, whereas multiple primer pairs are required for each exon to be amplified from genomic DNA. In either case, preparation cDNAs for printing requires thousands to tens of thousands of the plasmid preparations, PCR amplifications, and probe-purification steps. If more than a few array types are required, then the probe-preparation steps are best performed in a multiwell, high-throughput format that can be automated (Fig. 1).

cDNA or oligonucleotide arrays are printed using finely machined pins that mechanically spot the probes onto chemically derivatized or microscope polylysine-coated slides. The tip of each pin, which is typically split much like a fountain pen, is dipped into a single well of multiwell plates. A sufficient volume of probe is retained to spot the individual clones at the same relative position on multiple slides. Another pin format includes a small ring that holds the solution of probe as a thin film. A pin is then pushed through the film to punch out a small area of the film and deposit it on the surface of the matrix. The pins are then washed and dried before repeating the printing of the next cDNA probe onto all of the slides. Most high-speed robots use a multiple-pin format (up to 32 pins) and can print 100 or more slides with thousands of probes each, in a single day. The density of probe spot is



defined by the size and quality of the pins, by the arrangements of the pins within the robotic head, and by the software used to drive the robotics. Currently is possible to print up to 20,000 cDNA clones onto a single 1 inch  $\times$  3 inch microscope slide.

Although mechanical spotting using pins can yield high-quality arrays, it also suffers from several limitations. A significant limitation of chips produced by mechanical spotting is the variability in the volume of probe solution and hence the amount of probe deposited in each spot. The volume deposited is affected by surface characteristics, speed of the robot, time, and pressure of the pin on the slide surface, viscosity, and so on. Even when comparable volumes are deposited, evaporation from the pins or the sample wells during the printing process can change the concentration of the probes on the pin or in the wells. Although evaporation of the probe solution can be minimized by increased humidity in the printing area, the amount of probe deposited can still vary several-fold among spots. The density of spots on the array is limited by the diameter to which the pin tips can be machined and by the tolerance in the displacement of the pin holder by the robot. The rate limiting in printing arrays is the time it takes for the pin to touch the surface of the matrix. Shorter printing times are preferable not only for production capacity, but also because the probe solution retained by the pins is subject to evaporation, thereby changing the concentration of the probe solution to different arrays. Thus, a variety of alternative technologies such as piezoelectric dispensers and inkjet or thermal ejection printer heads to spray droplets of probe solution onto the matrix surface are being evaluated in a number of labs including our own.

Variability of printed arrays can be overcome by simultaneously hybridizing a given array with the target cDNA from the two cell types or states being compared, each of which is labeled with a different fluorescent molecule (Fig. 1). The relative amount of a specific mRNA expressed in the two cells can then be determined by measuring the amount of fluorescence from each fluor. A variety of array scanners with different capabilities are commercially available and usually include software for spot detection and identification, data capture, and quantitative analysis. Once fluorescence data are collected, they can be expressed as a ratio, such that the relative signals from each spot are internally controlled for variance in probe density on the array. By expressing the data as ratios, it is also possible to compare relative changes in expression among arrays despite a high level of inter-array variability. To further reduce variance within the data, the same probe is often replicated on a single array or the same hybridization is performed multiple times. Replicates usually include hybridizations

in which the dyes used to label the reference and test target are reversed to control for dye-specific differences. Nonetheless, variance remains significant consideration when comparing the expression of low-abundance genes. As fluorescence signals approach background levels, the variance increases such that even the ratios of intensities are subject to large fluctuations.

Another limitation of cDNA arrays is that it may not be possible to discern signals that are generated by the cross-hybridization of a labeled target sequence derived from one member of a gene family with the probe for another family member. The latter limitation could in theory be addressed using shorter oligonucleotide probes for each transcript and by selecting probes from regions of the cDNA where gene family members show little sequence identity. Despite these limitations, printed arrays have the advantage of the lower cost and the flexibility to readily alter the probe configuration.

## **6. POTENTIAL USES FOR MICROARRAYS IN THE STUDY OF APOPTOSIS**

### ***6.1. Apoptotic Signatures***

A central tenet of toxicology is that with the possible exception of rapid cell death, every toxic exposure leads to an alteration in the pattern of gene expression. This altered pattern of gene expression reflects the cell's attempt to cope with the toxic insult, and can range from induction of xenobiotic metabolism to the extreme of cell suicide or apoptosis. Likewise, the cell's response to normal biological signals (e.g., morphogens) or abnormal signals (e.g., inappropriate oncogene activation) may induce patterns of gene expression that initiate the apoptotic process. While numerous studies have looked at changes in the expression of a limited number of genes thought to play a role in these adaptive responses, the power of array technology is the ability to simultaneously compare the levels of thousands of genes. This global analysis of gene expression affords the opportunity to discern specific patterns or signatures of expression that are associated with particular classes of toxicants or biological signals. These signatures are likely to include classes of genes not previously implicated in response to specific toxic insults (41). As such the applications of array technologies will undoubtedly enhance our understanding of the cellular response to toxins and other signals. In the case of toxins, these types of studies should also provide insight into the mechanism of cell damage that may affect susceptibility to apoptosis. For example, agents that induce the expression of genes involved

in DNA repair almost certainly must be directly or indirectly genotoxic to the cell.

There is significant evidence to suggest that specific toxic exposures will produce discernable expression signatures. Studies in yeast and mammalian cells have demonstrated that a reproducible subset of genes will show altered expression in response to specific conditions such as anoxia, nutrient deprivation, exposure to alkylating agents, chemotherapeutic agents, and so on (41–43). It is therefore reasonable to hypothesize that toxicant signatures will exist for individual classes of toxins such as polycyclic aromatic hydrocarbons (PAH), alkylating agents, ionizing radiation, neurotoxins, and so forth. Moreover, the individual signatures will almost certainly reflect underlying mechanisms of toxicity such as oxidative stress, DNA damage, inhibition of oxidative phosphorylation, disruption of cell membrane potentials, and so on (44,45). Since many toxicants will have multiple mechanisms of action, a gene-expression signature will also reflect this complexity of mechanisms. As an example, the signature of PAHs will almost certainly include genes involved in their xenobiotic metabolism and genes that are involved in the response to oxidative stress. The ability of gene-expression signatures to provide insight into the underlying mechanisms would make it possible to predict the mechanism of toxicity unknown compounds. For example, if the expression signature of unknown compound includes a set of genes that are common by other inhibitors of apoptosis, then the unknown can be tentatively assigned to this class of agents.

Another exciting application of array technology is the possibility of defining thresholds of exposure below which there is no biological effect. Arguably, altered gene expression is the earliest measurable biological endpoint in response to a given exposure. Moreover, the signatures for doses of toxicant or signaling molecule that do not have any biological effect are likely to be distinct from the signatures of doses that induce cellular stress and adaptation, whereas signatures at even higher doses will reflect more acute cellular responses. The classical NOEL (no observable effect levels) is established by tests whose endpoints (mutation, transformation, DNA synthesis, apoptosis, etc.) rely on the integration of complex responses at the level of the cell, and in some cases at the level of the organism (teratology). By contrast, gene-expression signatures measure the earliest cellular responses and provide information on the nature of the cellular response. In addition, gene-expression signatures should reveal if the effects of multiple nontoxic doses are cumulative at the level of gene expression. The ability to obtain and compare signatures of many different inducers of apoptosis, at

different doses, and as complex mixtures will also make it possible to predict the lowest biologically relevant doses or dose regimens.

Another application of array technology is to dissect the biochemistry of apoptosis. For example, investigators might generate a set of mutants that inhibit apoptosis of a particular cell type during differentiation. Mutants that affect the same biochemical pathways should affect similar sets of genes. Thus mutants could be clustered on the basis of the patterns of gene expression they induce in the affected cell population. An example of such a cluster analysis of mutants affecting cell death and differentiation during haematopoiesis in the chicken is shown in the lower right corner of Fig. 1 (46).

## 6.2. Factors Affecting Gene-Expression Signatures

Although the application of microarray technology will have an enormous impact on understanding mechanisms of apoptosis, it is important to realize that the gene-expression signatures obtained will be highly sensitive to the assays conditions and methodologies. The data obtained will be affected by numerous factors ranging from the composition of the array to the source of the target nucleic acid.

Microarrays used to define expression profiles can include probes from all available genes or can be designed using the subset of genes suspected or already shown to be involved in the apoptotic response (some housekeeping genes are included as controls). An example of the latter type of array is by the Tox-Chip being designed by researchers at the National Institute for Environmental Health Sciences (N.I.E.H.S.) (47). While these arrays will be very informative, there is a good probability that they will detect only partial signatures for any given exposure. Ideally, the chips used to define signatures should include all possible genes. The importance of a comprehensive screen is illustrated by a recent study that examined the response of yeast cells to an alkylating agent using arrays harboring probes for the entire yeast gene set (41). The results yielded the expected result in that virtually all genes previously known to be induced by alkylating agents were detected as such by the microarray. However, the array detected 325 transcripts that were elevated and 76 that were decreased after exposure. Eighteen of the novel inducible additional genes were elevated to higher levels than the previously studied genes. Significantly, the data also allowed these researchers to conclude that alkylating agents induced activated a previously unsuspected program of gene expression to eliminate and replace adducted proteins. Neither the novel genes nor the protein-replacement pathways would

have been detected if the chip contained a subset of all yeast genes, and this underscores the need to develop comprehensive signatures for toxicants. Of course comprehensive screens are not yet possible for human cells. At present, the GeneChip Expression array from Affymetrix can simultaneously examine ~40,000 transcripts (<http://www.affymetrix.com>), with printed arrays are quickly approaching that number. While cost of comprehensive screens remains a major hindrance, it would seem prudent to make screens as comprehensive as possible. Lower-cost arrays with subsets of genes could then be designed and used for routine screening of compounds for functionally relevant signatures.

Other important considerations when using microarrays to study responses to inducers or inhibitors of apoptosis are the experimental parameters. The expression pattern detected by a single array represents a snapshot of the cellular response in time and physiological state. As already discussed earlier, the response of a cell to a given exposure will be a function of the dose. However, the response at the mRNA level will also vary as a function of time after exposure. Experience in yeast experiments clearly demonstrates that the induction or repression of genes follow predictable temporal patterns, which may fall into clusters for sets of genes that define an affected biochemical pathways (42). Moreover, the kinetics of the response could depend on dose. It is therefore important to examine toxicant signatures under a variety of experimental settings. Even when all experiments are carefully controlled, there will always be minor variations in conditions due to operator handling, small differences in cell density, temperature, and anoxia, all of which will contribute to the observed expression pattern in a given experiment. The impact of the inter-experiment variation can be minimized by performing replicate assays or by pooling mRNA from multiple experiments before analysis on arrays. In the former, outliers could be eliminated statistically, while in the latter, the spuriously elevated or decreased mRNAs would be averaged with levels in other experiments. Finally the choice of cell type will affect the observed signatures. It is likely that the response at the level of gene expression will vary among cell types, since many inducers or apoptosis are known to be highly tissue-specific.

Finally, if the cells are present in limited numbers, the amount of mRNA available may be insufficient to perform assay on the microarrays. In this case, the cells from numerous animals may need to be pooled for each assay. Alternatively, the mRNA from individual animals would have to be amplified prior to labeling of the target. In this case, care must be taken to ensure that the method of amplification does not distort the pattern of expression by preferential amplification of some targets. Exponential amplification such as occurs during PCR is thus inappropriate. Alternatives such as the production of cDNA libraries from single cells (48) are being evaluated for this purpose.

A major issue in toxicology testing is the difficulty in understanding and predicting individual variation in toxicant sensitivity. Toxicogenetics seeks to establish the genetic basis for these variations. A great deal of research has already identified numerous genetic polymorphisms in genes comprising biochemical pathways important for resistance to toxins (e.g. xenobiotic metabolism, DNA repair, etc.). In some cases a specific polymorphism has been linked to a specific phenotypes of chemical susceptibility. However, sensitivity to more complex effects of toxic exposure such as apoptosis, birth defects, and so on, may depend on the integrated effects of numerous polymorphisms. As a result, most attempts to find association between genetic polymorphisms in xenobiotic metabolizing genes and cancer risk have found only minimal and often conflicting effects, and even meta-analyses of the data can yield inconclusive results (49).

## 7. COMPUTATIONAL BIOLOGY

The previous section outlined available microarray technologies, some potential application to the study of apoptosis, as well as their limitations. Implicit in the previous discussion was the assumption that adequate computational and bioinformatics tools would be available for analysis of the unprecedented size and complexity of the data these studies would generate. The development of these tools remains a formidable challenge and may prove to be the rate-limiting step in the implementation of these exciting new methodologies. A number of programs for statistical evaluation of data have already been developed in both academic (16,50) and commercial settings. Computer software required falls into several categories. The first type deals with capture (spot identification, correction for background, data normalization, etc.), statistical analysis of the data, and may include the ability to compare expression levels between two cell types or conditions. This type of software is usually incorporated into the software provided with array scanners or can be obtained from academic investigators. Continued development in this statistical analysis software remains an area of active research. The second area for software development is for analysis of data across experimental conditions. For example, an investigator may want to find sets of genes that show common temporal profiles of altered expression after an exposure. Similarly, genes could be clustered on the basis of function categories, dose response, biochemical pathways, and so on. This type of analysis typically makes use of clustering algorithms. A discussion of these methods is beyond the scope of this chapter, and the reader is referred to the Reference Section for additional information.

The third and vastly more complex area for software development is for analysis of data across all experiments. For example, an investigator may wish to find patterns of gene expression common to all individuals that are sensitive to a complex mixture. Such a pattern might be used to predict the risk of individuals to that exposure. This example exemplifies the complexity and issues associated with the use of array technology in any setting, including toxicology. In addition to having adequate computing power and appropriate software for the required comparisons, one also needs to have publicly accessible databases containing the information gathered by many labs. The databases must also be annotated with experimental parameters to facilitate comparisons. The software used must allow for exchange of information among different laboratories and different computer platforms. Moreover, the software must be compatible with data generated by different microarray platforms. It might also be important to combine expression data with genotype data.

The successful application of array technology will require continued technology development, the establishment of public databases with accepted standards for data annotation, and the development of powerful new statistical and bioinformatics tools. Clearly many challenges and promises lie ahead.

## REFERENCES

1. Fleischmann, R. D., Adams, M. D., White, O., Clayton, R. A., Kirkness, E. F., Kerlavage, A. R., et al. (1995) Whole-genome random sequencing and assembly of *Haemophilus influenzae* Rd [see comments]. *Science* **269**, 496–512.
2. Velculescu, V. E., Zhang, L., Vogelstein, B., and Kinzler, K. W. (1995). Serial analysis of gene expression [see comments]. *Science* **270**, 484–487.
3. Underhill, P. A., Jin, L., Zeman, R., Oefner, P. J., and Cavalli-Sforza, L. L. (1996) A pre-Columbian Y chromosome-specific transition and its implications for human evolutionary history. *Proc. Nat. Acad. Sci. US* **93**, 196–200.
4. Liang, P. and Pardee, A. B. (1992) Differential display of eukaryotic messenger RNA by means of the polymerase chain reaction [see comments]. *Science* **257**, 967–971.
5. Zhao, N., Hashida, H., Takahashi, N., Misumi, Y., and Sakaki, Y. (1995) High-density cDNA filter analysis: a novel approach for large-scale, quantitative analysis of gene expression. *Gene* **156**, 207–213.
6. Zarbl, H., Aragaki, C., and Zhao, L. P. (1998) An efficient protocol for rare mutation genotyping in a large population. *Genetic Test.* **2**, 315–321.
7. Southern, E., Mir, K., and Shchepinov, M. (1999) Molecular interactions on microarrays. *Nature Genet.* **21 (Suppl.)**, 5–9.
8. Duggan, D. J., Bittner, M., Chen, Y., Meltzer, P., and Trent, J. M. (1999) Expression profiling using cDNA microarrays. *Nature Genet.* **21 (Suppl.)**, 10–14.

9. Chueng, V. G., Morley, M., Aguilar, F., Massimi, A., Kucherlapati, R., and Childs, J. (1999) Making and reading microarrays. *Nature Genet.* **21 (Suppl.)** 21, 15–19.
10. Lipshutz, R. J., Fodor, S. P. A., Gingeras, T. R., and Lockhart, D. J. (1999) High density synthetic oligonucleotide arrays. *Nature Genet.* **21 (Suppl.)**, 20–24.
11. Bowtell, D. D. (1999) Options available — from start to finish — for obtaining expression data by microarray. *Nature Genet.* **21 (Suppl.)**, 25–32.
12. Brown, P. O. and Botstein, D. (1999) Exploring the new world of the genome with DNA microarrays. *Nature Genet.* **21 (Suppl.)**, 33–37.
13. Cole, K. A., Krizman, D. B., and Emmert-Buck, M. R. (1999) The genetics of cancer: a 3D model. *Nature Genet.* **21 (Suppl.)**, 38–41.
14. Debouck, C. and Goodfellow, P. N. (1999) DNA microarrays in drug discovery and development. *Nature Genet.* **21 (Suppl.)**, 48–50.
15. Hacia, J. G. (1999) Resequencing and mutational analysis using oligonucleotide microarrays. *Nature Genet.* **21 (Suppl.)**, 42–47.
16. Bassett, D. E., Jr., Eisen, M. B., and Boguski, M. S. (1999) Gene expression informatics: it's all in your mine. *Nature Genet.* **21**, 51–55.
17. Chakravarti, A. (1999) Population genetics: making sense out of sequence. *Nature Genet.* **21 (Suppl.)**, 56–60.
18. Conner, B. J., Reyes, A. A., Morin, C., Itakura, K., Teplitz, R. L., and Wallace, R. B. (1983) Detection of sickle cell beta S-globin allele by hybridization with synthetic oligonucleotides. *Proc. Nat. Acad. Sci. US* **80**, 278–282.
19. Zarbl, H., Sukumar, S., Arthur, A. V., Martin-Zanca, D., and Barbacid, M. (1985) Direct mutagenesis of Ha-ras-1 oncogenes by N-nitroso-N-methylurea during initiation of mammary carcinogenesis in rats. *Nature* **315**, 382–385.
20. Drmanac, R., Labat, I., Brukner, I., and Crkvenjakov, R. (1989) Sequencing of megabase plus DNA by hybridization: theory of the method. *Genomics* **4**, 114–128.
21. Fodor, S. P., Read, J. L., Pirrung, M. C., Stryer, L., Lu, A. T., and Solas, D. (1991) Light-directed, spatially addressable parallel chemical synthesis. *Science* **251**, 767–773.
22. Khrapko, K. R., Lysov Yu, P., Khorlin, A. A., Ivanov, I. B., Yershov, G. M., Vasilenko, S. K., et al. (1991) A method for DNA sequencing by hybridization with oligonucleotide matrix. *DNA Sequence* **1**, 375–388.
23. Southern, E. M., Maskos, U., and Elder, J. K. (1992) Analyzing and comparing nucleic acid sequences by hybridization to arrays of oligonucleotides: evaluation using experimental models. *Genomics* **13**, 1008–1017.
24. Maskos, U. and Southern, E. M. (1993) A study of oligonucleotide reassociation using large arrays of oligonucleotides synthesised on a glass support. *Nucleic Acids Res.* **21**, 4663–4669.
25. Matson, R. S., Rampal, J., Pentoney, S. L., Jr., Anderson, P. D., and Coassin, P. (1995) Biopolymer synthesis on polypropylene supports: oligonucleotide arrays. *Anal. Biochem.* **224**, 110–116.



26. Southern, E. M., Case-Green, S. C., Elder, J. K., Johnson, M., Mir, K. U., Wang, L., and Williams, J. C. (1994) Arrays of complementary oligonucleotides for analysing the hybridisation behaviour of nucleic acids. *Nucleic Acids Res.* **22**, 1368–1373.
27. Marshall, A. and Hodgson, J. (1998) DNA chips: an array of possibilities. *Nature Biotechnol.* **16**, 27–31.
28. McGall, G., Labadie, J., Brock, P., Wallraff, G., Nguyen, T., and Hinsberg, W. (1996) Light-directed synthesis of high-density oligonucleotide arrays using semiconductor photoresists. *Proc. Nat. Acad. Sci. US* **93**, 13,555–13,560.
29. Wang, D. G., Fan, J. B., Siao, C. J., Berno, A., Young, P., Sapolsky, R., et al. (1998) Large-scale identification, mapping, and genotyping of single-nucleotide polymorphisms in the human genome. *Science* **280**, 1077–1082.
30. Lockhart, D. J., Dong, H., Byrne, M. C., Follettie, M. T., Gallo, M. V., Chee, M. S., et al. (1996) Expression monitoring by hybridization to high-density oligonucleotide arrays [see comments]. *Nature Biotechnol.* **14**, 1675–1680.
31. Wodicka, L., Dong, H., Mittmann, M., Ho, M. H., and Lockhart, D. J. (1997) Genome-wide expression monitoring in *Saccharomyces cerevisiae*. *Nature Biotechnol.* **15**, 1359–1367.
32. Fodor, S. P., Rava, R. P., Huang, X. C., Pease, A. C., Holmes, C. P., and Adams, C. L. (1993) Multiplexed biochemical assays with biological chips. *Nature* **364**, 555–556.
33. Drmanac, R. and Drmanac, S. (1999) cDNA screening by array hybridization. *Methods Enzymol.* **303**, 165–178.
34. Drmanac, S., and Drmanac, R. (1994) Processing of cDNA and genomic kilobase-size clones for massive screening, mapping and sequencing by hybridization. *Biotechniques* **17**, 328–329.
35. Drmanac, S., Kita, D., Labat, I., Hauser, B., Schmidt, C., Burczak, J. D., and Drmanac, R. (1998) Accurate sequencing by hybridization for DNA diagnostics and individual genomics. *Nature Biotechnol.* **16**, 54–58.
36. Pietu, G., Alibert, O., Guichard, V., Lamy, B., Bois, F., Leroy, E., et al. (1996) Novel gene transcripts preferentially expressed in human muscles revealed by quantitative hybridization of a high density cDNA array. *Genome Res.* **6**, 492–503.
37. Kho, C. J. and Zarbl, H. (1992) A rapid and efficient protocol for sequencing plasmid DNA. *Biotechniques* **12**, 228.
38. Schena, M., Shalon, D., Davis, R. W., and Brown, P. O. (1995) Quantitative monitoring of gene expression patterns with a complementary DNA microarray [see comments]. *Science* **270**, 467–470.
39. Schena, M., Shalon, D., Heller, R., Chai, A., Brown, P. O., and Davis, R. W. (1996) Parallel human genome analysis: microarray-based expression monitoring of 1000 genes. *Proc. Nat. Acad. Sci. US* **93**, 10,614–10,619.
40. Shalon, D., Smith, S. J., and Brown, P. O. (1996) A DNA microarray system for analyzing complex DNA samples using two-color fluorescent probe hybridization. *Genome Res.* **6**, 639–645.
41. Jelinsky, S. A. and Samson, L. D. (1999) Global response of *Saccharomyces cerevisiae* to an alkylating agent. *Proc. of the Nat. Acad. Sci. US* **96**, 1486–1491.

42. DeRisi, J. L., Iyer, V. R., and Brown, P. O. (1997) Exploring the metabolic and genetic control of gene expression on a genomic scale. *Science* **278**, 680–686.
43. Iyer, V. R., Eisen, M. B., Ross, D. T., Schuler, G., Moore, T., Lee, J. C. F., et al. (1999) The transcriptional program in the response of human fibroblasts to serum [see comments]. *Science* **283**, 83–87.
44. Marton, M. J., DeRisi, J. L., Bennett, H. A., Iyer, V. R., Meyer, M. R., Roberts, C. J., et al. (1998). Drug target validation and identification of secondary drug target effects using DNA microarrays [see comments]. *Nature Med.* **4**, 1293–1301.
45. Norman, T. C., Smith, D. L., Sorger, P. K., Drees, B. L., O'Rourke, S. M., Hughes, T. R., et al. (1999) Genetic selection of peptide inhibitors of biological pathways. *Science* **285**, 591–595.
46. Nieman, P. E., Ruddell, A., Jasoni, C., Thomas, S. J., Brandvold, K. A., Lee, R.-M., et al. (2001) Analysis of gene expression during *myc* oncogene-induced lymphomagenesis in the bursa of fabricius. *PNAS* **98**, 6378–6383.
47. Nuwaysir, E. F., Bittner, M., Trent, J., Barrett, J. C., and Afshari, C. A. (1999) Microarrays and toxicology: the advent of toxicogenomics. *Mol. Carcinogen.* **24**, 153–159.
48. Brady, G., and Iscove, N. N. (1993) Construction of cDNA libraries from single cells. *Methods Enzymol.* **225**, 611–623.
49. Taioli, E. (1999) International collaborative study on genetic susceptibility to environmental carcinogens. *Cancer Epidemiol. Biomark. & Prevent.* **8**, 727–728.
50. Ermolaeva, O., Rastogi, M., Pruitt, K. D., Schuler, G. D., Bittner, M. L., Chen, Y., et al. (1998) Data management and analysis for gene expression arrays. *Nature Genet.* **20**, 19–23.

## Microarray Analysis of Apoptosis

---

**Richard W. E. Clarkson, Catherine A. Boucher,  
and Christine J. Watson**

### 1. INTRODUCTION

Apoptotic cell death is a genetically regulated process and the balance between death and survival signals determines the fate of a cell. Apoptosis is important in development and in a number of pathological conditions including cancer and autoimmune diseases. Many transcription factors have been shown to regulate apoptosis in a range of biological systems. However, the downstream target genes and the mechanism of their action have not been clearly defined. The recent advent of gene microarray technology will allow the expression patterns of a large number of genes to be analyzed. Changes in transcription in response to an apoptotic stimulus can be identified and novel pathways defined.

Microarray is a rapidly developing field, with the capacity to revolutionize many fields of biomolecular research. This technology promises to deliver an explosion of information on the genetic basis of normal physiological processes and disease states by providing the opportunity to simultaneously compare the relative amounts of thousands of individual sequences from complex mixtures of nucleic acids. Based on traditional nucleic acid hybridization chemistry, it offers flexibility in choice of target/probe combinations and provides quantifiable data on relative expression levels.

The power of microarray based methods of expression analysis lies in the ease with which multiple expression profiles can be directly compared to provide increasingly stringent analysis of a complex biological system. In this review we provide an overview of the processes involved in microarray,

highlight potential problems and pitfalls, and discuss its application to apoptosis research.

## 2. WHAT IS MICROARRAY?

The technique can be subdivided into four processes:

1. Immobilization of nucleotides onto a solid substrate,
2. Fluorescence labeling of independent cDNA populations,
3. Hybridization of labeled probe to immobilized nucleotides, and
4. Scanning and analysis of comparative fluorescence.

This is illustrated schematically in Fig. 1.

The majority of effort has gone into optimizing the first process. This also requires complex and expensive equipment. In contrast, process 4 has received comparatively less attention and only recently has begun its own revolution. It is clear now that analysis is critical to eventual output.

There are two formats of microarray: oligonucleotide chips contain short (less than 60) nucleotides synthesized *in situ* on the solid support (1,2) and spotted DNA arrays where nucleic acids are robotically spotted onto a glass substrate (3). PCR product or plasmid DNA in 96/384-well format is transferred by specially engineered tips to multiple glass slides then dried and fixed to the glass substrate.

Oligo chips are expensive to make and technically more demanding at this stage than the alternative “spotting” methods. However oligo arrays are available commercially and retain the distinct advantage that each target gene is represented by four or more sequences on the array, which also includes mismatch sequences. These features provide improved hybridization controls.

In contrast, the ability to choose target DNAs, and the relative ease of spotting these onto solid substrates, has resulted in spotting methods becoming the popular choice of noncommercial research laboratories. For this reason we will focus on methods of arraying and hybridizing to spotting cDNA arrays.

## 3. HISTORICAL PERSPECTIVE

Methods of expression profiling are not new. Original techniques were based on semi-specific polymerase chain reaction (PCR), selectively amplifying subsets of RNA populations, and providing quantitative data on the relative abundancies of these transcripts between two given samples. These methods have proven successful in many areas of biomedical research,

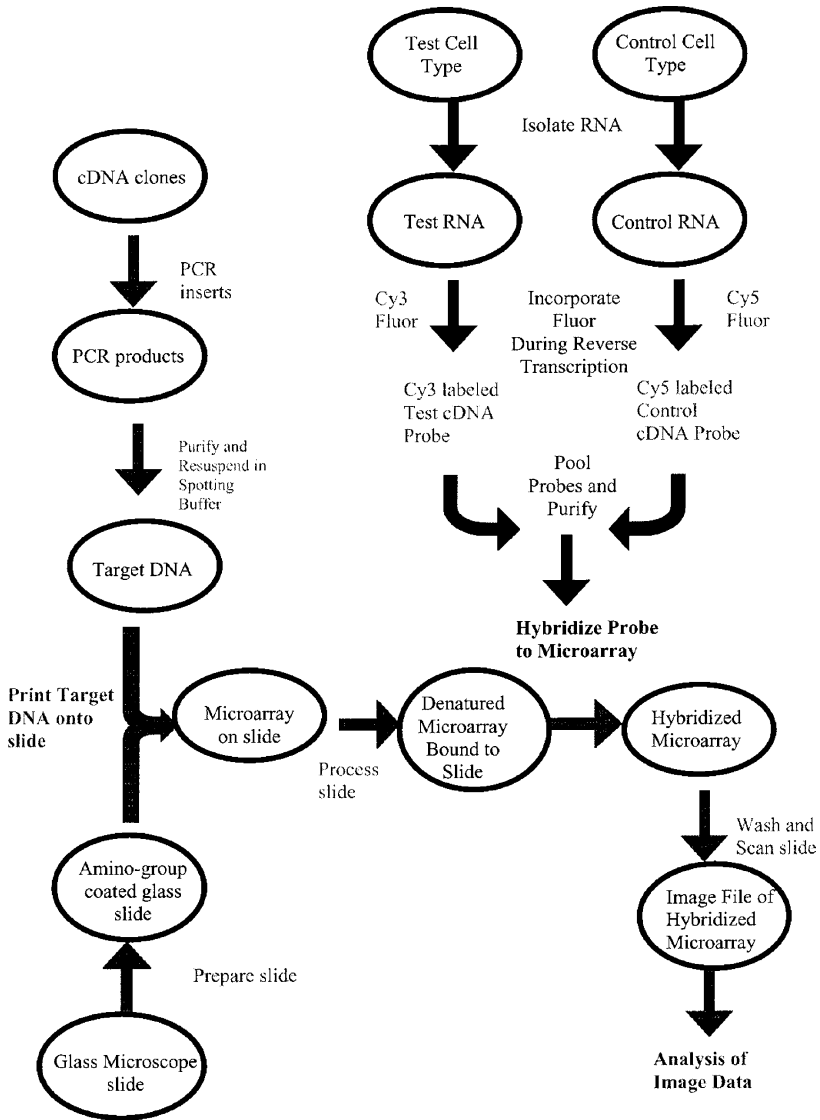


Fig. 1. A standard approach to microarray analysis using spotted cDNA arrays. Target DNA may alternatively consist of synthetic oligonucleotides. In some applications a single probe population is hybridized per slide.

however, there are inherent difficulties associated with these PCR-based procedures.

Recent advances in micro-manipulation and hybridization, fluorescence labeling, and large-scale sequencing projects have led to new methods of expression profiling and genome analysis, loosely termed microarray analysis. This is an oblique description for a number of methods that utilize hybridization of labeled complex RNA probes to immobilized nucleotides arrayed at high density on a solid substrate to provide quantifiable data on relative expression levels.

Originally described in analysis of plant gene expression, microarray was rapidly adopted for analysis of mammalian and lower eukaryotic transcriptomes. Until very recently, analyses were restricted to small (approx 1000 gene) subsets or complete genomes of lower eukaryotes such as yeast. The original application in humans, used to demonstrate application of the technique, was an analysis of heat-shock proteins in T cells (4).

#### **4. INITIAL CONSIDERATIONS IN EXPERIMENTAL DESIGN: PROBE VS TARGET**

Terminology relating to probe and target in the hybridization are interchangeable and for the purposes of this review we will refer to DNA immobilized on glass substrate as target and fluorescently labeled nucleic acids as probe.

The choice of targets in large-scale expression studies is largely dictated by the resources available. Ideally every gene in the genome would be represented on the array. This is only possible of course if the genome has been completely sequenced and every possible open reading frame could be PCR-amplified. This has been performed for yeast and *Arabidopsis* (the smallest higher eukaryotic genome known), but is no mean feat in mammalian species, which possess more complex genomes. An alternative approach is to utilize the increasingly comprehensive cDNA and expressed sequence tags (ESTs) collections, resources compiled from cDNA libraries from a variety of tissues and a number of different species. Unique cDNA clones may be chosen from these collections and used as gene-specific targets in arrays. In this way only relevant targets may be selected to be represented on the array, thus simplifying the spotting procedure. However this introduces potential clone-selection bias often evident when cDNA arrays are constructed from known gene sets. For example, small-scale apoptosis related gene arrays currently available from commercial sources are, by definition, limited to known apoptosis genes and therefore obviate the possibility of identifying unknown apoptosis genes.

For poorly characterized genomes or in circumstances where a particular tissue or developmental stage is not well-represented in the available resource of cDNA libraries, one may wish to array cDNA clones directly from libraries constructed in-house. Ideally, it would be preferable to have a limited duplication of cDNA clones on a microarray. If random clones are chosen from a cDNA library then the more abundantly expressed sequences will dominate the microarray. Therefore a sequence verified nonredundant set of clones is a better option. Dependant on the species of interest, such a set of clones may be available commercially or from academic establishments (such as a sequence verified set of human IMAGE consortium clones available from Research Genetics and soon to be available from the HGMP resource centre in the UK). However it must be noted that all sources of sequence verified clones will have some error in clone identification. Furthermore, novel and previously ill-defined genes will be unrepresented on the array.

Another option is the preparation of subtracted libraries to reduce redundancy. This method of library production enables one to enrich starting material for genes of interest, in essence providing a preliminary screen for cognate genes prior to the more specific screens ascribed by the subsequent hybridizations. These clones may not necessarily be sequenced prior to arraying, which takes advantage of the fact that rare transcripts represented only once in the microarray will be as equally informative as those genes multiply represented. This adaptation of the standard approach of arraying unique, sequence-verified, cDNA clones avoids the technically demanding, costly, and laborious requirements of sequencing all clones from the normalized library prior to arraying.

Alternatively, an enriched or normalized cDNA library may be an appropriate source of cDNA clones. Provided that the redundancy of the library is not too high, such a library will provide a good source of clones, which are specific to the tissue, cell type, and conditions of interest.

## **5. METHODOLOGY**

It is not the scope of this chapter to provide a detailed protocol for potential users to follow. Indeed this is impossible as the technology at this early stage is still in development and there are as many working protocols as there are research groups performing the technique. Rather, we aim to provide an insight into some of the important considerations. We refer the reader wishing to acquire a more comprehensive explanation of the protocol to an excellent review by Eisen and Brown (3) and to detailed methods available on the internet (<http://cmgm.stanford.edu/pbrown>, <http://www.biorobotics.co.uk>).

As mentioned earlier, the microarray process can be subdivided into four steps. Each of these will be discussed in turn.

## ***5.1. Immobilization of Nucleotides onto a Solid Substrate: Preparation of Gene Set and Arraying Nucleic Acids***

### *5.1.1. Preparation of Gene Set*

The target DNA can be plasmid preparations of cDNA clones, PCR-amplified inserts of cDNA clones, or PCR-amplified open reading frames (ORFs). The most suitable will depend on availability and ease of use.

The PCR template can either be prepared plasmid DNA or bacterial cell lysates. The primers can be standard oligonucleotides or 5-amine modified, depending on what slide binding chemistry is adopted (*see* Subheading 5.1.2.).

If plasmid DNA is used then a high proportion of the DNA on the microarray will be vector-derived. As the DNA forms a monolayer on the slide the quantity of DNA binding to the slide is restricted and the presence of vector DNA will limit the number of cDNA molecules available for hybridization. This in turn will affect the intensity of signal achieved.

PCR amplification requires large quantities of PCR reagents in order to produce a sufficient quantity of DNA. Although this can be expensive, it does maximize the number of molecules available for hybridization. If cDNA clones are available then amplification of the inserts using vector specific primers may be more efficient than amplifying ORFs with gene-specific primers. However, for some systems, amplification of ORFs direct from genomic DNA might be the only option. An example of this is bacterial gene sets derived from sequencing of bacterial genomes.

It is desirable to purify the PCR products prior to arraying in order to remove PCR-reaction components and cellular debris from the amplified target DNA, which would otherwise increase the printed spot size and interfere with the binding of the DNA to the slide surface. Several alternative methods could be used including: (1) ethanol or isopropanol precipitation, or (2) 96-well PCR purification kits from TeleChem, Qiagen and Millipore.

Generally 4  $\mu\text{g}$  of each PCR product from a 100  $\mu\text{L}$  reaction is needed for spotting and a small aliquot of the PCR reaction should be run on an agarose gel to verify amplification of a pure PCR product and to estimate the quantity of product.

Due to the large scales involved, gene sets are optimally stored in 384-well format, and most robotics accommodate this system. Archival material, in the form of glycerol stocks of the bacterial cultures, bacterial lysate plates,



purified PCR products, or 384-well printing source plates, can be stored at  $-70^{\circ}\text{C}$ . Fresh printing run 384-well source plates can be prepared from archived purified stocks as required.

### 5.1.2. *Arraying Nucleic Acids*

While control elements are important, other microarray structural features such as landmark elements will prove useful. A landmark element is labeled DNA printed at defined locations throughout the array, such as the four corners of the array or subarrays. These elements make it easier for the analysis software to locate an array for data acquisition.

When making arrays, it is advisable to print all clones in duplicate or triplicate, thereby providing multiple measurements, for averaging purposes, of mRNA expression level for each clone.

A minimum concentration of target DNA should be  $200\text{ ng}/\mu\text{L}$ . This is sufficient to produce a spot with a saturated DNA monolayer. The maximum source DNA concentration is about  $1\text{ }\mu\text{g}/\mu\text{L}$ . Higher concentrations can increase the risk of comet-tails and other artifacts caused by localized reattachment of excess spot material to the slide surface during the post-array processing. Spot centers are routinely  $200\text{ }\mu\text{m}$  apart, resulting in a capacity of around 80,000 spots on a standard microscope slide.

Various different spotting solutions have been described including 1X Array-IT micro-spotting solution (TeleChem International, cat. no. MSS-1), 5X SSC, 3X SSC,  $150\text{ mM}$  sodium phosphate buffer, pH 8.5, and 1X PCR buffer. We find the spotting buffers providing optimal spot size shape and effective binding of the target DNA to the slide are either 1X Array-IT or  $150\text{ mM}$  sodium phosphate/0.01% SDS.

There are several different approaches to binding DNA onto microscope slides, but they can be essentially divided into two groups; those that involve hydrogen bonding or those that involve covalent linkage. Hydrogen bonding can occur between amine groups coated on the slide and phosphate groups in the DNA backbone. Microscope slides can be coated with either poly-L-lysine or aminosilane to give an amine group coated slide. Once the DNA is spotted onto the slide, ultraviolet (UV) crosslinking or oven baking allows some covalent bonds to be formed between the amine groups and the DNA. The remaining free amine groups on the slide should be blocked. This is achieved by treatment with succinic anhydride (a molecule with two active carboxyl groups). A condensation reaction takes place and for every succinic anhydride molecule two peptide bonds are formed with the poly-L-lysine/amino silane. Poly-L-lysine or amino silane slides can be prepared in-house (5,6) or purchased (poly-L-lysine:

P 0425, Sigma; amino silane: CMT-GAPS slides 2549, Corning; Silanated slides, CSA-25, TeleChem).

For poly-L-lysine slides, homemade slides can be cleaner, with a more even surface-coating and lower background fluorescence, than commercially prepared slides that are currently available. However, commercially available CMT-GAPS slides (cat. no. 2549, Corning) are exceptionally clean and of very high quality.

While there are no significant differences between the spot size, morphology, and surface-binding properties of the two coatings, aminosilane may be more physically robust than poly-L-lysine and less prone to surface damage.

Covalent bonding can occur between active groups (such as aldehyde, epoxy, or isothiocyanate) coating the slide and amine-modified DNA. The amine groups can be synthetically attached to the PCR primers during the synthesis of the oligonucleotides. The PCR primers can then be used to amplify the cDNAs giving the amine modified DNA. In-house slides can be prepared by treating aminosilane slides with phenylmercuriisothiocyanate (5). Alternatively, activated slides can be purchased (3D-Link activated slides, Surmodics; Silylated slides, CSS-25, TeleChem). These active slides are moisture sensitive and only once the target DNA has been spotted onto them can they be exposed to moisture. This then deactivates the groups to prevent unwanted probe binding to the slide.

#### 5.1.2.1. PREPARATION OF POLY-L-LYSINE COATED GLASS SLIDES

This method is based on a protocol that is provided in ref. 6. It has been suggested by some researchers that, following coating, slides should be left to season for at least a week before use. The surface of the seasoned slides is likely to be more arid than that of the freshly coated slides and this feature may contribute to smaller spot sizes. However, some workers report no discernable improvement in the surface-binding properties of slides used immediately after coating and those that have been left to season. Recommended slides are Gold Star, single frosted-end, washed, 76 × 26 mm glass microscope slides (cat. no. KTH 002). Of those slides tested, these displayed the lowest levels of background fluorescence.

#### 5.1.2.2. POSTARRAY PROCESSING OF PRINTED SLIDES

In general, the postarray processing allows the binding reaction to take place, the deactivation of active groups on the slide surface, the removal of unbound DNA, and the denaturation of the target DNA ready for hybridization. The processes will be chemistry/slide-specific and manufacturer's protocols should be followed.

### 5.1.2.3. POSTARRAY PROCESSING OF POLY-L-LYSINE SLIDES

As mentioned, this process is based on the method detailed in ref. 6. Once in solution, the blocking agents do not remain active for long, so it is important to prepare fresh solutions and to use immediately. In particular, the time between the point at which the succinic anhydride is completely dissolved and when the slides are plunged into the blocking solution is to be kept to the absolute minimum. Furthermore, 1-methyl-2-pyrrolidinone oxidizes upon exposure to air, a feature denoted by a yellow discoloration of the fluid.

It is essential that, with the exception of the ethanol wash, the solutions used in the protocol are agitated vigorously during use. Failure to do so will increase the risk of generating “comet-tails” and other undesirable patterns of background caused by localized reattenuation of excess cDNA material from the spots.

The salt deposits, which make the printed array visible, are washed off during slide processing. It is essential that the microarray position is clearly marked on the slide surface in order to accurately position the slide cover-slip during subsequent hybridizations.

Some protocols recommend the inclusion of a rehydration step prior to slide processing, the purpose of which is presumably to redistribute more evenly the material within a spot. This step may be unnecessary.

## **5.2. Fluorescence Labeling of Two Independent cDNA Populations: Probe Preparation**

### *5.2.1. Probe Preparation*

To compare the levels of gene expression between two cell types, RNA is extracted and reverse-transcribed to produce cDNA probes, incorporating fluorescently labeled nucleotides in the process. These two differently labeled probes are pooled and hybridized to the microarray. Once the slide has been washed to remove unhybridized probe from the microarray, it is scanned and two image files are collected (one for each fluor detected). The intensity of signal detected, for any one spot, will be proportional to the quantity of mRNA present in the cell type from which the probe was generated. As the amount of DNA bound to the surface of the slide cannot be fully controlled, the exact amount of mRNA present in the cell type cannot be quantified. However, using software to analyze the two image files, relative levels of expression between the two cell types can be calculated by comparing the intensity of signal between the two laser channels. Several variations of this procedure are possible, e.g., a vector probe could replace the control complex probe, total, or mRNA-derived probes can be used and if only small amounts of RNA are available, then perhaps an additional probe amplification step may be required.

At least two probes are required, the test probe and the control probe. The test probe can be derived from either mRNA or total RNA. The control probe can either be a complex probe derived from RNA of a control cell type or a probe that will hybridize to all target DNA such as a vector probe. If a complex control probe is used, then levels of expression can be directly compared between two complex probes and small differences between samples can be detected. The quantity of complex probe needed will be governed by the complexity of the RNA, and in general, the larger the quantity of RNA used the better the probe. For human RNA 50–100  $\mu\text{g}$  total RNA or 1–2  $\mu\text{g}$  polyA+ mRNA can be used.

A probe that can detect all target DNA (such as a vector probe) will allow the relative quantification of DNA in each spot to be determined. Expression levels can then be compared across several slides after the inevitable differences in quantity of target DNA binding to the slide have been taken into account. This approach can only be taken if all target DNA samples are tagged with the same DNA element.

There is a complex relationship between the concentration of input RNA for a given gene and the intensity of probe signal, depending on sequence, length, and purity. Thus, microarray is best at determining the relative hybridization signals across an array of targets, especially when two alternately labeled hybridizations are performed on the same target, which eliminates target variability.

Probe selection is dependent on the experimental design, and in the classic examples of differential expression profiling may include comparisons of nucleic acids based on pre- and posttreatment of cells, animals, or tissues; different disease states; different tissues or cell types; and subcellular localization. The number and type of comparison determine the complexity of data produced. The simplest experiment would involve the direct comparison of two nucleic acid samples which, depending on the complexity of the samples compared, may provide a few or many hundreds of differences. This highlights an important aspect of experimental design. Heterogeneous tissues provide a source of variability that is difficult to control for, and use of such tissues should be carefully considered.

When comparing hybridization results between two cell types, the same type and quantity of RNA should be used to generate both probes. If sufficient material is available, probes can be directly generated by incorporating fluorescent nucleotides during a reverse-transcription reaction. Otherwise an additional RNA amplification step will be needed. This is not desirable because it could cause problems with transcript representation.

#### 5.2.1.1. RNA ISOLATION

Successful hybridizations depend critically on the quality and purity of both the starting RNA and of the labeled end-product. As with all RNA work, RNase-free reagents should be used throughout. Purified ddH<sub>2</sub>O used to prepare solutions should be treated with 0.1% diethylpyrocarbonate (DEPC) overnight and then autoclaved.

If only small quantities of RNA are available, then RNA amplification using T7 RNA polymerase to produce transcripts from double-stranded cDNA may be necessary (3).

#### 5.2.1.2. PROBE LABELING

It is important that the chosen fluorescent dyes are compatible with the scanner excitation wavelengths. Most scanners excite at 532 nm and 635 nm, making Cy3 and Cy5 (Amersham or NEN) compatible. Either dUTP- or dCTP-labeled nucleotides can be used, with the corresponding unlabeled nucleotide concentration reduced. Fluorescent dyes are photosensitive, so measures should be taken to minimize their exposure to light. Probe-labeling reactions, hybridizations, and so forth should be foil-wrapped or performed in light-proof containers wherever possible.

#### 5.2.1.3. VECTOR PROBE PRODUCTION

Fluorescent-labeled PCR product can be produced by adapting a standard PCR reaction by including fluorescent dCTP but keeping the total dCTP concentration the same as standard, with the ratio of fluorescent to unfluorescent dCTP being 1:4. Using the same vector primers as used to amplify the target DNA, amplify the multiple cloning site of the appropriate pure vector DNA.

#### 5.2.1.4. PROBE PURIFICATION

Before setting up a microarray hybridization, the labeled probes must be purified, concentrated, and resuspended in the hybridization buffer containing the appropriate salts, blocking agents, and detergents.

### ***5.3. Hybridization of Labeled Probe to Immobilized Nucleotides***

Hybridizations should be carried out under a sealed coverslip in a humid chamber. Geneframes or coverslips sealed with Cowgum can be used to hybridize in a humid box in an oven. However, this method is not recommended as problems can occur if sealant is deposited on the slide after

hybridization. Alternatively, Corning (cat. no. 2551) or TeleChem International (cat. no. AHC-1) hybridization chambers can be used in a waterbath. These chambers are preferable as humidification can be ensured and the seal does not touch the coverslip or slide. The coverslip used should just cover the area of the microarray, and the volume of hybridization adjusted accordingly. It is essential that no air bubbles are introduced under the coverslip when setting up hybridizations and care must be taken to avoid this. However, if bubbles do appear under the coverslip, these should not be tapped out since this could result in damage to the slide surface coating and, therefore, to the array.

#### 5.3.1. Prehybridization Set-Up

The active groups on the slide surface should be deactivated during the post array processing. However, a prehybridization of bulk DNA to the slide can ensure a clean background (use general blocking reagents as mentioned below for the hybridization step). This prehybridization should take place immediately prior to hybridization and is based on standard hybridization protocols.

#### 5.3.2. Hybridization Set-Up

Hybridizations can either occur at 65°C or 42°C (if 50% formamide is included). General and species specific blocking elements should be included in the hybridization. For human RNA-derived probes in a 25 µL hybridization, use of 10 µL of 1 mg/mL CoT-1 DNA helps to block repetitive human DNA, 1 µL of 4 mg/µL yeast tRNA acts as a nonspecific hybridization blocker and 1 µL of 8 mg/mL poly dA blocks the oligo dT. The CoT-1 DNA and the tRNA can be added to the probe just prior to purification.

#### 5.3.3. Slide Washing

Hybridization components such as SDS and SSC fluoresce and, unless washed from the slide surface prior to scanning, will cause diffuse low-level background. This background can be minimized by immediately spin-drying slides by low-velocity centrifugation after washing. Washing is based on standard hybridization protocols.

### 5.4. Scanning and Analysis of Comparative Fluorescence

#### 5.4.1. Slide Scanning and Signal Quantification

The expression levels of different genes on the microarray are visualized by confocal laser scanning of the hybridized slide. There are a number of

different scanners on the market which detect Cy3 and Cy5 (or their spectral homolog) and at least one manufacturer produces instruments that can detect additional fluors.

It is useful to scan slides at every stage of the process, to check on the background level of fluorescence on the slides, and to check that the DNA has been bound effectively (by analyzing the intensity of the landmark spots).

Slides can be scanned at several different laser intensities in order to ensure that all levels of expression are detected and that the spot intensity is not saturated.

#### *5.4.2. Data Analysis*

Image analysis software packages extract data from TIFF files generated from scanning the slide. In general, a circle is drawn around each spot and the integrated or mean intensity of signal within the spot is calculated. Background signal-intensity data is also extracted together with standard deviation errors. This data can be exported in a tab-delineated format and imported into a spread-sheet packages (such as Excel) or into the data mining packages. Also composite images can be generated where two images from the same slide are shown as one. Both the image analysis software and spread-sheet packages are capable of giving a graphical presentation of the data. The data-mining packages look for trends and patterns in the data from a set of several slides.

## **6. TECHNICAL CONSIDERATIONS**

The following issues and more are discussed and reviewed elsewhere in detail (3,7,8).

### **6.1. Cost**

To prepare microarrays requires costly robotics equipment and large-scale sequencing analysis. This is prohibitively expensive for all but the larger research and clinical laboratories and biotech industry; for small-scale expression studies or in cases where small numbers of arrays are required, it is not cost-effective. For this reason many researchers opt to acquire pre-made arrays or amplified cDNA sets from commercial sources. A growing number of specific cDNA subsets are now commercially available as arrays. These include cell-cycle and apoptosis gene arrays.

## 6.2. Reproducibility

Spot integrity and reproducibility in arrays is one of the paramount concerns. While relative binding of labeled probe is intrinsic to each spot on the array, large variation in DNA concentration or impurities may significantly interfere with uniform hybridization signals. Similarly amounts of DNA loaded per spot can dramatically affect performance of the final array. Too much DNA may result in comet formation, high background, and an inconsistent loss of bound DNA from the slide; too little may result in poor binding and low fluorescent signals. Each commercial arrayer will recommend optimal conditions, which should be heeded.

## 6.3. Controls

An important aspect of any microarray experiment is the design of several controls. This has been an area of intense debate and, where possible, more than one internal control should be included that will meet at least one of the following variables:

1. The quantity of target DNA binding to the slide,
2. The quality of the spotting and binding processes of the target DNA onto the slide,
3. The quality of the RNA samples,
4. The efficiency of the reverse transcription and fluorescent labeling of the probes,
5. The efficiency of blocking repetitive elements in the target DNA, and
6. Variation in background fluorescence on the slide.

The ideal internal control clone for microarray expression normalization would be derived from a gene whose expression level is invariant between the different states under investigation. This has been a problem for quantitative PCR studies for many years and is just as challenging for microarray. Unfortunately, such a clone is unlikely to be identified before carrying out an experiment. A pool of some 30–50 candidate normalization clones should therefore be contained within the array.

Following data acquisition it becomes possible to select a sub-set of clones for expression normalization.

External controls are generally synthetic mRNAs or clones of mRNA derived from an organism unrelated to—and therefore unlikely to cross-hybridize with—the organism under investigation. These RNAs can be spiked



into the labeling reaction at different concentrations and used to assess the efficiency of the reaction. It might be possible to use such RNAs for expression normalization. However care will need to be taken, as the overall level of RNA expression may vary between the different states under investigation.

A single PCR can produce up to 1000 dots. These reactions should be devoid of glycerol, peg, or gelatin, which may interfere with the spotting process. Dehydration is one of the most important issues to be addressed in the arraying and hybridization steps. In an uncontrolled environment PCR samples will dehydrate, reducing the number of potential slides and increasing the amount of DNA loaded per slide during a run. If large-scale arrays are constructed or several hundred slides are arrayed, simultaneously, the effect of dehydration can be significant.

With most high-throughput, automated processes, batch testing of reagents and equipment is also a vital component of successful reproducibility. In particular, commercially available slides should be tested for their consistency between batches and all solutions should be monitored carefully not to exceed shelf lives, which may often be determined empirically.

## **7. TO ARRAY OR NOT TO ARRAY?**

Many research projects that aim to establish the identity of differentially expressed genes from two or more samples would not necessarily benefit from the microarray approach compared to more conventional methods such as subtractive library screening or differential display. Initial considerations as to the suitability of this technique to a particular application include: whether more than two samples are being compared, how many differences might be expected, and what proportion of the total number of transcripts from the target tissue are known or have been cloned. In addition, the practical issues of availability of array robotics and analysis hardware and technical expertise must all be considered.

The prime consideration of array analysis is the genes that are represented on the immobilized array. Obviously no data can be obtained on a gene that is not represented on the array. This is a significant disadvantage of pre-made arrays using known genes when one is interested in identifying potentially novel or previously uncharacterized genes.

Other considerations are heterogeneity of tissue and sensitivity problems with respect to low-abundance transcripts.

## 8. RESEARCH APPLICATIONS

### 8.1. Expression Profiling

A consequence of the flexibility of microarrays is the wide range of possible applications. The microarray technique has been applied to genetic mapping (8–10), mutation analyses (11), and genetic screening (12). However it is in the field of comparative-expression profiling that this technology has gained most attention and is likely to yield the greatest amount of information.

Already, many microarray studies have been published and validate the use of this expensive technology. Perhaps the best examples include human cancer (13–16) encompassing the monitoring of tumor progression (17,18) and leading to the reclassification of tumors (17,19). Other diseases have also been subject to array analysis such as rheumatoid arthritis (20) and Batten disease (21).

Basic biological questions have been addressed using microarray. Examples include cell cycle (22) and targets of transcriptional regulators such as BRCA1 (23), PAX3-FKHR (24), and *WT1* (25).

Total expression of brain has been investigated using microarrays (26) and physiological responses have also been examined in the studies of receptor tyrosine kinase pathways and serum growth factors (27,28).

### 8.2. Other Microarray Applications

In addition to expression profiling, microarray approaches are used in comparative genome hybridization (CGH) studies, and single nucleotide polymorphism (SNP) analysis. For CGH studies, cDNA or genomic clones are microarrayed and probes of labeled whole genomic DNA from tumor and control are compared (29,30). For any spot, the ratio of signal intensity from the two probes is proportional to the copy number of the corresponding DNA sequence in the tumor. This allows detection of deletions and amplifications of segments in the tumor DNA.

Two alternative methods can be used for SNP analysis using microarrays. The first is based on differential hybridization (31) and the other on minisequencing (32). For differential hybridization, a set of oligonucleotides (containing the SNP of interest) is arrayed onto a glass slide. The set com-

prises of overlapping oligonucleotides with both sequence alternatives included. PCR products of sample DNA (containing the SNP) are then hybridized to the microarray at varying stringencies in order to distinguish which sequence is present in the sample. Multiplex PCR followed by hybridization to an array of several sets of oligo nucleotides allows many SNPs to be typed at the same time.

Alternatively, oligonucleotides are arrayed onto the glass slide and a one-base minisequencing reaction is carried out on the slide with the arrayed oligonucleotides as the primer and sample PCR products as the template. SNP is typed by scanning the array to determine which fluorescent dideoxynucleotide has been incorporated. Again many SNPs can be typed at once by minisequencing from a multiplex of PCR products.

### **8.3. Apoptosis Research Applications**

Microarray technology has already been used in a number of apoptosis-related studies. In our laboratory, we have carried out a preliminary microarray analysis of genes, which are induced following the initiation of involution in the mouse mammary gland. Involution is characterized by extensive apoptosis of the epithelial cells. We have previously shown that at least three transcription factors, Stat3, IRF-1, and NF- $\kappa$ B, have either pro-apoptotic or survival functions in mammary epithelia (33–36). The downstream targets of these transcription factors during mammary epithelial-cell apoptosis have been identified using microarrays. An example of our preliminary data is presented in Fig. 2.

A variety of microarray approaches have been adopted in other laboratories, including the use of apoptosis chips containing only gene sequences currently implicated in apoptosis regulation. An example of this is the study of Jones et al (37) who hybridized 205 apoptosis-related genes with RNA from retinitis pigmentosa (apoptotic) and normal retinas. Wang and colleagues (38) used a 6591 gene oligo array to look at apoptosis induced by etoposide, identifying previously undescribed candidates downstream of p53. A much larger array (11,000 genes) was utilized by Voehringer to investigate the effects of ionizing irradiation-induced gene expression in apoptosis sensitive and resistant B cell lymphoma cell lines (39). A number of redox and mitochondrial elements were identified that control the sensitivity/resistance to apoptosis. Their data suggest that a multigenic program

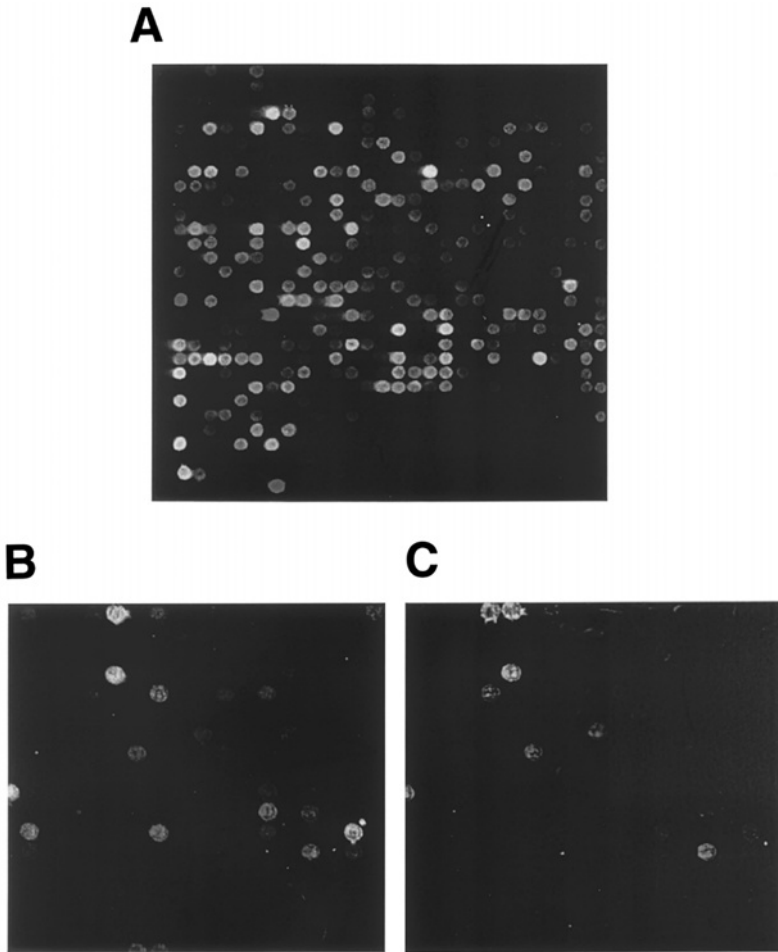


Fig. 2. Resultant scan from a cDNA microarray analysis of Stat3-specific gene targets in mammary epithelial cells. (A) Portion of a 15,000 mouse cDNA array, hybridized with Cy3 (inactive Stat3) and Cy5 (active Stat3)-labeled cDNA probes from a mouse mammary epithelial cell line. Note the range of hybridization intensities between cDNAs “spots” on the array, representing relative differences in the expression of these transcripts in the complex probe populations. (B) and (C) Differential hybridization to individual cDNAs on the same part of the array is evident in separate scans of Cy-3 (B) and Cy-5 (C) labeled probes. These cDNA clones therefore represent likely gene targets of the Stat3 transcription factor.

is involved in controlling sensitivity to apoptosis and that genes involved in uncoupling mitochondrial electron transport and loss of membrane-potential control the sensitivity to apoptosis.

One of the major advantages of microarray technology is that it allows the simultaneous characterization of sets of genes that may be involved in a complex cellular process. Thus, it is eminently suitable for apoptosis studies and lends itself particularly well to studies on the effects of pharmacological agents on apoptosis induction.

## ACKNOWLEDGMENTS

We wish to thank Dr. Nabeel Affara (Dept. of Pathology, University of Cambridge) and Dr. David Latto (BioRobotics UK Ltd.) for their extensive contribution to the microarray methodologies described in this review.

## REFERENCES

1. Fodor, S. P. A., Rava, R. P., Huang, X. H. C., Pease, A. C., Holmes, C. P., and Adams, C. L. (1993) Multiplexed biochemical assays with biological chips. *Nature* **364**, 555–556.
2. Pease, A. C., Solas, D., Sullivan, E. J., Cronin, M. T., Holmes, C. P., and Fodor, S. P. A., (1994) Light-generated oligonucleotide arrays for rapid DNA-sequence analysis. *Proc. Nat. Acad. Sci. US* **91**, 5022–5026.
3. Eisen, M. B. and Brown, P. O. (1999) DNA arrays for analysis of gene expression. *Methods Enzymol.* **303**, 179–205.
4. Schena, M., Shalon, D., Heller, R., Chai, A., Brown, P. O., and Davis, R. W. (1996) Parallel human genome analysis: Microarray-based expression monitoring of 1000 genes. *Proc. Natl. Acad. Sci. USA* **93**, 10,614–10,619.
5. Guo, Z., Guilfoyle, R. A., Thiel, A. J., Wang, R. F., and Smith, L. M., (1994) Direct fluorescence analysis of genetic polymorphisms by hybridization with oligonucleotide arrays on glass supports. *Nucleic Acids Res.* **22**, 5456–5465.
6. Shalon, D., Smith, S. J., and Brown, P. O., (1996) A DNA microarray system for analyzing complex DNA samples using two-color fluorescent probe hybridization. *Genome Res.* **6**, 639–645.
7. Greenfield, A. (2000) Applications of DNA microarrays to the transcriptional analysis of mammalian genomes. *Mammalian Genome* **11**, 609–613.
8. Chee, M., Yang, R., Hubbell, E., Berno, A., Huang, X. C., Stern, D., et al. (1996) Accessing genetic information with high-density DNA arrays. *Science* **274**, 610–614.
9. Gerton, J. L., DeRisi, J., Shroff, R., Lichten, M., Brown, P. O., and Petes, T. D. (2000) Global mapping of meiotic recombination hotspots and coldspots in the yeast *Saccharomyces cerevisiae*. *Pro. Nat. Acad. Sci.US* **97**, 11,383–11,390.

10. Lashkari, D. A., DeRisi, J. L., McCusker, J. H., Namath, A. F., Gentile, C., Hwang, S. Y., et al. (1997) Yeast microarrays for genome wide parallel genetic and gene expression analysis. *Proc. Nat. Acad. Sci. US* **94**, 13,057–13,062.
11. Kononen, J., Bubendorf, L., Kallioniemi, A., Barlund, M., Schraml, P., Leighton, S., et al. (1998) Tissue microarrays for high-throughput molecular profiling of tumor specimens. *Nature Med.* **4**, 844–847.
12. DeRisi, J., Penland, L., Brown, P. O., Bittner, M. L., Meltzer, P. S., Ray, M., et al. (1996) Use of a cDNA microarray to analyse gene expression patterns in human cancer. *Nature Genet.* **14**, 457–460.
13. Alizadeh, A., Eisen, M., Botstein, D., Brown, P. O., and Staudt, L. M. (1998) Probing lymphocyte biology by genomic-scale gene expression analysis. *J. Clin. Immunol.* **18**, 373–379.
14. Golub, T. R., Slonim, D. K., Tamayo, P., Huard, C., Gaasenbeek, M., Mesirov, J. P., et al. (1999) Molecular classification of cancer: Class discovery and class prediction by gene expression monitoring. *Science* **286**, 531–537.
15. Perou, C. M., Jeffrey, S. S., Van de Rijn, M., Rees, C. A., Eisen, M. B., Ross, D. T., et al. (1999) Distinctive gene expression patterns in human mammary epithelial cells and breast cancers. *Proc. Nat. Acad. US* **96**, 9212–9217.
16. Scholl, F. A., Betts, D. R., Niggli, F. K., and Schafer, B. W. (2000) Molecular features of a human rhabdomyosarcoma cell line with spontaneous metastatic progression. *Brit. J. Cancer* **82**, 1239–1245.
17. Alizadeh, A. A., Eisen, M. B., Davis, R. E., Ma, C., Lossos, I. S., Rosenwald, A., et al. (2000) Distinct types of diffuse large B-cell lymphoma identified by gene expression profiling. *Nature.* **403**, 503–511.
18. Backert, S., Gelos, M., Kobalz, U., Hanski, M. L., Bohm, C., Mann, B., et al. (1999) Differential gene expression in colon carcinoma cells and tissues detected with a cDNA array. *Inter. J. Cancer* **82**, 868–874.
19. Wellmann, A., Thieblemont, C., Pittaluga, S., Sakai, A., Jaffe, E. S., Siebert, P., and Raffeld, M. (2000) Detection of differentially expressed genes in lymphomas using cDNA arrays: identification of clusterin as a new diagnostic marker for anaplastic large-cell lymphomas. *Blood* **96**, 398–404.
20. Heller, R. A., Schena, M., Chai, A., Shalon, D., Bedilion, T., Gilmore, J., et al. (1997) Discovery and analysis of inflammatory disease-related genes using cDNA microarrays. *Proc. Nat. Acad. Sci. US* **94**, 2150–2155.
21. Pearce, D. A., Ferea, T., Nosel, S. A., Das, B., and Sherman, F. (1999) Action of *BTN1*, the yeast orthologue of the gene mutated in Batten disease. *Nature Genet.* **22**, 55–58.
22. DeRisi, J. L., Iyer, V. R., and Brown, P. O. (1997) Exploring the metabolic and genetic control of gene expression on a genomic scale. *Science* **278**, 680–686.
23. Harkin, D. P., Bean, J. M., Miklos, D., Song, Y. H., Truong, V. B., Englert, C., et al. (1999) Induction of GADD45 and JNK/SAPK-dependent apoptosis following inducible expression of BRCA1. *Cell* **97**, 575–586.
24. Khan, J., Bittner, M. L., Saal, L. H., Teichmann, U., Azorsa, D. O., Gooden, G. C., et al. (1999) cDNA microarrays detect activation of a myogenic transcription program by the PAX3-FKHR fusion oncogene. *Proc. Nat. Acad. Sci. US* **96**, 13,264–13,269.

25. Lee, S. B., Huang, K., Palmer, R., Truong, V. B., Herzlinger, D., Kolquist, K. A., et al. (1999) The Wilms tumor suppressor WT1 encodes a transcriptional activator of amphiregulin. *Cell* **98**, 663–673.
26. Sandberg, R., Yasuda, R., Pankratz, D. G., Carter, T. A., Del Rio, J. A., Wodicka, L., et al. (2000) Regional and strain-specific gene expression mapping in the adult mouse brain. *Proc. Nat. Acad. Sci. US* **97**, 11,038–11,043.
27. Fambrough, D., McClure, K., Kazlauskas, A., and Lander, E. S. (1999) Diverse signaling pathways activated by growth factor receptors induce broadly overlapping, rather than independent, sets of genes. *Cell* **97**, 727–741.
28. Iyer, V. R., Eisen, M. B., Ross, D. T., Schuler, G., Moore, T., Lee, J. C. F., et al. (1999) The transcriptional program in the response of human fibroblasts to serum. *Science* **283**, 83–87.
29. Pinkel, D., Seagraves, R., Sudar, D., Clark, S., Poole, I., Kowbel, D., et al. (1998) High resolution analysis of DNA copy number variation using comparative genomic hybridization to microarrays. *Nature Genet.* **20**, 207–211.
30. Pollack, J. R., Perou, C. M., Alizadeh, A. A., Eisen, M. B., Pergamenschikov, A., Williams, C. F., et al. (1999) Genome-wide analysis of DNA copy-number changes using cDNA microarrays. *Nature Genet.* **23**, 41–46.
31. Wang, D. G., Fan, J. B., Siao, C. J., Berno, A., Young, P., Sapolsky, R., et al. (1998) Large-scale identification, mapping, and genotyping of single-nucleotide polymorphisms in the human genome. *Science* **280**, 1077–1082.
32. Pastinen, T., Kurg, A., Metspalu, A., Peltonen, L., and Syvanen, A. C. (1997) Minisequencing: a specific tool for DNA analysis and diagnostics on oligonucleotide arrays. *Genome Res.* **7**, 606–614.
33. Chapman, R. S., Lourenco, P. C., Tonner, E., Flint, D. J., Selbert, S., Takeda, K., et al. (1999) Suppression of epithelial apoptosis and delayed mammary gland involution in mice with a conditional knockout of Stat3. *Genes Dev.* **13**, 2604–2616.
34. Chapman, R. S., Duff, E. K., Lourenco, P. C., Tonner, E., Flint, D. J., Clarke, A. R., and Watson, C. J. (2000) A novel role for IRF-1 as a suppressor of apoptosis. *Oncogene*, in press.
35. Clarkson, R. W. E., Heeley, J. L., Chapman, R., Aillet, F., Hay, R. T., Wyllie, A., and Watson, C. J. (2000) NF-kappa B inhibits apoptosis in murine mammary epithelia. *J. Biol. Chem.* **275**, 12,737–12,742.
36. Clarkson, R. W. E., and Watson, C. J. (1999) NF-kappa B and apoptosis in mammary epithelial cells. *J. Mammary Gland Biol. Neoplasia* **4**, 165–175.
37. Jones, S. E., Jomary, C., Grist, J., Stewart, H. J., and Neal, M. J. (2000) Altered expression of secreted frizzled-related protein-2 in retinitis pigmentosa retinas. *Invest. Ophthalmol. Visual Sci.* **41**, 1297–1301.
38. Wang, Y. X., Rea, T., Bian, J. H., Gray, S., and Sun, Y. (1999) Identification of the genes responsive to etoposide-induced apoptosis: application of DNA chip technology. *FEBS Lett.* **445**, 269–273.
39. Voehringer, D. W., Hirschberg, D. L., Xiao, J., Lu, Q., Roederer, M., Lock, C. B., et al. (2000) Gene microarray identification of redox and mitochondrial elements that control resistance or sensitivity to apoptosis. *Proc. Nat. Acad. Sci. US.* **97**, 2680–2685.

## ELISAs for Quantification of Bcl-2 Family Activities and Active Caspases

---

Calvin F. Roff, Amy M. Walz, Lisa B. Niehoff,  
David J. Sdano, Antoinette M. Bennaars,  
Jeffrey A. Cooper, Becky L. Senft,  
Anatoli A. Sorkin, Steven P. Stoesz,  
and Paul A. Saunders

### 1. INTRODUCTION

Enzyme-linked immunosorbent assays (ELISAs) have long been used to quantify cytokines and other proteins that are secreted from cells. ELISAs enable the user to assay multiple samples, to obtain reproducible quantitative results, and to design studies with quantifiable endpoints. Intracellular activities intimately involved in apoptosis, such as control of mitochondrial permeability to holocytochrome c and activation of a specific caspase, are quantified by the ELISAs described in this chapter. The cytochrome c ELISA is generally used to quantify the activities of the proteins belonging to the Bcl-2 family. The active caspase ELISA quantifies a specific active caspase among a background of latent caspase and other active caspases.

A schematic representing proposed positions in the apoptotic pathway occupied by the Bcl-2 family and caspase family of proteins is shown in Fig. 1. In this scheme, the effect of an apoptosis-inducing signal, most often generated in response to stress (e.g., loss of a cytokine binding to its cell surface receptor, free radicals, or DNA damage), can be mediated by the Bcl-2 family proteins (1–4). One mechanism by which the Bcl-2 family of proteins regulate apoptosis is by controlling the release of proteins from mitochondria. Pro-apoptotic Bcl-2 family members (e.g., Bid, Bax, Bad, Bim, Bkl,



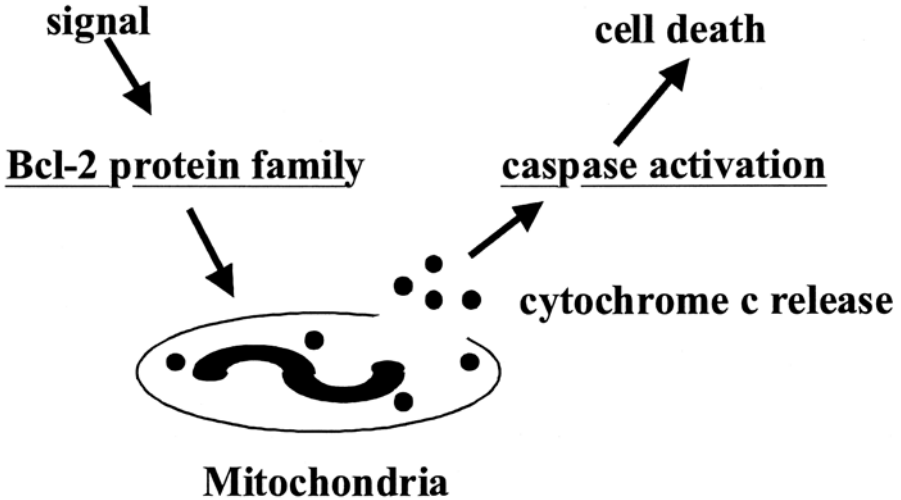


Fig. 1. Schematic showing the position of mitochondria relative to the Bcl-2 family of proteins and caspases. Cells receive an incoming apoptosis signal that causes pro-apoptotic Bcl-2 family proteins to alter the integrity of the outer mitochondrial membrane. Anti-apoptotic Bcl-2 family members can prevent the actions of the pro-apoptotic members. Cytochrome c is released from the mitochondria. Released cytochrome c causes activation of caspases. Active caspases cleave intracellular proteins and cause cell death.

Bak, Bok, Hrk, Bik, and Bcl-x<sub>S</sub>) appear to facilitate release of integral mitochondrial factors and anti-apoptotic members (e.g., Bcl-2, Bcl-x<sub>L</sub>, Mcl-1, A1/Bfl-1, Bcl-w, Boo/Diva, Brag-1) appear to prevent release of these factors from the mitochondria. Protein interaction, namely oligomerization, of the Bcl-2 family proteins, appears to be part of the molecular mechanisms that govern the release of other proteins from the mitochondria. The proteins cytochrome c (5,6), apoptosis-inducing factor-1 (7), and Smac/DIABLO (8,9) have been shown to be released from mitochondria of dying cells and to have roles in the apoptotic process. Release of cytochrome c into the cytosol initiates formation of a pro-apoptotic protein complex or "apoptosome" through oligomerization of Apaf-1 and caspase-9 (10–14). In most cell types studied, formation of the apoptosome activates the caspase protease cascade by activating caspase-9, which then activates caspase-3 and caspase-7 by cleaving at the junctions of the large and small subunits (15). The active caspase proteases then act as executioners by cleaving vital intracellular proteins (16).

Bcl-2 family proteins are attractive targets for drug development. Conceivably, inhibitors of the pro-apoptotic members would block apoptosis prior to cytochrome c release and caspase activation and may have therapeutic value for conditions that appear to involve excess apoptosis (e.g., neurodegenerative disorders and ischemia associated with stroke and heart attack). Activators of the pro-apoptotic members or inhibitors of the anti-apoptotic members would have value in treating disorders that appear to progress as a result of too little apoptosis (e.g., cancer and autoimmunity).

Inhibitors of caspases are being developed to prevent cell death in medical situations involving acute insults. Some caspase inhibitors increase *in vivo* cell survival in model systems involving ischemia (17,18). Targeted inhibition of caspases may also increase the chances of cell survival. Inhibiting caspase-9 that starts the caspase cascade in response to cytochrome c release would limit proteolytic damage, but would not prevent release of cytochrome c from mitochondria. Inhibiting caspase-8 or caspase-10 that start the cascade in response to death-inducing ligands (20) would block caspase-mediated proteolysis. Compounds that activate caspases also have potential applications for inducing cell death.

The cytochrome c release assay described in this section can be used as an index of the biological activity of Bcl-2 family proteins or biologicals that are designed to act as Bcl-2 family proteins. Cytochrome c released from mitochondria in response to the pro-apoptotic Bcl-2 family members and inhibition of release when an anti-apoptotic Bcl-2 family member is added with the pro-apoptotic member is quantified by a cytochrome c ELISA. The assay is also capable of detecting inhibitors of Bcl-2 protein interactions and can be used to screen for agonists or antagonists to the Bcl-2 proteins through mechanisms other than oligomerization (e.g., inhibition of protein transport through the mitochondrial membrane). Thus, the cytochrome c release assay expands the mechanistic basis for screening large libraries for compounds capable of inhibiting the Bcl-2 family members. A modification of the cytochrome c release assay for application to automated screening of large libraries is described.

The active caspase ELISAs quantify the events closely following the release of cytochrome c from mitochondria. The active caspase ELISA quantifies a single active caspase family member (19). The procedure uses the covalent modification of the active site cysteine with a biotinylated inhibitor to label active caspases and selected capture on a plate coated with a caspase-specific monoclonal antibody (MAb). In this chapter, a typical characterization of an active caspase ELISA is included as a demonstration of proof that the ELISA quantifies a specific active caspase. The ability of the assay to

simultaneously quantitate two active caspases, namely active caspase-3 and active caspase-7, in apoptotic cells is also demonstrated.

## **2. QUANTIFICATION OF THE BCL-2 FAMILY ACTIVITIES USING THE CYTOCHROME C RELEASE LONG-FORMAT ASSAY**

### ***2.1. Method Overview***

A cytochrome c ELISA is used to quantify the amount of cytochrome c released from mitochondria in response to added Bcl-2 family members. Mouse liver mitochondria are isolated by differential centrifugation or mitochondria can be further enriched on a gradient of Percoll. In the long-format cytochrome c release assay described in Fig. 2A, incubation of mitochondria with the Bcl-2 family protein(s) is performed in a microcentrifuge tube. Assay buffer and Bcl-2 family protein(s) are added to the tube and the assay is started by addition of mitochondria. The mixture is incubated at 30°C for 0.5–1 h and mitochondria are then pelleted by centrifugation. The cytochrome c released from the mitochondria remains in the supernatant. The supernatant is diluted and aliquots are incubated in wells of the ELISA plate in the presence of horseradish peroxidase (HRP)-conjugated detection antibody for 2 h. The plate is washed and hydrogen peroxide and 3, 3', 5, 5'-tetramethylbenzidine (TMB) are added to the wells for HRP-catalyzed color development. Acid is added after 0.5 h to stop the reaction and the absorbance at 450 nm is determined. A standard curve is generated with purified rat cytochrome c. The ELISA, excluding sample preparation, takes 2.5 h to perform.

### ***2.2. Quantification of Bcl-2 Family Protein Members' Activities***

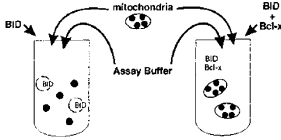
Bid was added to mitochondria to demonstrate the assay's ability to quantify a pro-apoptotic Bcl-2 family member's activity. As shown in Fig. 3A, addition of recombinant human Bid caused cytochrome c release from mitochondria in a dose-dependent manner. Bid is cleaved by caspase-8 to generate a carboxyl terminal 15 kDa fragment and an amino-terminal 7 kDa fragment, which remain associated (21,22). Cleaved Bid has been shown to be more potent than uncleaved Bid in releasing cytochrome c from mitochondria (21–23). Cleavage significantly ( $p < 0.05$ , paired *t*-test,  $n = 6$ ) increased the potency of Bid, decreasing the  $EC_{50}$  (concentration to obtain 50% maximal effect) from  $90 \pm 24$  nM to  $30 \pm 4$  nM in an assay involving

### Cytochrome c (●) Release Assay

#### A Long format: 180+ minutes

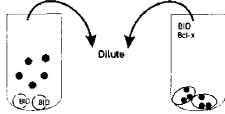
**Step 1** — 30 minutes

- To a microcentrifuge tube add:
  - assay buffer
  - Bcl-2 family member (s)
  - start assay by adding mitochondria
- Incubate at 30° C for 30 minutes



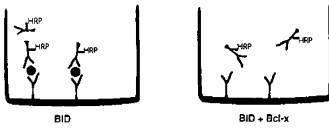
**Step 2** (time depends on number of samples)

- Centrifuge to pellet mitochondria
- Dilute supernatant



**Step 3** — 120 minutes

- To the wells of the cytochrome c ELISA plate add:
  - assay buffer containing HRP-conjugated cyt. c detection antibody
  - aliquot of diluted supernatant
- incubate at room temp. for 120 minutes



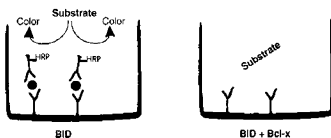
**Step 4** — 2 minutes

- Wash wells



**Step 5** — 30 minutes

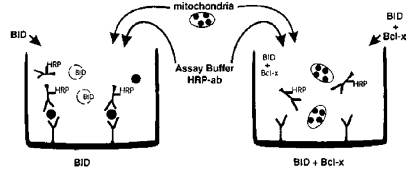
- incubate with HRP substrate for 30 minutes
- Add stop solution
- Read absorbance at 450 nm



#### B Short format: 35 minutes

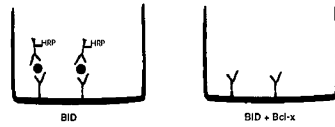
**Step 1** — 30 minutes

- To the wells in the cytochrome c ELISA plate add:
  - assay buffer containing HRP-conjugated cyt. c detection antibody (HRP-ab)
  - Bcl-2 family member(s)
  - start assay by adding mitochondria
- Incubate at 30° C for 30 minutes



**Step 2** — 2 minutes

- Wash wells



**Step 3** — 3 minutes

- incubate with HRP substrate for 3 minutes
- Add stop solution
- Read absorbance at 450 nm

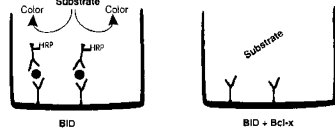


Fig. 2. Schematic showing the long-format (A) and short-format (B) cytochrome c release assays.

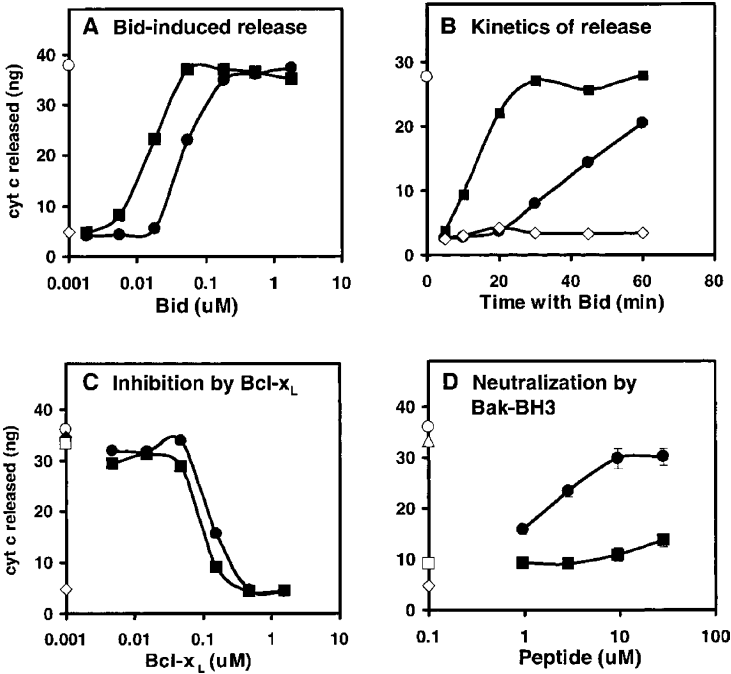


Fig. 3. Quantification of Bcl-2 family activities with the long-format cytochrome c release assay. Results are the average of duplicate measurements in (A) and are averages of triplicate measurements  $\pm$  SEM in (B–D) (many error bars in panels [B–D] are obscured by the symbols). In panels (A–D) open circles indicate cytochrome c detected when Triton X-100 was added to mitochondria and open diamonds indicate cytochrome c detected when no Bcl-2 family proteins were added to mitochondria. All incubations of mitochondria except those in (B) were for 30 min. (A) Recombinant human Bid (solid circles) and caspase-8-cleaved human Bid (squares) induce release of cytochrome c from isolated mouse liver mitochondria in a dose-dependent manner. (B) Kinetics of 52 nM (solid squares) and 5.2 nM (solid circles) human cleaved Bid-induced cytochrome c release from isolated mouse liver mitochondria. (C) Bcl-x<sub>L</sub> inhibition of caspase-8-cleaved human Bid and cleaved mouse Bid induced cytochrome c release. Mitochondria were incubated with 52 nM cleaved human Bid without (solid diamond) or with (solid squares) the indicated concentrations of mouse Bcl-x<sub>L</sub>. Mitochondria were also incubated with 17 nM cleaved mouse Bid without (open square) or with (solid circles) the indicated concentrations of mouse Bcl-x<sub>L</sub>. (D) A synthetic peptide (GQVGRQLAIIGDDINR) corresponding to the amino acid 72-87 BH3 region of Bak prevents Bcl-x<sub>L</sub> from inhibiting caspase-8-cleaved mouse Bid induction of cytochrome c release. Mitochondria were incubated with 17 nM caspase-8-cleaved mouse Bid without (triangle) or with (open square) 155 nM mouse Bcl-x<sub>L</sub> and the indicated concentrations of Bak-BH3 (solid circle) or the corresponding Bak peptide (GQVGRQAAIIGDDINR) with a L to A substitution (solid squares).

a 30 min incubation at 30°C (Fig. 3A). Others have used the ELISA to demonstrate that N-myristoylated cleaved Bid is a more potent inducer of cytochrome c release than non-N-myristoylated cleaved Bid (23). The rate of cytochrome c release from mitochondria was also measured (Fig. 3B). When 5.2 nM caspase-8 cleaved Bid was included with mitochondria, release started after a 20-min lag and then increased linearly at 0.4 ng cytochrome c/min. When 52 nM cleaved Bid was included, release was prompt and at a rate of 1.2 ng cytochrome c/min until 90% of total cytochrome c was released. The results indicate that the assay is capable of quantifying activities of proteins that target the mitochondria and induce cytochrome c release, effects of post-translational modifications on the activities of these proteins, and the kinetics at which these proteins exert their activity.

The ability of the assay to quantify interactions between pro-apoptotic and anti-apoptotic Bcl-2 family proteins was examined by adding anti-apoptotic recombinant mouse Bcl-x<sub>L</sub> with pro-apoptotic-cleaved Bid. Addition of Bcl-x<sub>L</sub> with human- or mouse-cleaved Bid inhibited the cytochrome c releasing activity of Bid in a dose-dependent fashion (Fig. 3C). The EC<sub>50</sub> for Bcl-x<sub>L</sub> inhibition of 52 nM human caspase-8-cleaved Bid was 108 ± 8 nM (n = 4) and the EC<sub>50</sub> for inhibition of 17 nM mouse caspase-8-cleaved Bid was 83 ± 8 nM (n = 4). The results indicate that mouse Bcl-x<sub>L</sub> is capable of inhibiting the activities of cleaved bid from both human and mouse and the assay is capable of quantifying this inhibition.

The assay was also tested to determine if it could detect perturbations of interactions between pro-apoptotic and anti-apoptotic Bcl-2 family members. Interactions between the pro-apoptotic members and the anti-apoptotic members appear to involve interaction of the BH3 region of the pro-apoptotic member with an anti-apoptotic member (24–26). A synthetic peptide corresponding to the BH3 region (amino acids 72–87) of human Bak was tested for the ability to interfere with the interaction between Bid and Bcl-x<sub>L</sub>. If the Bak BH3 peptide interferes with the interaction between Bid and Bcl-x<sub>L</sub>, Bid would be free to release cytochrome c from mitochondria in the presence of Bcl-x<sub>L</sub>. Increasing amounts of the Bak BH3 peptide were added to assays containing 155 nM mouse Bcl-x<sub>L</sub> and 17 nM mouse-cleaved Bid (Fig. 3D). Inhibition of Bid by Bcl-x<sub>L</sub> was prevented by the Bak BH3 peptide in a dose-dependent manner, thereby enabling Bid to release cytochrome c from the mitochondria (Fig. 3D). The EC<sub>50</sub> for the Bak BH3 peptide reversal of 155 nM Bcl-x<sub>L</sub> inhibition of 17 nM cleaved Bid was 2.9 ± 0.5 μM (n = 4). A peptide with a single leucine to alanine substitution (L78A) was used as a control to ensure that the structural BH3 motif was responsible for preventing Bcl-x<sub>L</sub> from inhibiting Bid. The L78A substitu-

tion has been shown to neutralize activities of the Bak BH3 peptide (27). This L78A Bak BH3 peptide did not prevent Bcl-x<sub>L</sub> from inhibiting Bid (Fig. 3D). The results demonstrate that the assay is capable of quantifying the effects of antagonists or agonist of the Bcl-2 family that act to inhibit protein interactions. A synthetic peptide was used in this study as a model for demonstration purposes. However, the same assay format has the potential to quantify effects of nonpeptide molecules on interactions between the pro-apoptotic and anti-apoptotic members. The assay also has the potential to quantify antagonistic effects of small molecules on the pro-apoptotic Bcl-2 family members.

### 3. CYTOCHROME C RELEASE SHORT-FORMAT ASSAY FOR HIGH-THROUGHPUT SCREENING

#### 3.1. Method Overview

We have developed a short-format method that considerably shortens the time required to perform the cytochrome c release assay. Using the long-format assay described on the previous pages, incubation of the Bcl-2 members with mitochondria requires 30 min and the ELISA requires an additional 150 min, resulting in a total assay time of 3 h. The long-format assay also requires extensive sample handling (e.g., centrifugation and dilutions). Results can be obtained from the short-format assay in as little as 15 min and most of the sample handling is eliminated.

The entire short format assay (described in Fig. 2B) is performed in the well of the ELISA plate coated with antibodies that capture cytochrome c. Cytochrome c release assay buffer containing HRP-conjugated detection antibody is added to the well. Bcl-2 family protein(s) is/are then added. The assay is initiated by adding mitochondria. The dish is incubated at 30°C for 10–30 min. Only released cytochrome c is available for binding to capture and detection antibodies. Unreleased cytochrome c remains in the mitochondria and is removed during washing of the well. After the desired time the plate is washed and HRP substrates are added. The 15-min short format assay is composed of a 10-min incubation of the mitochondria with the Bcl-2 proteins, 2 min for washing, and 3 min for color development. The 35-min short-format assay includes a 30-min incubation followed by 2 min for washing and 3 min for color development. The short-format assay takes a fraction of the time required to perform the long-format assay and fewer handling steps are required. The simplicity and speed of the assay are well-suited for automated high throughput screening for compounds that modulate cytochrome c release.

### ***3.2. Detection of Bcl-2 Protein Family Member Activities with the Short-Format Assay***

Results typical of those obtained when mitochondria, HRP-conjugated detection antibody, and Bcl-2 family members were incubated in assay buffer in wells of the ELISA plate for 30 min at 30°C are shown in Fig. 4A. Caspase-8 cleaved human Bid was used to demonstrate that the short format detects protein-induced cytochrome c release (Fig. 4A). Bcl-x<sub>L</sub> was added with cleaved Bid to demonstrate that the short format detects inhibition of a pro-apoptotic Bcl-2 family member by an anti-apoptotic member (Fig. 4A). In the 35-min assay, Bid-induced release of cytochrome c was concentration-dependent with an EC<sub>50</sub> of 38 nM (Fig. 4B). The difference between the EC<sub>50</sub> of 38 nM determined in the 35-min short-format assay was not statistically different (*z* test, *p* < 0.05) from the EC<sub>50</sub> of 30 ± 4 nM determined in the 3-h long format assay (Fig. 3A). Appreciable release caused by cleaved Bid can also be detected in a 15-min short-format assay conducted in the well of the ELISA plate (Fig. 4C) and inhibition of Bid was apparent when Bcl-x<sub>L</sub> was included in the 15-min short-format assay (Fig. 4C).

### ***3.3. Advantages of the Long-Format and Short-Format Assays***

Many of the parameters (e.g., rate of cytochrome c release in response to various concentrations of Bcl-2 family members and rates at which capture and HRP-detection antibodies bind released cytochrome c) have been examined in the short and long format assays. The 15-min assay represents the least time in which the short-format assay can be performed to detect cytochrome c release. As shown in Fig. 3B, the amount of cytochrome c released after 10 min with 52 nM human cleaved Bid is a fraction of that released after 30 min. Thus, a 30-min incubation of mitochondria with Bcl-2 family members is preferred over the 10-min incubation in the short-format assay. Binding of added cytochrome c by the ELISA capture and detection antibodies is biphasic with a rapid initial phase where >70% of the added cytochrome c is detected in less than 5 min followed by a slow phase required to obtain equilibrium between the capture and detection antibodies. The 35-min short-format assay takes advantage of the fact that maximal or near maximal release of cytochrome c from the mitochondria is within 30 min and that >70% of the released cytochrome c is detected in the ELISA. The long format ensures that binding of the capture and detection antibodies is at equilibrium, thereby making the assay quantitative. Therefore, the short format is the method of choice when seeking qualitative yes or no answers when screening for compounds that are agonists or antagonists to the Bcl-2 family proteins, and the long-format assay is preferred when quantitative results are desired.



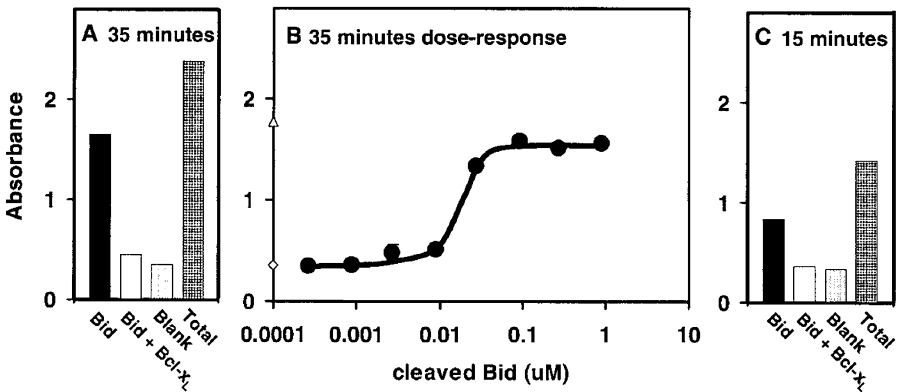


Fig. 4. Detection of cytochrome c release from mitochondria in the short format cytochrome c release assay. (A) Assay buffer, HRP-detection antibody, and 52 nM caspase-8-cleaved human Bid (solid bars), 52 nM human cleaved Bid and 156 nM mouse Bcl-x<sub>L</sub> (open bars), no additions (light gray bars), or Triton X-100 (stippled bars), were added to a 96-well ELISA plate coated with cytochrome c capture antibody. Mitochondria were added and the plate was incubated at 30 °C for 30 min (A) or 10 min (C). The wells were washed for 2 min and color developing reagent was added for 3 min. (B) shows a 35-min assay in which the concentration of human cleaved Bid was varied. Open triangle indicates cytochrome c detected when Triton X-100 was added to mitochondria and open diamond indicates cytochrome c detected when no Bcl-2 family proteins were added to mitochondria.

## 4. QUANTIFICATION OF ACTIVE CASPASES WITH THE ACTIVE CASPASE ELISAS

### 4.1. Method Overview

The active caspase ELISAs are used to quantify events that occur downstream of cytochrome c release from mitochondria or that are initiated by death-inducing ligands. The active caspase ELISAs described here are specific for a single active caspase family member and do not detect latent caspases. A biotinylated peptide containing a reactive fluoromethyl ketone group is used to tag the active site cysteine of active caspases. The caspase active site cysteine displaces the fluoride on the inhibitor to generate a stable thioether bond between the active caspase and the biotinylated inhibitor. The cysteines of latent caspases do not displace the fluoride. Thus, only active caspases in the cells are tagged with biotin through the covalent

attachment of the biotinylated inhibitor. The biotinylated inhibitor is added directly to the cells via addition to culture medium. After 1 h, cells are lysed and the caspase is then captured on a plate coated with a caspase-specific MAb. Protein containing the biotinylated-inhibitor adduct and subsequently captured on the antibody-coated dish is detected with HRP-streptavidin and color generation is with substrate for HRP. Biotinylated-inhibitor-modified caspase or chemically biotinylated large subunit is used to generate a standard curve. As demonstrated by use of the ELISAs described in this chapter to measure active caspase-3 and active caspase-7, the caspase specificity of the assay can be modified by changing the caspase specificity of the capture antibody coated on the plates. Methods to verify that the active caspase ELISA is specific for a single caspase and that the active caspase ELISA detects active caspase without detecting caspase zymogen are also demonstrated. We also used cleavage of natural substrates, cleavage of peptide substrates, and proteolytic processing of caspase-7 to demonstrate their use for assessing the active state of caspases. Similar results for caspase-3 have been reported previously (28).

#### ***4.2. Cleavage of Poly(ADP-Ribose) Polymerase (PARP) in Apoptotic Jurkat Cells***

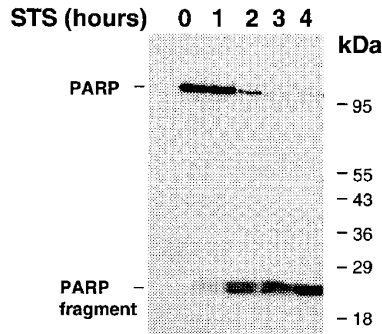
Jurkat cells treated with staurosporine (STS) were used as a model system for the simultaneous quantification of active caspase-7 and active caspase-3. PARP, a natural substrate for caspase-3 (29,30), is cleaved in apoptotic cells to generate a 23 kDa fragment. PARP was cleaved in the first hour with staurosporine (STS) and full-length PARP was nearly depleted by 3 h (Fig. 5A). The results show that Jurkat cells initiate an immediate and rapid apoptosis response to STS.

#### ***4.3. Caspase-7 Processing in Apoptotic Jurkat Cells***

Caspase-7 polypeptide can be proteolytically processed into the forms shown in Fig. 6A. Precursor caspase 7 is a 303 amino acid (aa) polypeptide containing 3 regions: aa 1–23 pro-region (Pro), aa 24–198 large subunit (LSU), and aa 199–303 small subunit (SSU). Cleavage at Asp<sup>23</sup> generates Pro and LSU-SSU. Cleavage at Asp<sup>198</sup> generates Pro-LSU and SSU. Cleavage at both Asp<sup>23</sup> and Asp<sup>198</sup> generates Pro, LSU, and SSU. Anti-caspase-7 LSU detects forms containing the LSU (i.e., precursor, Pro-LSU, LSU-SSU, and LSU). Anti-caspase-7 SSU detects forms containing SSU (i.e., precursor, LSU-SSU, and SSU).

Proteolytic processing of caspase-7 (31,32) was examined by Western blotting extracts from Jurkat cells treated with STS. Extracts were Western-blotted with anti-caspase-7 LSU and anti-caspase-7 SSU (Fig. 6B). All pre-

### A PARP cleavage



### B DEVD-afc cleavage activity

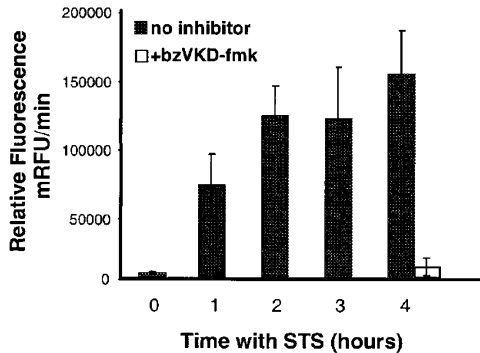


Fig. 5. (A) Cleavage of PARP in Jurkat cells treated with STS. Extracts from Jurkat cells treated with STS for the indicated times were subjected to Western blotting with anti-PARP. (B) DEVD-afc cleavage activity in extracts of Jurkat cells treated with STS. Jurkat cells were cultured with STS for the indicated times, extracted, and the amount of DEVD-afc cleavage activity in the extracts was determined (solid bars). Parallel cultures of Jurkat cells were incubated with bzVKD-fmk during the final hour of a 4 h incubation with STS, extracted, and the amount of DEVD-afc cleavage activity was determined (open bar). Results are averages  $\pm$  SEM,  $n = 6$ .

cursor caspase-7 was proteolytically processed in cells treated with STS for 3 h. Most caspase-7 was cleaved at Asp<sup>23</sup> and Asp<sup>198</sup> to generate LSU and SSU, consistent with the findings that many active caspases are composed of 2

LSUs and 2 SSUs (33,34). Some LSU-SSU was detected in cells treated with STS for 1 hour, and less was detected in cells treated with STS for longer times. Trace amounts of Pro-LSU were detected in cells treated with STS for 1–4 h. The results show that caspase-7 is proteolytically processed in Jurkat cells induced to undergo apoptosis by treatment with STS.

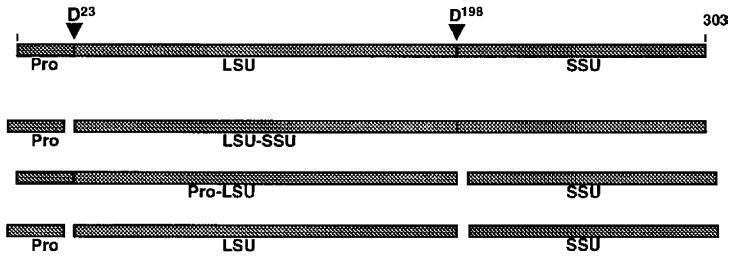
#### ***4.4. Proteins Covalently Modified by Biotinylated Inhibitor***

Covalent bond formation between the caspase active site cysteine and the biotinylated inhibitor, carbobenzoxy-Val-Lys(N $\epsilon$ -biotinyl)-Asp(O-methyl)fluormethylketone (bzVKD-fmk), is used to distinguish active from latent caspases (28,35). The ability of bzVKD-fmk to enter apoptotic cells and form covalent bonds with proteins was confirmed by treating cells with STS for the indicated times and then for 1 hour with bzVKD-fmk. Extracts were solubilized in SDS sample buffer and then Western-blotted with HRP-streptavidin to detect proteins containing the biotinylated inhibitor adduct (Fig. 6B, HRP-SA blot). Bands of 18–22 kDa were prominently labeled after 1 h with STS. A prominent 25 kDa band and other higher molecular-weight polypeptides were also labeled after 2 h with STS. There was an increase in labeling of the 25 kDa and higher molecular weight bands at 3 h with STS. Although the polypeptides containing covalent bzVKD-fmk adducts cannot be identified by this method, it is clear that bzVKD-fmk covalently modifies a subset of cellular proteins.

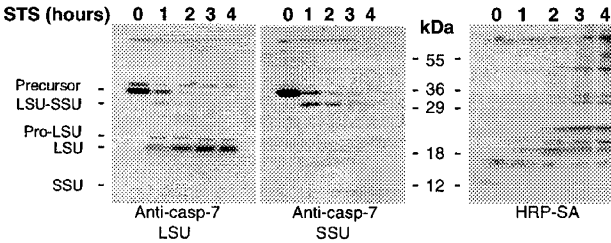
Inhibition of cellular DEVD-afc cleavage activity by bzVKD-fmk was confirmed by adding bzVKD-fmk to the culture medium during the final hour of a 4 h incubation with STS. DEVD-x (where x is a chromophore or fluorophore) is a preferred substrate for both caspase-3 and caspase-7 (36,37). Cleavage of DEVD-afc reflects activities of caspase-3, caspase-7, and any other caspase with significant amounts of DEVD-afc cleavage activity (37). The cleavage of DEVD-afc in cell extracts can, therefore, only be used as an indicator that caspases are active. Jurkat cell DEVD-afc cleavage activity was high after 1 h treatment with STS and continued to increase at 2 h. Maximal activity was maintained between 2 and 4 h with STS. bzVKD-fmk inhibited cellular DEVD-afc cleavage by greater than 90% in Jurkat cells treated with STS for 4 h (Fig. 5B). The results suggest that bzVKD-fmk formed covalent bonds with the active site cysteine of active caspase-3, active caspase-7, and other active caspases that are responsible for DEVD-afc cleavage activity.

The aforementioned results demonstrate that in Jurkat cells treated with STS, the natural caspase substrate PARP is cleaved, DEVD-afc cleavage activity is activated, caspase-7 is proteolytically processed, and bzVKD-

### A Processing of caspase-7



### B Total cell extracts



### C Captured polypeptides

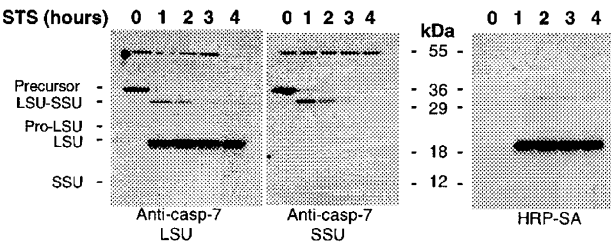


Fig. 6. (A) Caspase-7 forms generated by caspase cleavage; Pro, pro-region; LSU, large subunit; and SSU, small subunit. (B) Western blot of cell extracts. Extracts from Jurkat cells incubated with STS for the indicated times and then for 1 h with bzVKD-fmk and STS were subjected to Western blotting with anti-caspase-7 LSU (Anti-LSU), anti-caspase-7 SSU (Anti-SSU), or HRP-streptavidin (HRP-SA). (C) Western blots of captured polypeptides. After incubation with STS for the indicated times and then 1 h with bzVKD-fmk and STS cells were extracted as described in Methods for capture on 6-well dishes coated with caspase-7 capture antibody. Captured material was solubilized in SDS sample buffer and subjected to Western blotting with anti-caspase-7 LSU (Anti-casp-7 LSU), anti-caspase-7 SSU (Anti-casp-7 SSU), or HRP-streptavidin (HRP-SA).

fmk enters apoptotic cells where it forms covalent bonds with proteins including the caspases responsible for DEVD-afc cleavage.

#### ***4.5. Specificity of the Active Caspase-7 ELISA***

Specificity of the active caspase-7 ELISA was determined by analyzing captured polypeptides. Capture antibody is the caspase-7-specific antibody coated in the ELISA 96-well plates and is different from the anti-caspase-7 antibodies used for western blotting. Polypeptides that are bound by the capture antibody are referred to as “captured.” Jurkat cells were incubated with STS for 0–4 h and then with bzVKD-fmk for an additional 1 h. Cell extracts were incubated in 6-well plates coated with caspase-7 capture antibody. After washing, polypeptides captured on the plate were solubilized in SDS sample buffer and Western-blotted. Captured polypeptides were blotted with anti-caspase-7 LSU and anti-caspase-7 SSU to detect polypeptides derived from caspase-7. Captured polypeptides were blotted with HRP-streptavidin to detect the polypeptides covalently modified with the bzVKD-fmk inhibitor. Captured polypeptides covalently modified with bzVKD-fmk is the material that the ELISA quantifies.

It is important to clarify that active caspase is selectively modified by bzVKD-fmk and that precursor caspase is not and therefore does not contribute to the ELISA signal. Caspase-7 precursor was captured but was not modified by bzVKD-fmk. Precursor was detected in polypeptides captured from untreated cells and cells treated with STS for 1 h by blotting with anti-LSU and anti-SSU but was not detected by HRP-streptavidin (Fig. 6C). Therefore, precursor does not contribute to signal in the ELISA because it is not covalently modified by the bzVKD-fmk inhibitor that is required for binding of HRP-streptavidin.

Caspase-7 LSU was the major captured bzVKD-fmk modified polypeptide detected by HRP-streptavidin (Fig. 6C). The amount of LSU detected at 1 h in shorter exposures (results not shown) of the anti-LSU blot was less than the amount detected at 2–4 h. Minor amounts of LSU-SSU and Pro-LSU covalently modified with bzVKD-fmk were present in captured material. Signal generated in the active caspase-7 ELISA is, therefore, primarily due to bzVKD-fmk modified LSU with minor contribution by bzVKD-fmk-modified LSU-SSU and Pro-LSU. All bzVKD-fmk containing bands had corresponding bands when blotted with anti-caspase-7 LSU except for one. Pro-LSU was detected in cell extracts (Anti-LSU blot, Fig. 6B) but was not readily detected by anti-LSU in captured material (Anti-LSU blot, Fig. 6C) whereas a band with the appropriate mobility was detected by HRP-streptavidin (HRP-SA blot, Fig. 6C). Although the basis for this discrep-

ancy is not known, the amount of this material detected by HRP-streptavidin is trivial when compared to the amount of LSU. The results suggest that all captured polypeptides modified with bzVKD-fmk were forms of caspase-7.

Additional experiments can be carried out to support the possibility that the LSU-SSU is a transient intermediate in the processing of precursor to LSU and SSU. In this model, the intermediate consists of an intact LSU-SSU polypeptide chain and a LSU and a SSU derived from another precursor to form a  $(\text{LSU-SSU})_1(\text{LSU})_1(\text{SSU})_1$  intermediate. Alternatively, the LSU-SSU modified by bzVKD-fmk is unique in that it becomes active and is not cleaved at Asp<sup>198</sup>.

Specificity of the anti-caspase-7 LSU capture antibody can also be determined by quantifying the signal generated with other recombinant active caspases that were covalently modified at the active site cysteine with biotin-Asp-fmk. Detection of biotin-Asp-fmk modified caspases-2, -3, -8, or -10 in the active caspase-7 ELISA was minimal or nonexistent. Nor did caspase-2, -3, -8, or -10 interfere with detection of caspase-7 standard (results not shown).

#### ***4.6. Simultaneous Quantification of Active Caspase-3 and Active Caspase-7 in Apoptotic Cells***

The active caspase ELISAs enable the user to quantify two distinct proteases with very similar substrate specificities in the same cell extract. Active caspase-3 and active caspase-7 were quantified in the same extracts from Jurkat cells treated for various durations with STS. bzVKD-fmk was added to the culture medium and cells were extracted 1 h later. Active caspase-3 and active caspase-7 were quantified with the active caspase-3 and the active caspase-7 ELISAs, respectively. The levels of both active caspases increased dramatically at 1 h with STS and continued to increase in the following hour (Fig. 7A). The levels plateaued at 3 h and were decreased slightly at 4 h. Using purified caspases to generate a standard curve for assigning mass amounts, 4.1 ng of active caspase-3 per  $10^6$  cells and 2.2 ng of active caspase-7 per  $10^6$  cells were quantified in extracts from Jurkat cells treated with STS for 3 h. Jurkat cells were also induced to undergo apoptosis by treatment with anti-Fas. Anti-Fas aggregates cell-surface death receptors and initiates the caspase cascade through activation of caspase-8. The amount of active caspase-3 and active caspase-7 increased rapidly in response to anti-Fas (Fig. 7B). In Jurkat cells treated with anti-Fas for 4 h, 3.23 ng active caspase-3 per  $10^6$  cells and 2.73 ng active caspase-7 per  $10^6$  cells were detected.

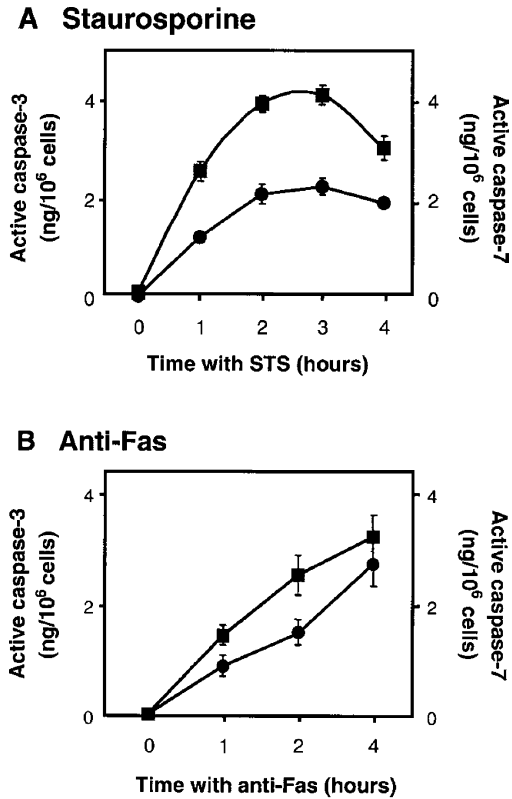


Fig. 7. Quantification of active caspase-3 and active caspase-7 in apoptotic Jurkat cells. Jurkat cells were incubated with 1  $\mu$ M STS (A) or 100 ng/mL anti-Fas (B) for the indicated times and then for 1 h with 10  $\mu$ M bzVKD-fmk. Active caspase-3 (squares) and active caspase-7 (circles) were quantified using the active caspase-3 and active caspase-7 ELISAs. Results are averages  $\pm$  SEM for triplicate measurements. Some error bars are obscured by the symbols.

We confirmed that this assay could be used to quantify active caspase-3 and active caspase-7 in other cell types. Active caspase-3 and active caspase-7 were quantified in the extracts from STS-treated human neuroblastoma (CHP-100 and SH-SY5Y) and promyelocytic leukemia (HL60) cells (Table 1). The amount of active caspase-3 was found to be much higher than the amount of active caspase-7 in these cell types. Very low or no amounts of active caspases were detected in control cells (cells not treated with STS). Active caspase-3 and active caspase-7 were also quantified in human breast adenocarcinoma (MCF-7) cells that do not express caspase-3 (28,38). No



**Table 1**  
**Active Caspase-3 and Active Caspase-7 in STS-Treated Cells<sup>a</sup>**

Cell line	STS (h)	Active caspase-3 ng/10 <sup>6</sup> cells	Active caspase-7 ng/10 <sup>6</sup> cells
CHP100	7	5.78	0.64
HL60	6	1.52	0.26
MCF-7	4	0.00	0.45
SHSY5Y	7	2.43	0.63

<sup>a</sup>Results are averages of duplicate measurements.

active caspase-3 was detected whereas 0.45 ng active caspase-7 per 10<sup>6</sup> MCF-7 cells was detected (Table 1).

## 5. DISCUSSION OF ASSAY LIMITATIONS

We have demonstrated quantitative assays for measuring two intracellular events associated with apoptosis. The cytochrome c ELISA quantifies cytochrome c or an event involved in releasing cytochrome c from mitochondria. The active caspase ELISA quantifies the activation of specific caspases. Both ELISAs enable the user to assay multiple samples, obtain reproducible quantitative results, and to design studies with well-defined endpoints.

We have characterized the activities of several recombinant human and mouse Bcl-2 family proteins (Bcl-2, Bcl-x<sub>L</sub>, Bcl-w, Bax, Bid, and caspase-8 cleaved Bid) with the cytochrome c ELISA. Dose responses, kinetics, inhibition, and the effects of protein-protein interactions have been quantified. Conducting the cytochrome c release assay in the well of the ELISA plate decreases the time required to perform the assay from 3 h to 35 min. Similar dose responses for induction of cytochrome c release caused by cleaved Bid were obtained with the 35 min and 3 h release assays, indicating that the short format can detect intermediate levels of cytochrome c release. The short format is applicable to automation for screening million-member libraries. Mitochondria obtained from one mouse liver is sufficient to perform 4000 assays in the 96-well plates and scale-up is performed simply by increasing the amount of starting tissue.

Chimeric green fluorescent protein (GFP)-Bcl-2 family member proteins have also been used to monitor activities of the Bcl-2 family members. A chimeric GFP-Bax relocates from the cytosol to the mitochondria in response to the appropriate apoptosis-inducing signal (39). Thus, subcellular localization could be used to monitor response to compounds targeted at

inhibiting this movement. GFP-cytochrome c chimeras have been expressed in human cells. GFP-cytochrome c is sequestered in the mitochondria in healthy cells and is released from mitochondria when apoptosis is induced by the appropriate signal (40). Optical analysis of GFP-cytochrome c distribution could be used to detect inhibition or induction of cytochrome c release. These methods require penetration of the test compounds into the cell thereby eliminating candidate compounds that are cell-impermeable. These assays would also detect inhibitors that act far upstream of Bax relocation or cytochrome c release.

Other methods have been employed to monitor Bcl-2 family protein activities or interactions. Physical measurements can be used to monitor the effects of the Bcl-2 family members on lipid micelles. Bcl-2 (41,42), Bcl-x<sub>L</sub> (43), Bax (42,44–46), and Bid (47) form pores in lipid membranes/micelles that are quantifiable by electrophysical methods or by monitoring release of small molecules (e.g., fluorescein). In many instances the formation of pores is greatest under rather acidic conditions, making the biological significance of these measurements uncertain. Monitoring dimerization of members of the Bcl-2 family has been proposed as a screening tool for examining small molecules that interfere with dimerization. Dimerization between Bcl-2 family members has been examined by surface plasmon resonance (48) and in ELISA formats that detect both partners of the dimer (46,49). However, great care must be exercised in interpreting the results of dimerization assays. Detergents have been found to cause conformational changes that lead to heterodimerization of Bax with Bcl-x<sub>L</sub> in the test tube whereas there is strong evidence that this heterodimerization does not occur *in vivo* (50–52).

Each of these assays has drawbacks associated with them. The major obstacle for developing rapid screens for inhibitors of cytochrome c release from mitochondria is that enriched mitochondria have a finite time in which they can be used. We are in the process of testing mitochondria preparations to determine the stability of the mitochondria with respect to use in the cytochrome c release assay. Mitochondria stored on ice for 4 h (the longest time we have tested at the time of this writing) can be used in the cytochrome c release assay. Therefore, it is possible to run multiple assay cycles with one preparation of mitochondria. The short format cytochrome c release assay is not affected by cell permeability, makes no assumptions about the mechanism of action, does not use cultured cells, is targeted at the process to be inhibited (i.e., cytochrome c release from mitochondria), and is a colorimetric assay easily monitored by spectrophotometric plate readers. This assay would, therefore, increase the chances of detecting lead compounds to be subsequently modified to increase potency, cell permeability, and pharmacological efficacy.

Caspase activation can occur downstream of cytochrome *c* release from mitochondria or after cell-surface death receptors are engaged. Apoptosis-inducing ligands can directly activate caspases by recruiting caspase-8 or caspase-10 to protein complexes formed on the cytoplasmic portions of the receptors (20). ELISAs for quantification of specific active caspases in cultured cells are used to quantify these events. By using the capture of the large subunit that contains the active site cysteine modified with the biotinylated inhibitor as an indicator of the active caspase state, it is now possible to specifically quantify active caspase-3 or caspase-7 without interference by other active caspases.

The active caspase ELISA quantifies a specific caspase that contained an active site intracellularly. The mass amounts detected by the ELISA is dependent on the percentage of cellular active caspase that was modified by bzVKD-fmk and the standard used to generate a standard curve. It is important to note that not all of the active caspase may be modified in cells. The standard is made with biotin-Asp-fmk (or normalized to active caspase modified with biotin-Asp-fmk) and intracellular active caspases are modified with bzVKD-fmk. Therefore, we believe that the most appropriate presentation of data is “the amount of active caspase-3 or active caspase-7 detected relative to the standard.” Others have used caspase-specific antibodies coated on plates to capture a specific caspase. After capturing, the activity of the caspase is determined with a fluorogenic substrate. The ELISA described in this section avoids problems that could generate erroneous results. Labeling of the active caspases by bzVKD-fmk *in situ* avoids loss or gain of activity during extraction. A thioether bond is extremely stable and the thioether bond formed between the biotinylated inhibitor and the active site cysteine is stable to repetitive heating to 98°C for 5 min in SDS sample buffer. The possibility that the thioether bond can be hydrolyzed by cellular enzymes has not been explored. However, this hypothetical hydrolysis would have to occur in the presence of high amounts (10  $\mu$ M in the medium) of bzVKD-fmk that gives maximal labeling of active caspase-3 (28) or in 6 M urea that is included in the extraction buffer. The use of denaturing extraction buffer in the active caspase-ELISA also aids in dissociating complexes thereby preventing masking of sites required for binding by the capture antibody.

We have used four different endpoints to assess caspase activation; PARP cleavage, DEVD-afc cleavage, proteolytic processing of caspase-7, and quantification of active caspase-3 and active caspase-7 with the ELISAs. Of these methods, only the active caspase-3 and active caspase-7 ELISAs are capable of quantifying active caspase-3 and active caspase-7 with any certainty. DEVD-afc cleavage is often reported as caspase-3 activity. Clearly

caspase-7 and other caspases are able to cleave this substrate. The same is true of peptide inhibitors. Use of bzVKD-fmk to covalently modify caspase-3 and caspase-7 is an example of how broad the inhibitor specificity can be. bzVKD-fmk has a biotin on the epsilon amino of the lysine chain and modifies the active site cysteine of caspase-3 and caspase-7 and inhibits cellular DEVD-afc cleavage activity by greater than 90%. We have found that bzVKD-fmk also covalently modifies active caspase-2 *in situ* (results not shown). Cleavage of caspases has often been used to indicate caspase activation. However, cleaved caspases may be catalytically inactive. Caspase subunits detected by western blots could be from holoenzyme with activity, subunits not a part of a holoenzyme, or from holoenzyme that is inhibited by an inhibitor of apoptosis protein (IAP) (53). The presence of IAPs in cells complicates interpretations of Western blots where proteolytic processing is detected.

The active caspase ELISAs distinguish subunits that form an active enzyme from subunits not a part of an active enzyme by requiring an active site for modification by the biotinylated inhibitor. The ability of the active caspase-3 and active caspase-7 ELISAs to distinguish between an active holoenzyme and a holoenzyme inhibited by an IAP or by noncovalent inhibitory drug candidates has not been tested. The IAP, XIAP, inhibits small peptide substrate cleavage activity of caspase-3 and caspase-7 by binding to the caspases (54–56). Thus, XIAP may prevent bzVKD-fmk from covalently modifying the active site cysteine and XIAP inhibition would be reflected by a decrease in signal in the ELISA. The IAP, survivin, may not prevent bzVKD-fmk from covalently modifying the active site cysteine. Survivin has been reported to inhibit caspase cleavage of protein substrates, but not peptide substrates (57).

## 6. MATERIALS

The Jurkat (human acute T-cell leukemia, clone E6-1) cell line was from ATCC. Cytochrome c ELISA (#MCTC0), active caspase-3 ELISA (#KM300), active caspase-7 ELISA (#KM700), bzVKD-fmk (#FMK011 or included with kits), human Bid (#846-BD), mouse Bid (#860-MM), caspase-8-cleaved human Bid (#882-B8), caspase-8 cleaved mouse Bid (#883-M8), mouse Bcl-x<sub>L</sub> (#878-BC) missing the carboxyl terminal mitochondria targeting sequence, Bak-BH3 synthetic peptide (#881-BA), Bak L to A synthetic peptide (#879-BK), and HRP conjugated to streptavidin, recombinant human caspase 2 (#702-C2), caspase 3 (#707-C3), caspase 7 (#823-C7), caspase 8 (#705-C8), and caspase 10 (#834-CP) were from R&D Systems. Biotinylated standards for the ELISAs were made and assayed as previously

described. Standards were stored at  $-20^{\circ}\text{C}$ . Boc-D-fmk and DEVD-afc were from Enzyme Systems Products. Staurosporine was obtained from Sigma and was used at a concentration of  $1.0\ \mu\text{M}$ . Triton X-100, Tween-20, leupeptin, pepstatin A, aprotinin, phenylmethylsulfonylfluoride (PMSF), and Percoll were from Sigma. Stock solutions for leupeptin and pepstatin A at  $25\ \text{mg/mL}$  in dimethylsulfoxide (DMSO) were stored at  $-20^{\circ}\text{C}$ . When used, these inhibitors were diluted 1:1000 into the indicated buffer. Stock PMSF was made fresh at  $100\ \text{mM}$  in isopropanol and diluted 1:1000 into the indicated buffer. Phosphate-buffered saline (PBS) was  $8.1\ \text{mM}\ \text{Na}_2\text{HPO}_4$ ,  $1.5\ \text{mM}\ \text{KH}_2\text{PO}_4$ ,  $\text{pH}\ 7.5$ ,  $0.137\ \text{M}\ \text{NaCl}$ , and  $2.7\ \text{mM}\ \text{KCl}$ . Protein determination was with the Coomassie Protein Assay Reagent (Pierce) using bovine serum albumin (BSA) as standard.

## 7. DETAILED METHODS

### 7.1. Isolation of Mouse Liver Mitochondria

Mitochondria were isolated from mouse liver by a modified version of the previously described procedure (58). All steps were at  $4^{\circ}\text{C}$  unless noted otherwise. Mouse liver was rinsed twice with PBS and then homogenized in  $5\ \text{mL}/0.5\ \text{g}$  tissue of Buffer A ( $225\ \text{mM}$  mannitol,  $75\ \text{mM}$  sucrose,  $0.1\ \text{mM}$  EGTA,  $1\ \text{mg/mL}$  of fatty acid-free BSA (Sigma),  $10\ \text{mM}$  HEPES-KOH,  $\text{pH}\ 7.4$ ) with 10 strokes using a Tenbroeck ground-glass homogenizer. The resulting slurry was homogenized with 30 strokes of a tight-fitting pestle in a Dounce homogenizer. Homogenate was diluted with  $5\ \text{mL}$  of Buffer A and centrifuged for 10 min at  $600g$ . The resulting supernatant was centrifuged for 10 min at  $15,000g$ . Supernatant was discarded and the pellet containing mitochondria was resuspended by repeated pipetting in  $10\ \text{mL}$  of Buffer B ( $225\ \text{mM}$  mannitol,  $75\ \text{mM}$  sucrose,  $0.1\ \text{mM}$  EGTA,  $10\ \text{mM}$  HEPES-KOH,  $\text{pH}\ 7.4$ ) and then centrifuged at  $15,000g$ . The resulting pellet was resuspended by repeated pipetting in  $8\ \text{mL}$  of Buffer C ( $395\ \text{mM}$  sucrose,  $0.1\ \text{mM}$  EGTA,  $10\ \text{mM}$  HEPES-KOH,  $\text{pH}\ 7.4$ ). Results obtained with this crude preparation of mitochondria are similar to results obtained with mitochondria prepared by further fractionation on gradients of Percoll as described below. When using the crude mitochondria preparation, the pellet is resuspended in  $1.7\ \text{mL}$  of buffer C. Results with the short format cytochrome c ELISA (Fig. 3) were obtained with the crude mitochondria preparation. Results shown in Fig. 2 were obtained with mitochondria prepared by additional fractionation on gradients of Percoll.

Mitochondria were further enriched on a gradient of Percoll by centrifugation in polyallomer tubes in a Beckman SW28.1 rotor. Percoll-containing solutions were prepared by mixing Percoll (100%) with Buffer D ( $1.28\ \text{M}$

sucrose, 0.4 mM EGTA, 40 mM HEPES-KOH, pH 7.4). To obtain 10 mL of 60% Percoll, 6.0 mL of Percoll, 1.5 mL of Buffer D, and 2.5 mL deionized water were mixed. To obtain 20 mL of 26% Percoll, 5.2 mL of Percoll, 3.7 mL of Buffer D and 11.1 mL of water were mixed. All Percoll-containing solutions were adjusted to pH 7.4 with HCl. Five milliliters of the 60% Percoll added to the bottom of the centrifuge tube was carefully overlaid with 9 mL of 26% Percoll. Three milliliters of the fraction from the 15,000g pellet containing resuspended mitochondria were overlaid on the 26% Percoll. Material was centrifuged at 41,000g for 30 min. Mitochondria at the interface formed between the 26% and 60% Percoll were collected in a volume of approx 0.5 mL. The protein concentration of the 0.5 mL of mitochondria isolated in a single centrifuge tube was approx 2.3 mg/mL.

## 7.2. Cytochrome *c* Release Assay

Aliquots of 4  $\mu$ L of mitochondria were used in each 25  $\mu$ L assay. This is equivalent to 9  $\mu$ g of mitochondrial protein containing approx 35–40 ng of cytochrome *c*. The integrity of the enriched mitochondria was routinely assessed by determining the amount of cytochrome *c* released when mitochondria were incubated under assay conditions without any inducers of cytochrome *c* release. Typically, the amount of cytochrome *c* spontaneously released from enriched mitochondria during a 30-min incubation at 30°C was less than 15% of the total cytochrome *c*.

Proteins to be tested were diluted in buffer E (10 mM HEPES-KOH, pH 7.4, 100 mM KCl), at five times their final concentration in the assay. Assay volume was 25  $\mu$ L and assays were performed in 0.5 mL microcentrifuge tubes. Assays used Buffer F (125 mM KCl, 0.5 mM MgCl<sub>2</sub>, 3.0 mM succinic acid, 3.0 mM glutamic acid, 10 mM HEPES-KOH, pH 7.4, containing 25  $\mu$ g/mL leupeptin, 25  $\mu$ g/mL pepstatin, 3  $\mu$ g/mL aprotinin, 100 mM PMSF, and 10  $\mu$ M of the caspase inhibitor Boc-Asp-FMK). Protease inhibitors were added immediately to Buffer F prior to its use.

An aliquot of 5  $\mu$ L of the test protein(s) was added to 16  $\mu$ L of Buffer F. To initiate the assay, 4  $\mu$ L of mitochondria were added and the tube was capped. The assay mixture was gently mixed by gentle vortexing for 5–10 s and incubated in a 30°C water bath for 30 min. Samples were then centrifuged in a microcentrifuge at 16,000g for 5 min at 4°C. A 15  $\mu$ L aliquot of the supernatant was removed and stored at –20°C. One set of samples was not centrifuged and was used to determine total cytochrome *c*.

Samples were thawed immediately prior to quantifying cytochrome *c* with the mouse/rat cytochrome *c* ELISA. Triton X-100 was added to all samples to obtain a final concentration of 0.5%. Samples were vortexed, diluted 100-fold with cytochrome *c* ELISA diluent, and then vortexed again. Aliquots of

100  $\mu\text{L}$  of the 100-fold diluted sample were assayed in triplicate in the rat/mouse cytochrome c ELISA.

### 7.3. Short Format for Cytochrome C Release Measurements

The cytochrome c ELISA kit 96-well plate was incubated three times with PBS for 10 min per incubation. To each well was added 32  $\mu\text{L}$  of buffer F containing 20  $\mu\text{g}$  of BSA. HRP-conjugated detection antibody in conjugate diluent free of detergents was added to obtain the desired concentration. Then Bcl-2 family proteins diluted in buffer E were added. The volume of each well was adjusted to 42  $\mu\text{L}$  with buffer E. Mitochondria were diluted into buffer C, and 8  $\mu\text{L}$  (approx 1.8  $\mu\text{g}$  of protein) was added to each well. The plate was floated in a 30°C water bath for the desired time. Then 200  $\mu\text{L}$  of buffer E were added and the wells were washed 5 times with 300  $\mu\text{L}$  per wash of buffer E and 100  $\mu\text{L}$  of color development reagents was added. After 3 min, stop solution was added and absorbance was measured at 450 nm using 540 nm as a reference wavelength. To determine total detectable cytochrome c, Triton X-100 was added to mitochondria to a final concentration of 0.1%.

### 7.4. Immunoblotting

Samples for western immunoblotting and for blotting with HRP-streptavidin were prepared by adding a two- to fivefold concentrate of sodium dodecyl sulfate (SDS)-reducing sample buffer to obtain a 1X SDS sample buffer concentration (1X SDS sample buffer is 0.0625 M Tris(hydroxymethyl)aminomethane, pH 6.8, 10 mM dithiothreitol (DTT), 3% SDS, 5% glycerol, and bromophenylblue) and then heating sample at 90–100°C for 1–3 min. Electrophoresis was on 15% polyacrylamide gels and transfer to Immobilon-P (Millipore) was for 40 min at 250 mAmps, constant current, using a Trans-Blot SD Semi-Dry Transfer Cell (Bio-Rad). Blocking, incubation with antibodies, and washing membranes were as described in the package inserts provided by the antibody suppliers. Western blotting anti-caspase 7 SSU (AF823) and anti PARP (AF600) were from R&D Systems. (Monoclonal anti-caspase-7 LSU antibody used for Western blotting was a gracious gift from Dr. Yuri Lazebnik at Cold Spring Harbor Laboratory). Secondary reagents were HRP-protein A (Amersham), HRP-sheep anti-mouse IgG (Amersham) and HRP-rabbit anti-goat IgG (Zymed). HRP was detected with the enhanced chemiluminescence-detection reagent (Amersham). To detect biotinylated inhibitor-modified protein membranes containing the transferred proteins were incubated with 25 mM Tris(hydroxymethyl)aminomethane, pH 7.5, 0.15 M NaCl, 0.05% Tween-20 containing 3% BSA at room temperature for 1 h to block and then with 40 mL

of the buffer containing 1% BSA and 100 ng HRP-streptavidin/ml at room temperature for 1 h. Membranes were washed 5–10 times with the buffer and then developed with enhanced chemiluminescence reagent.

### **7.5. DEVD-afc Cleavage Activity**

Cells were pelleted by centrifugation at 1000g, resuspended in PBS, and recentrifuged. Cells were solubilized in ice-cold active caspase-3 ELISA extraction buffer without urea and protease inhibitors at  $1 \times 10^7$  p mL. Extracts were kept on ice for approx 30 min prior to starting the assay. Immediately before starting the assay, 1 M DTT was added to each sample to a final concentration of 10  $\mu$ M. Aliquots of 90  $\mu$ L of cell extract were pipetted into a 96-well plate and the assay was started by addition of 10  $\mu$ L of 1 mM DEVD-afc in DMSO. Fluorescence was monitored every 40 s for 15 min using a fluorescent plate reader (SpectraMAX GeminiXS, Molecular Devices) using wavelengths of 400 nm for excitation, 505 nm for emission, and 495 nm for emission cutoff. Results are expressed as the rate of fluorescence generation. Fluorescence increased linearly with all samples.

### **7.6. Preparation of Cell Extracts and Conditions for Active Caspase ELISA**

Preparation of cell extracts and ELISA conditions were as described in the package insert provided with the active-caspase-3 and active caspase-7 ELISAs. Briefly, after inducing apoptosis and culture with 10  $\mu$ M bzVKD-fmk, cells and culture medium were transferred to a tube and centrifuged at room temperature at 1000g for 5 min. The cell pellet was rinsed with 1 mL PBS per  $10^7$  cells, centrifuged, and then cells were solubilized in extraction buffer (extraction buffer and diluents were made as described in or provided with the active caspase kits) containing 6 M urea, 25  $\mu$ g/mL leupeptin, 25  $\mu$ g/mL pepstatin, 3  $\mu$ g/mL aprotinin, and 100  $\mu$ M PMSF at  $10^7$  cells/mL by vortexing for 1 min at room temperature. Extracts were stored overnight at 4°C before placing at -20°C for longer storage. Samples were diluted with calibrator diluent and 100  $\mu$ L of sample were incubated in wells of antibody-coated microtiter plates for 2 h at room temperature. Wells were washed 5 times with wash buffer and 100  $\mu$ L of HRP-streptavidin were then added to each well. After 1 h wells were washed 5 times with wash buffer and 100  $\mu$ L of color reagent were added to each well. After 30 min, color development was terminated by addition of 100  $\mu$ L of stop solution to each well. Plates were read on a Molecular Devices Thermo<sub>max</sub> Microplate reader. Optical density at 450 nm was determined using 540 nm as a reference wavelength.



### 7.7. Recovery of Captured Polypeptides

To identify the biotinylated proteins that were captured by the caspase-7 capture antibody coated on the plates,  $3 \times 10^7$  Jurkat cells were incubated for the indicated times with  $1 \mu\text{M}$  STS. bzVKD-fmk was then added to the medium to give a final concentration of  $10 \mu\text{M}$ . After 1 h, cells were washed with PBS, solubilized in 1 mL of extraction buffer (extraction buffer and diluents were made as described in or provided with the active caspase kits) containing 6 M urea and protease inhibitors and stored overnight at  $4^\circ\text{C}$ . Extracts were diluted with 4 mL ELISA calibrator diluent and incubated for 2 h at room temperature in a 6-well dish coated with caspase-7 capture antibody. Captured material was washed 4 times with ELISA wash buffer and then 1 time with PBS. Captured proteins were solubilized directly into 200  $\mu\text{L}$  SDS sample buffer. Captured proteins were separated by SDS-PAGE, and transferred to immobilon membranes (Millipore) that were subsequently incubated with HRP-streptavidin or anti-caspases-7 LSU or anti-caspase-7 SSU.

## REFERENCES

1. Gross, A., McDonnell, J. M., and Korsmeyer, S. J. (1999) BCL-2 family members and the mitochondria in apoptosis. *Genes Dev.* **10**, 1899–1911.
2. Green, D. and Kroemer, G. (1998) The central executioners of apoptosis: caspases or mitochondria? *Trends Cell Biol.* **8**, 267–271.
3. Kroemer, G. (1997) The proto-oncogene Bcl-2 and its role in regulating apoptosis. *Nature Med.* **3**, 614–620.
4. Green, D. R. and Reed, J. C. (1998) Mitochondria and apoptosis. *Science* **281**, 1309–1312.
5. Kluck, R. M., Bossy-Wetzel, E., Green, D. R., and Newmeyer, D. D. (1997) The release of cytochrome c from mitochondria: a primary site for Bcl-2 regulation of apoptosis. *Science* **275**, 1132–1136.
6. Yang, J., Liu, X., Bhalla, K., Kim, C. N., Ibrado, A. M., Cai, J., et al. (1997) Prevention of apoptosis by Bcl-2: release of cytochrome c from mitochondria blocked. *Science* **275**, 1129–1132.
7. Joza, N., Susin, S. A., Daugas, E., Stanford, W. L., Cho, S. K., Li, C. Y. J., et al. (2001) Essential role of the mitochondrial apoptosis-inducing factor in programmed cell death. *Nature* **410**, 549–554.
8. Du, C., Fang, M., Li, Y., Li, L., and Wang, X. (2000) Smac, a mitochondrial protein that promotes cytochrome c-dependent caspase activation by eliminating IAP inhibition. *Cell* **102**, 33–42.
9. Ekert, P. G., Silke, J., Hawkins, C. J., Verhagen, A. M., and Vaux, D. L. (2001) DIABLO promotes apoptosis by removing MIHA/XIAP from processed caspase 9. *J. Cell Biol.* **152**, 483–490.
10. Liu, X., Kim, C. N., Yang, J., Jemmerson, R., and Wang, X. (1996) Induction of apoptotic program in cell-free extracts, requirement for dATP and cytochrome c. *Cell* **86**, 147–157.

11. Li, P., Nijhawan, D., Budihardjo, I., Srinivasula, S. M., Ahmad, M., Alnemri, E. S., and Wang, X. (1997) Cytochrome c and dATP-dependent formation of Apaf-1/caspase-9 complex initiates an apoptotic protease cascade. *Cell* **91**, 479–489.
12. Saleh, A., Srinivasula, S. M., Acharya, S., Fishel, R., and Alnemri, E. S. (1999) Cytochrome c and dATP-mediated oligomerization of Apaf-1 is a prerequisite for procaspase-9 activation. *J. Biol. Chem.* **274**, 17,941–17,945.
13. Zou, H., Liu, X., and Wang, X. (1999) An APAF-1-cytochrome c multimeric complex is a functional apoptosome that activates procaspase-9. *J. Biol. Chem.* **274**, 11,549–11,556.
14. Hu, Y., Benedict, M. A., Ding, L., and Nunez, G. (1999) Role of cytochrome c and dATP/ATP in Apaf-1-mediated caspase-9 activation and apoptosis. *EMBO J.* **18**, 3586–3595.
15. Slee, E. A., Harte, M. T., Kluck, R. M., Wolf, B. B., Casiano, C. A., Newmeyer, D. D., et al. (1999) Ordering the cytochrome c-initiated caspase cascade: hierarchical activation of caspases-2, -3, -6, -7, -8, and -10 in caspase-9-dependent manner. *J. Cell Biol.* **144**, 281–292.
16. Thornberry, N. A. and Lazebnik, Y. (1998) Caspases: enemies within. *Science* **281**, 1312–1316.
17. Hara H., Friedlander, R. M., Gagliardini, V., Ayata, C., Fink, K., Huang, Z., et al. (1997) Inhibition of Interleukin 1 $\beta$  converting enzyme family proteases reduces ischemic and excitotoxic neuronal damage. *Proc. Natl. Acad. Sci. USA* **94**, 2007–2012.
18. Cheng, Y., Deshmukh, M., D'Costa, A., Demaro, J. A., Gidday, J. M., Shah, A., et al. (1998) Caspase inhibitor affords neuroprotection with delayed administration in a rat model of neonatal hypoxic-ischemic brain injury. *Clin. Invest.* **101**, 1992–1999.
19. Bossy-Wetzel, E., Newmeyer, D. D., and Green, D. R. (1998) Mitochondrial cytochrome c release in apoptosis occurs upstream of DEVD-specific caspase activation and independently of mitochondrial transmembrane depolarization. *EMBO J.* **17**, 37–49.
20. Ashkenazi, A. and Dixit, V. M. (1998) Death receptors: signaling and modulation. *Science* **281**, 1305–1308.
21. Luo, X., Budihardjo, I., Zou, H., Slaughter, C., and Wang, X. (1998) Bid, a Bcl-2 interacting protein, mediates cytochrome c release from mitochondria in response to activation of cell surface death receptors. *Cell* **94**, 481–490.
22. Li, H., Zhu, H., Xu, C. J., and Yuan, J. (1998) Cleavage of BID by caspase 8 mediates the mitochondrial damage in the Fas pathway of apoptosis. *Cell* **94**, 491–501.
23. Zha, J., Weiler, S., Oh, K. J., Wei, M. C., and Korsmeyer, S. J. (2000) Post-translational N-myristoylation of BID for targeting mitochondria and apoptosis. *Science* **290**, 1761–1765.
24. Chittenden, T., Flemington, C., Houghton, A. B., Ebb, R. G., Gallo, G. J., Elangovan, B., et al. (1995) A conserved domain in Bak, distinct from BH1 and BH2, mediates cell death and protein binding functions. *EMBO J.* **14**, 5589–5596.

25. Hanada, M., Aime-Sempe, C., Sato, T., and Reed J. C. (1995) Structure-function analysis of Bcl-2 protein. *J. Biol. Chem.* **270**, 11,962–11,969.
26. Sattler, M., Liang, H., Nettlesheim, D., Meadows, R. P., Harlan, J. E., Eberstadt, M., et al. (1997) Structure of Bcl-x<sub>L</sub>-Bak peptide complex: recognition between regulators of apoptosis. *Science* **275**, 983–986.
27. Holinger, E. P., Chittendon, T., and Lutz, R. J. (1999) Bak BH3 peptides antagonize Bcl-x<sub>L</sub> function and induce apoptosis through cytochrome c-independent activation of caspases. *J. Biol. Chem.* **274**, 13,298–13,304.
28. Saunders, P. A., Cooper, J. A., Roodell, M. M., Schroeder, D. A., Borchert, C. J., Isaacson, A. L., et al. (2000) Quantification of active caspase 3 in apoptotic cells. *Anal. Biochem.* **284**, 114–124.
29. Casciola-Rosen, L., Nicholson, D. W., Chong, T., Rowan, K. R., Thornberry, N. A., Miller, D. K., and Rosen (1996) Apopain/ CPP32 cleaves proteins that are essential for cellular repair: a fundamental principle of apoptotic death. *J. Exp. Med.* **183**, 1957–1964.
30. Lazebnik, Y. A., Kaufmann, S. H., Desnoyers, S. Poirier, G. G., and Earnshaw, W. C. (1994) Cleavage of poly(ADP-ribose) polymerase by a proteinase with properties like ICE. *Nature* **371**, 346–347.
31. Fernandez-Alnemri, T., Takahashi, A., Armstrong, R., Krebs, J., Fritz, L., Tomaselli, K. J., et al. (1995) Mch3, a novel human apoptotic cysteine protease highly related to CPP32. *Cancer Res.* **55**, 6045–6052.
32. Lippke, J. A., Sarnecki, C., Caron, P. R., and Su, M. S. (1996) Identification and characterization of CPP32/Mch2 homolog 1, a novel cysteine protease similar to CPP32. *J. Biol. Chem.* **271**, 1825–1828.
33. Walker, N. P. C., Talanian, R. V., Brady, K. D., Dang, L. C., Bump, N. J., Ferenz, C. R., et al. (1994) Crystal structure of the cysteine protease interleukin-1 $\beta$ -converting enzyme: a (p20/p10)<sub>2</sub> homodimer. *Cell* **78**, 343–352.
34. Rotonda, J., Nicholson, D. W., Fazil, K. M., Gallant, M., Gareau, Y., Labelle, M., et al. (1996) The three-dimensional structure of apopain/ CPP32, a key mediator of apoptosis. *Nature Struct. Biol.* **3**, 619–625.
35. Mittl, P. R. E., Di Marco, S., Krebs, J. F., Bai, X., Karanewsky, D. S., Priestle, et al. (1997) Structure of recombinant human CPP32 in complex with the tetrapeptide acetyl-Asp-Val-Ala-Asp fluoromethyl ketone. *J. Biol. Chem.* **272**, 6539–6547.
36. Gurtu, V., Kain, S. R., and Zhang, G. (1997) Fluorometric and colorimetric detection of caspase activity associated with apoptosis. *Anal. Biochem.* **251**, 98–102.
37. Thornberry, N. A., Rano, T. A., Peterson, E. P., Rasper, D. M., Timkey, T., Garcia-Calvo, M., et al. (1997) A combinatorial approach defines specificities of members of the caspase family and granzyme B. *J. Biol. Chem.* **272**, 17,907–17,911.
38. Janicke, R. U., Sprengart, M. L., Wati, M. R., and Porter, A. G. (1998) Caspase-3 is required for DNA fragmentation and morphological changes associated with apoptosis. *J. Biol. Chem.* **273**, 9357–9360.
39. Wolter, K. G., Hsu, Y.-T., Smith, C. L., Nechushtan, A., Xi, X.-G., and Youle, R. J. (1997) Movement of Bax from the cytosol to mitochondria during apoptosis. *J. Cell Biol.* **139**, 1281–1292.

40. Goldstein, J. C., Waterhouse, N. J., Juin, P., Evan, G. I., and Green, D. R. (2000) The coordinate release of cytochrome c during apoptosis is rapid, complete and kinetically invariant. *Nature Cell Biol.* **2**, 156–162.
41. Schendel, S. L., Xie, Z., Montal, M. O., Matsuyama, S., Montal, M., and Reed J. C. (1997) Channel formation by antiapoptotic protein Bcl-2. *Proc. Natl. Acad. Sci. USA* **94**, 5113–5118.
42. Schlesinger, P. H., Gross, A., Yin, X.-M., Yamamoto, K., Saito, M., Waksman, G., and Korsmeyer, S. J. (1997) Comparison of the ion channel characteristics of proapoptotic BAX and antiapoptotic Bcl-2. *Proc. Natl. Acad. Sci. USA* **94**, 11,357–11,362.
43. Minn, A. J., Velez, P., Schendel, S. L., Liang, H., Muchmore, S. W., Feslik, S. W., et al. (1997) Bcl-x<sub>L</sub> forms an ion channel in synthetic lipid membranes. *Nature* **385**, 353–357.
44. Basanez, G., Nechushtan, A., Drozhinin, O., Chanturiya, A., Choe, E., Tutt, S., et al. (1999) Bax, but not Bcl-x<sub>L</sub>, decreases the lifetime of planar phospholipid bilayer membranes at subnanomolar concentrations. *Proc. Natl. Acad. Sci. USA* **96**, 5492–5497.
45. Antonsson, B., Conti, F., Clavatta, A.M., Montessuit, S., Lewis, S., Martinou, I., et al. (1997) Inhibition of Bax channel-forming activity by Bcl-2. *Science* **277**, 370–372.
46. Shimizu, S., Ide, T., Yanagida, T., and Tsujimoto, Y. (2000) Electrophysiological study of a novel large pore formed by Bax and the voltage-dependent anion channel that is permeable to cytochrome c. *J. Biol. Chem.* **275**, 12,321–12,325.
47. Schendel, S. L., Azimov, R., Pawlowski, K. Godzik, A., Kagan, B. L., and Reed, J. C. (1999) Ion channel activity of the BH3 only Bcl-2 family member, BID. *J. Biol. Chem.* **274**, 21,932–21,936.
48. Xie, Z. and Reed, J. C. (2000) Analysis of dimerization of Bcl-2 family proteins by surface plasmon resonance. *Methods Enzymol.* **322**, 266–274.
49. Diaz, J. L., Oltersdorf, T., and Fritz, L. C. (2000) Monitoring interactions of Bcl-2 family proteins in 96-well plate assays. *Methods Enzymol.* **322**, 255–266.
50. Hsu, Y. T. and Youle R. J. (1997) Nonionic detergents induce dimerization among members of the Bcl-2 family. *J. Biol. Chem.* **272**, 13,829–13,834.
51. Hsu, Y. T., Wolter, K. G. and Youle R. J. (1997) Cytosol-to-membrane redistribution of Bax and Bcl-x<sub>L</sub> during apoptosis. *Proc. Natl. Acad. Sci. USA* **94**, 3668–3672.
52. Hsu, Y. T. and Youle R. J. (1997) Bax in murine thymus is a soluble monomeric protein that displays differential detergent-induced conformations. *J. Biol. Chem.* **273**, 10,777–10,783.
53. Green, D. R. (2000) Apoptotic pathways: paper wraps stone blunts scissors. *Cell* **102**, 1–4.
54. Deveraux, Q., Takahashi, R., Salvesen, G. S., and Reed, J. C. (1997) X-linked IAP is a direct inhibitor of cell-death proteases. *Nature* **388**, 300–304.
55. Deveraux, Q. L., Roy, N., Stennicke, H. R., Arsdale, T. V., Zhou, Q., Srinivasula, S. M., et al. (1998) IAPs block apoptotic events induced by caspase-8 and cytochrome c by direct inhibition of distinct caspases. *EMBO J.* **17**, 2215–2223.

56. Takahashi, R., Deveraux, Q., Tamm, I., Welsh, K., Assa-Munt, N., Salvesen, G. S., and Reed, J. C. (1998) A single BIR domain of XIAP sufficient for inhibiting caspases. *J. Biol. Chem.* **273**, 7787–7790.
57. Shin, S., Sung, B.-J., Cho, Y.-S., Kim, H.-J., Ha, N.-C., Hwang, J.-I., et al. (2001) An anti-apoptotic protein human survivin is a direct inhibitor of caspase-3 and -7. *Biochem.* **40**, 1117–1123.
58. Brustovetsky, N. and Dubinsky, J. M. (2000) Dual responses of CNS mitochondria to elevated calcium. *J. Neurosci.* **20**, 103–113.

## A

- Allele-specific oligonucleotide hybridization, limitations, 78
- Annexin V assay,
  - basis and limitations, 4, 13, 21
  - fluorescent dyes, 21
  - laser-scanning cytometry, cell staining and fluorescence measurement, 48
  - materials, 47, 48
  - overview, 47
- Apoptosis, *see also* specific assays, definition, 1
  - endpoints, biochemical, 3
  - morphological features, 1–3, 12, 59
  - tissue section analysis, *see* Tissue sections, apoptosis analysis,types, 62

## B

- Bax, mitochondrial translocation in apoptosis, 16, 40
- Bcl-2,
  - apoptosis regulation, 119, 120
  - cytochrome c release assay using enzyme-linked immunosorbent assay for Bcl-2 activity quantification, limitations, 136, 137

- long-format assay,
  - Bid incubation, 122, 125
  - pro-apoptotic and anti-apoptotic Bcl-2 protein interactions, 125, 126
  - protocol, 141, 142
- mitochondria isolation, 140, 141
- overview, 119, 122
- selection of assay format, 127
- short-format assay for high-throughput screening,
  - Bid incubation, 127
  - principles, 126
  - protocol, 142
- immunocytochemistry, 65
- therapeutic targeting, 121
- verotoxin II interactions, 7

## C

- Calcium,
  - cell death regulation, 19
  - fluorescence assays, 19
- Cardiolipin, fluorescent dyes for determination, 12, 17
- Caspases,
  - apoptosis regulation, 120
  - basis and limitations of assays, 4

- enzyme-linked
  - immunosorbent assay
  - for activity
  - quantification,
  - captured polypeptide
    - recovery, 144
  - caspase-7 processing,
    - 129–131, 133, 134, 144
  - cell extract preparation, 143
  - limitations, 138, 139
  - overview, 119, 121, 122,
    - 128, 129
  - poly(ADP-ribose)
    - polymerase
      - cleavage, 129
  - proteins covalently
    - modified with
      - biotinylated
        - inhibitors, 131, 133,
          - 142, 143
    - simultaneous caspase-3/
      - caspase-7 assay,
        - 134–136
- fluorescence activation
  - assays, 20
- fluorochrome labeled
  - inhibitors of caspases
    - assay using laser-
      - scanning cytometry,
    - cell staining and analysis,
      - 53, 54
  - materials, 53
  - overview, 52
- immunocytochemistry in
  - tissue sections, 63–65
- inhibitors, 121
- poly(ADP-ribose) polymerase
  - cleavage, *see* Poly(ADP-
    - ribose) polymerase
  - posttranslational regulation, 8
    - types, 64
- Cell death, rationale for pathway
  - elucidation, 3, 6
- Cell membrane integrity assays,
  - basis and limitations, 5
- CGH, *see* Comparative genomic
  - hybridization
- Chromatin condensation assay,
  - laser-scanning cytometry,
    - cell staining and
      - measurement, 44
    - limitations, 45
    - materials, 43, 44
    - overview, 42, 43
    - ultrastructural analysis, 72, 73
- Cisplatin, apoptosis induction, 6
- Comparative genomic
  - hybridization (CGH),
    - microarray analysis, 112
- Complementary DNA arrays, *see*
  - Microarray analysis
- Confocal microscopy, apoptosis
  - applications, 25, 26
- Cytochrome c,
  - apoptosis regulation, 120
  - enzyme-linked
    - immunosorbent assay,
    - release assays for Bcl-2
      - activity quantification,
    - limitations, 136, 137
    - long-format assay,
      - Bid incubation, 122, 125
    - pro-apoptotic and anti-
      - apoptotic Bcl-2
        - protein
          - interactions,
          - 125, 126
    - protocol, 141, 142

- mitochondria isolation, 140, 141
- overview, 119, 122
- selection of assay format, 127
- short-format assay for high-throughput screening, Bid incubation, 127
- principles, 126
- protocol, 142
- mitochondrial translocation in apoptosis, 16
- Cytoplasmic acidification, fluorescence assay, 17, 18
- Cytoskeletal alterations, fluorescence assays, 20
- D**
- Dichloropfluorescein diacetate, cytosolic oxidant assay, 12, 18
- DNA microarray, *see* Microarray analysis
- Doxorubicin, apoptosis induction, 6
- E**
- ELISA, *see* Enzyme-linked immunosorbent assay
- Enzyme-linked immunosorbent assay (ELISA), caspase activity quantification, captured polypeptide recovery, 144
- caspase-7 processing, 129–131, 133, 134, 144
- cell extract preparation, 143
- limitations, 138, 139
- overview, 119, 121, 122, 128, 129
- poly(ADP-ribose) polymerase cleavage, 129
- proteins covalently modified with biotinylated inhibitors, 131, 133, 142, 143
- simultaneous caspase-3/caspase-7 assay, 134–136
- cytochrome c release assays for Bcl-2 activity quantification, limitations, 136, 137
- long-format assay, Bid incubation, 122, 125
- pro-apoptotic and anti-apoptotic Bcl-2 protein interactions, 125, 126
- protocol, 141, 142
- mitochondria isolation, 140, 141
- overview, 119, 122
- selection of assay format, 127
- short-format assay for high-throughput screening, Bid incubation, 127
- principles, 126
- protocol, 142
- DEVD-afc cleavage activity, 143
- immunoblotting, 142, 143
- materials, 139, 140
- Expression profiling, microarray analysis, 112



**F**

- Fas ligand,  
immunocytochemistry, 65
- FLICA assay, *see* Fluorochrome labeled inhibitors of caspases assay
- Flow cytometry,  
apoptosis applications, 23–25  
cell-cycle stage specific  
apoptosis assay, 27–29  
combined reduced thiol,  
NADP(H), and  
mitochondrial  
membrane potential  
assay, 28–30  
intracellular calcium assays, 19  
laser-scanning cytometry, *see*  
Laser-scanning  
cytometry  
limitations, 37
- Fluorescence resonance energy  
transfer (FRET), caspase  
activation assay, 20
- Fluorochrome labeled inhibitors  
of caspases (FLICA)  
assay, laser-scanning  
cytometry,  
cell staining and analysis, 53, 54  
materials, 53  
overview, 52
- FRET, *see* Fluorescence resonance  
energy transfer

**G**

- Glutathione,  
combined reduced thiol,  
NADP(H), and  
mitochondrial  
membrane potential

flow cytometry assay,  
28–30

fluorescence assay, 12, 18

**I**

- In situ* end labeling (ISEL), tissue  
sections, 66, 67
- In situ* nick translation (ISNT),  
tissue sections, 66, 67
- ISEL, *see In situ* end labeling
- ISNT, *see In situ* nick translation

**J**

JAM assay, basis and limitations, 4

**L**

- Lamin B, immunocytochemistry,  
66
- Laser-scanning cytometry (LSM),  
accuracy and sensitivity, 39, 40  
annexin V assay,  
cell staining and  
fluorescence  
measurement, 48  
materials, 47, 48  
overview, 47
- chromatin condensation assay,  
cell staining and  
measurement, 44  
limitations, 45  
materials, 43, 44  
overview, 42, 43
- fluorochrome labeled  
inhibitors of caspases  
assay,  
cell staining and analysis,  
53, 54  
materials, 53  
overview, 52
- instrumentation, 38, 39

- mitochondrial transmembrane potential assay, cell staining and
  - fluorescence measurement, 46
- dyes, 45, 46
- materials, 45, 46
- overview, 45
- temperature sensitivity, 46, 47
- poly(ADP-ribose) polymerase cleavage assay, cell attachment and fixation, 55
- cell staining and analysis, 55, 56
- materials, 55
- overview, 54
- principles, 37, 38
- protein translocation studies, 40
- recorded parameters, 39
- slide attachment of cells, advantages, 40
- cytocentrifugation, 41
- live cells, 41, 42
- overview, 40, 41
- TUNEL assay, cell fixation, 50
- DNA strand break labeling, 50, 51
- materials, 50
- overview, 49, 50
- LSM, *see* Laser-scanning cytometry
- M**
- Microarray analysis, advantages, 97, 98
- apoptotic signatures, factors affecting, 89–91
- mutant analysis, 89
- threshold establishment, 88, 89
- toxicant signatures, 87, 88
- applications, 8, 78, 112, 113, 115
- comparison with other high-throughput techniques, 77, 78
- complementary DNA arrays, filter spotting and printing, 83, 85, 86
- fluorescently-labeled nucleotides, 84, 85
- limitations, 86, 87
- principles, 80, 81
- probe preparation, 85
- replicate hybridizations, 86, 87
- computational biology, 91, 92
- considerations, 111
- controls, 110, 111
- costs, 109
- experimental design, 100, 101
- historical perspective, 98, 100
- hybridization, materials, 107, 108
- posthybridization, 108
- prehybridization, 108
- washing, 108
- immobilization of nucleotides onto solid substrates, arraying, 103, 104
- gene set preparation, 102, 103
- poly-L-lysine coated slide preparation, 104
- postarray processing, poly-L-lysine slides, 105
- printed slides, 104
- limitations, 7

- oligonucleotide arrays,
  - advantages, 81
  - approaches, 78, 79
  - GeneChip system, 81, 83
  - high-density array
    - oligonucleotide preparation, 79, 80
  - synthesis, *in situ*, 79, 81
- overview, 98
- probe preparation,
  - control probe, 105, 106
  - fluorescent labeling, 106, 107
  - purification, 107
  - RNA isolation, 107
  - sequence selection, 106
  - vector probe, 107
- reproducibility, 110
- slide scanning and
  - quantitative analysis, 108, 109
- Microtiter plate, *see* Plate reader
- Mitochondrial assays,
  - apoptosis-induced changes, 15
  - basis and limitations, 5, 13
  - Bax translocation, 16
  - cardiolipin assays, 17
  - combined reduced thiol, NADP(H), and mitochondrial membrane potential flow cytometry assay, 28–30
  - cytochrome c translocation, 16
  - fluorescent dyes,
    - mass determination, 12
    - transmembrane potential determination, 12, 15
  - laser-scanning cytometry,
    - mitochondrial transmembrane potential assay, cell staining and fluorescence measurement, 46
    - dyes, 45, 46
    - materials, 45, 46
    - overview, 45
    - temperature sensitivity, 46, 47
  - permeability transition assay, 16
  - respiration, 15
  - ultrastructural evaluation, 71, 72
- N
- NAD(P)H,
  - combined reduced thiol, NADP(H), and mitochondrial membrane potential flow cytometry assay, 28–30
  - flow cytometry, 24, 25
  - fluorescence detection of levels, 12
- Necrosis,
  - definition, 11
  - features, 11, 12
- Nuclear fragmentation assays,
  - cell fixation, 14
  - DNA degradation, 14
  - fluorescent assay
    - optimization, 14, 15
  - fluorescent DNA-binding dyes, 12, 14

**O**

- Oligonucleotide arrays, *see* Microarray analysis
- Oxidative stress, fluorescent assays, 18, 19

**P**

- PARP, *see* Poly(ADP-ribose) polymerase
- PCR, *see* Polymerase chain reaction
- Phosphatidylserine, annexin V binding, 21, 47, 65  
plasma membrane translocation, 65
- Plate reader, fluorescent assays in apoptosis, 21, 23
- Poly(ADP-ribose) polymerase (PARP), caspase cleavage, 54, 66  
enzyme-linked immunosorbent assay of cleavage, 129  
immunocytochemistry, 66  
laser-scanning cytometry cleavage assay, cell attachment and fixation, 55  
cell staining and analysis, 55, 56  
materials, 55  
overview, 54
- Polymerase chain reaction (PCR), gene set preparation for microarray analysis, 102, 103
- Programmed cell death, definition, 1

**S**

- Single nucleotide polymorphism (SNP), microarray analysis, 112, 113
- Single-stranded DNA, monoclonal antibody detection, 67, 68
- SNARF-1, cytoplasmic acidification assay, 17, 18
- SNP, *see* Single nucleotide polymorphism

**T**

- Terminal deoxynucleotidyl dUTP nick end labeling (TUNEL), basis and limitations, 4, 13  
laser-scanning cytometry, cell fixation, 50  
DNA strand break labeling, 50, 51  
materials, 50  
overview, 49, 50  
tissue sections, 66, 67
- Tissue sections, apoptosis analysis, apoptotic cell abundance, 61, 62  
apoptotic protein immunocytochemistry, 65, 66  
caspase immunocytochemistry, 63–65  
cell volume in quantification, 69, 70  
classification of apoptosis, 62  
DNA fragmentation assays, 66–68  
molecular analysis with histopathology, 63  
morphological changes, 59–61

- quantitative analysis, 68, 69
- ultrastructural evaluation, 71–73
- TRAIL, *see* Tumor necrosis factor-related apoptosis-inducing ligand
- Tumor necrosis factor-related apoptosis-inducing ligand,
  - immunocytochemistry, 65
- TUNEL, *see* Terminal deoxynucleotidyl dUTP nick end labeling
- V**
- Verotoxin II, Bcl-2 interactions, 7